

RESONANT AMPLITUDE RESPONSE OF MACHINE FOUNDATIONS ON COHESIVE SOIL

Robert L. Kondner*

SYNOPSIS

Resonant vertical displacement amplitude response of prototype circular footings supported on cohesive soil and subjected to vertical sinusoidal loading of a nature prevalent in machine foundations is presented using the methods of dimensional analysis in conjunction with kinematic and force parameters in phase diagram representation. The response is nonlinear but is presented in terms of a non-dimensional resonant amplitude parameter, dynamic stress amplitude transmitted to the supporting soil, and transmission factor of the soil-foundation system in both graphic and analytic form. The physical variables include the size and mass of the footing, applied dynamic force, eccentricity factor, displacement, and energy dissipation. Size effects are conveniently handled in non-dimensional form. Static stress level was maintained constant at 4.25 psi with footing diameters ranging from 5 ft. 2 in. to 10 ft. 4 in., total weights from 12,820 lbs. to 51,280 lbs., and applied force amplitudes between 525 lbs. and 52,000 lbs. The results may shed insight into other studies of resonant amplitude response of machine foundations.

INTRODUCTION

The major source of objectionable response of machine foundations is the occurrence of resonant phenomena. When the operational speed of the machinery coincides with the natural frequency of the soil-foundation system, resonance occurs and the amplitude of motion of the foundation is greatly amplified. Excessive foundation motion may lead to serious structural damage, excessive wear of the machinery, or objectionable performance. Most work on machine foundations have been directed at the analysis, determination, and prediction of the natural frequencies of the soil-foundation systems. Considerably less attention has been devoted to the consequences of resonance; namely, the resonant amplitudes of the foundation motion. Because of the energy dissipation inherent in any physical system such as a soil-foundation system, the resonant amplitudes have finite values. It is highly desirable to be able to estimate the values of these resonant amplitudes in order to compare them with acceptable displacement tolerances of the foundation.

*Associate Professor of Civil Engineering, Technological Institute, Northwestern University
Evanston, Illinois U.S.A.

The resonant response of a soil-foundation system is a function of many factors, including size and mass of the foundation, mass and distribution of mass of the machinery, operational characteristics of the machinery, properties of the soil supporting the foundation, magnitude and nature of the applied forcing function, frequency of oscillation, applied static stress, etc. The interrelated effects of these factors on the value of the natural frequency have not yet been determined. It is generally recognized that the response of a soil-foundation system is a nonlinear problem of a highly indeterminate nature. However, highly idealized, simplified representations or models of these systems have been utilized to provide the foundation engineer with methods (however limited) for attempting the estimation of prototype response. These expedient solutions are limited with regard to the scope of their applicability to represent actual field conditions. Most experimental studies of machine foundations are on models or relatively small footings with prototype investigations quite limited in scope.

The present paper deals with the analysis and formulation of the vertical mode resonant amplitude response of large scale prototype circular footings supported on cohesive soil and subjected to vertical vibratory loading of a nature prevalent in machine foundations. The physical variables considered include the size and mass of the footing, applied dynamic force, frequency of loading, damping of the system, and footing displacement as well as the phase angle between applied force and displacement. Static stress level was maintained constant at 4.25 psi with footing diameters ranging from 5 ft. 2 in. to 10 ft. 4 in., total weights from 12,820 lbs. to 51,280 lbs., and applied force amplitudes between 525 lbs. and 52,000 lbs. The methods of dimensional analysis are used in setting up functional relationships among the variables. A point by point amplitude linear approximation of assumed harmonic motion is used and kinematic as well as force parameters are represented in phase diagram form.

DIMENSIONAL ANALYSIS

The highly indeterminate nonlinear nature of the response of soil-foundation systems makes dimensional analysis a convenient method of expressing the physical phenomena in functional form in terms of a finite number of physical quantities. Such methods as used to formulate relationships among physical quantities may be briefly summarized as follows. If there are 'm' physical quantities containing 'n' fundamental units, which can be related by an equation, then there are (m-n), and only (m-n), independent, non-dimensional parameters, called π terms, such that the π terms are arguments of some indeterminate, homogeneous function K:

$$K(\pi_1, \pi_2, \pi_3, \dots \dots \pi_{m-n}) = 0 \quad (1)$$

Using a force, length, and time system of fundamental units, the physical quantities given in Table I have been selected considering the steady state vertical oscillation of a circular foundation supported on a cohesive soil and subjected to a sinusoidally applied vertical force.

TABLE I

PHYSICAL QUANTITY	SYMBOL	FUNDAMENTAL UNITS
1. Amplitude of footing displacement	x	L
2. Total weight of foundation	W	F
3. Diameter of footing	d	L
4. Amplitude of applied force	F _D	F
5. Forcing frequency	ω	T ⁻¹
6. Restoration parameter of soil	q	FL ⁻²
7. Dissipation parameter of soil	η	FL ⁻² T
8. Natural frequency of system	p	T ⁻¹

It is recognized that the stress-strain-time relations for cohesive soils may be complicated nonlinear viscoelastic in nature; however, for simplicity, it is assumed that the soil can be described implicitly in terms of characteristic restoration and dissipation parameters. The characteristic restoration parameter is quite general and may take many forms including a shear or compression modulus, compressive strength, compliance function, or relaxation modulus function, depending upon the circumstances under consideration. The dissipation parameter may represent many forms including a damping coefficient, friction coefficient or viscosity. The natural frequency is not a physical property of a soil but a function of a soil-foundation system and, hence, a function of the other physical quantities of the soil, loading, and foundation. Ordinarily, it might not be included as an independent physical quantity. However, since its expression in terms of the other physical quantities is not known, it is listed separately. Certain operational characteristics of the machinery may be included in the applied force amplitude. The other quantities of Table I are straightforward.

The eight physical quantities and three fundamental units give rise to five independent, non-dimensional π terms. These can be methodically obtained, algebraically transformed, and substituted into Eq. (1) to give

$$K \left[\frac{x}{d}, \frac{F_D}{d^2 q}, \frac{W}{d^2 q}, \frac{\omega}{p}, \frac{\omega \eta}{q} \right] = 0 \quad (2)$$

Since the amplitude of the footing displacement explicitly appears in only one π term, it may be considered the dependent variable and written as:

$$\frac{x}{d} = \psi \left[\frac{F_D}{d^2 q}, \frac{W}{d^2 q}, \frac{\omega}{p}, \frac{\omega \eta}{q} \right] \quad (3)$$

In Eq. (3) and hereafter the symbol ψ denotes "some function of" but not necessarily the same

function for each equation. This avoids the use of numerous subscripts and superscripts as a means of differentiating between equations:

The non-dimensional π terms may be interpreted in the following manner. Amplitude of footing displacement is given in terms of the footing diameter and expressed as the amplitude parameter, x/d . The term F_D/d^2q may be considered proportional to the ratio of the applied dynamic stress to the resisting stress and, hence, an applied dynamic Cauchy Number. Analogously, the parameter W/d^2q may be considered proportional to the ratio of the static stress level to the static resisting stress or static Cauchy Number. The term $\omega\eta/q$ may be considered the ratio of the viscous to restoring stresses and related to the familiar dissipation factor of viscoelasticity known as the loss tangent which is associated with the phase angle between the applied force and displacement. The frequency ratio is ω/p .

The prototype test results analyzed in this paper are resonant displacement amplitudes for a constant static stress level; thus, $\omega/p = 1$ and W/d^2q may be considered approximately constant. Subject to the condition on ω/p and W/d^2q , Eq. (3) can be simplified to the form

$$\frac{\Delta}{d} = \psi \left[\frac{F_D}{d^2q}, \frac{\omega\eta}{q} \right] \quad (4)$$

where Δ is the value of x at resonance. Eq. (4) is the extent to which dimensional analysis alone is helpful. The explicit form of Eq. (4) must be determined experimentally.

THEORETICAL CONSIDERATIONS

As previously noted, the dynamic prototype soil-foundation problem is nonlinear. Since the motion in nonlinear vibration may be periodic but not harmonic, the assumption of a harmonic wave form inherently leads to the concept of linearity. Depending upon the degree of nonlinearity, it is possible to use a harmonic approximation for the response, particularly when only amplitude data are being considered on an individual point by point basis.

Assuming a harmonic wave form for the steady state displacement response of prototype footings under harmonic vibratory loading, the displacement can be written as

$$y = x \sin \omega t \quad (5)$$

while the velocity, \dot{y} , and acceleration, \ddot{y} , can be written

$$\dot{y} = x\omega \cos \omega t = \dot{x} \cos \omega t \quad (6)$$

$$\text{and} \quad \ddot{y} = -x\omega^2 \sin \omega t = \ddot{x} \sin \omega t \quad (7)$$

Considering the forcing function as a harmonic function of the same frequency as the displacement but out of phase with the displacement by a time interval, Δt , gives

$$F_d = F_0 \sin(\omega t + \delta) \quad (8)$$

where $\delta = \omega(\Delta t)$ and F_0 is the amplitude of the dynamic force wave.

Since the displacement is a sine function, the velocity is a cosine function and the

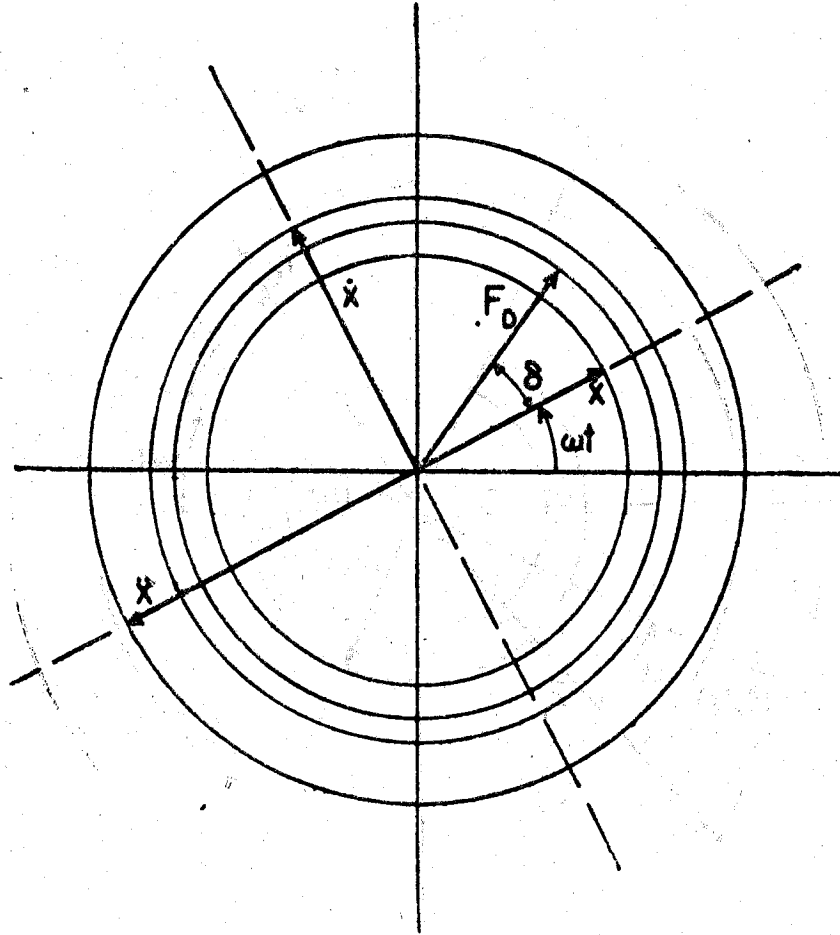


Figure 1 Phase Diagram: Kinematic Parameters and Force

acceleration is a negative sine function; the velocity and acceleration are 90° and 180° , respectively, out of phase with the displacement. Fig. 1 is a vector diagram of the displacement, velocity and acceleration. The angles between the vectors are called phase angles and the diagram itself is called a phase diagram. Since all of the vectors in Fig. 1 are rotated at the same frequency, they may be considered as turning like the spokes of a wheel, preserving their relative positions in the wheel.

D'Alembert's principle utilizes the inertial term $m\ddot{x}$ as a force whose direction is opposite to that of the acceleration vector. The restoring function vector $R_2(x)$ is opposite to that of the displacement and the dissipation function vector $R_1(\dot{x})$ is in the opposite direction of the velocity. Thus, the phase diagram for the force system can be constructed as given in Fig. 2

for the situation in which the forcing function F_D leads the displacement function by the phase angle δ . By resolving the forcing function into two components perpendicular and parallel to the displacement vector and then applying the equilibrium conditions at an instant of time, one obtains the following relations :

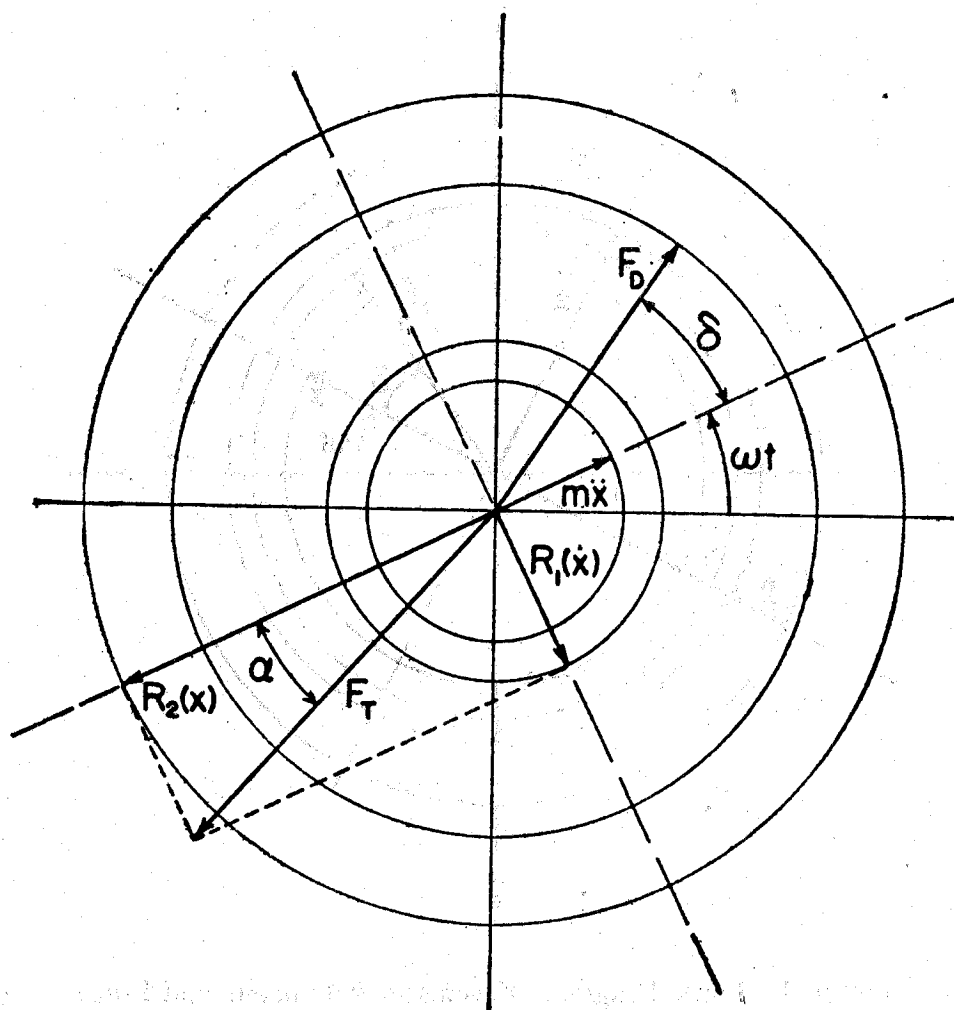


Figure 2 Phase Diagram: Force Parameters

$$R_1(\dot{x}) - F_D \sin \delta = 0 \quad (9)$$

and

$$m\ddot{x} - R_2(x) + F_D \cos \delta = 0 \quad (10)$$

Eqs. (9) and (10) give the amplitude of the dissipation function as

$$R_1(\dot{x}) = F_D \sin \delta \quad (11)$$

and the restoring function amplitude as

$$R_2(x) = m\ddot{x} + F_D \cos \delta \quad (12)$$

The same relations can be obtained directly from the equation of motion using Eqs. (7) and

(8) and evaluating the results at $\omega t=0$ and $\omega t=\pi/2$.

The amount of displacement of the footing is a function of the amount of force transmitted to the cohesive soil supporting the footing. This transmitted force, F_T , is made up of the two components R_1 and R_2 , as indicated in Fig. 2; that is, the transmitted force is the vector sum of the force transmitted through the dissipation mechanism or damper and the force transmitted through the restoring mechanism. The amplitude or modulus of the transmitted force vector is denoted as F_T . Fig. 3 is a vector force polygon for the response

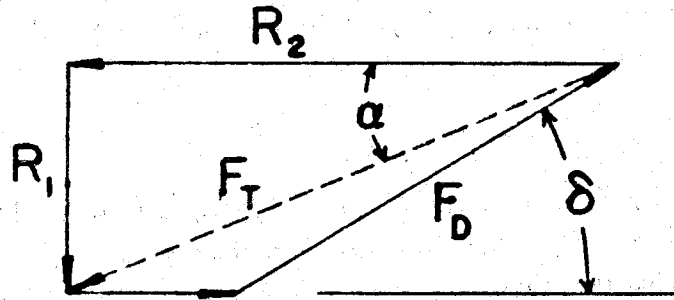


Figure 3 Force Vector Polygon

given in Fig. 2. All force vectors are shown in Fig. 3. However, F_T is equivalent to the vector sum of R_1 and R_2 and can be combined with the applied force amplitude, F_D , and the inertial force amplitude to form a force triangle. From Newton's second law, the resultant of all the external forces acting on the footing system must be exactly equal to the product of the mass and acceleration with the direction of the acceleration. Thus, the external resultant force vector cannot have a component normal to the acceleration vector. This leads to the relation

$$F_T \sin \alpha = F_D \sin \delta \quad (13)$$

and the transmitted force amplitude is

$$F_T = F_D \frac{\sin \delta}{\sin \alpha} \quad (14)$$

As indicated in Fig. 3,

$$\alpha = \tan^{-1} \left(\frac{R_1}{R_2} \right) \quad (15)$$

Substitution of Eqs. (11) and (12) into Eq. (15) gives

$$\alpha = \tan^{-1} \left[\frac{F_D \sin \delta}{m\ddot{x} + F_D \cos \delta} \right] \quad (16)$$

and $\sin \alpha$ can be conveniently obtained from a table of the values of the trigonometric functions.

The transmission factor, T.F., is the ratio of the transmitted force to applied force. At

resonance, the transmission factor can be written as

$$(T.F.)_r = \frac{F_T}{F_D} = \frac{\sin \delta}{\sin \alpha} \quad (17)$$

and the resonant transmitted force amplitude can be written

$$F_T = F_D (T.F.)_r \quad (18)$$

It is interesting to note that the transmission factor is both non-dimensional and a measure of the energy dissipation parameter of the system. Hence, the transmission factor can be considered related to $\omega\eta/q$. Since Eq. (4) is in functional form, the transmission factor may be substituted for $\omega\eta/q$ to give

$$\frac{\Delta}{d} = \psi \left[\frac{F_D}{d^2 q}, (T.F.)_r \right] \quad (19)$$

Since the arguments of Eq. (14) are independent and non-dimensional, they can be algebraically transformed as desired provided the final two arguments are also independent and non-dimensional. Multiplying the two arguments together and elimination of $F_D/d^2 q$ gives the parameters $[F_D (T.F.)_r/d^2 q]$ and $(T.F.)_r$. Dividing the first of these by $\pi/4$ and using Eq. (18) gives

$$\frac{F_D (T.F.)}{\frac{\pi d^2}{4} q} = \frac{F_T}{Aq} = \frac{\sigma_{DT}}{q} \quad (20)$$

where A is the cross sectional area of the footing and σ_{DT} is the dynamic stress amplitude transmitted to the supporting soil at resonance. Thus, Eq. (19) can be written

$$\frac{\Delta}{d} = \psi \left[\frac{\sigma_{DT}}{q}, (T.F.)_r \right] \quad (21)$$

The explicit form of the functional relation of Eq. (21) must be determined by experiment.

PROTOTYPE TEST RESULTS

The author has been involved in the analysis of the results of a number of prototype footing tests conducted using vertical sinusoidal forces generated by the centrifugal force due to a rotating eccentrically mounted mass. The test results analyzed in this paper were obtained from reinforced concrete circular footings with diameters of 5 ft., 2 in., 7 ft. 4 in., 9 ft. 2 in., and 10 ft. 4 in. supported on the surface of a relatively uniform silty clay. Unfortunately, extensive soil test data were not available from the test area. Each footing was loaded to a static pressure of 4.25 psi with ballast symmetrically placed and secured to the footing. The static pressure included the weight of the footing, weight of the vibrator, and ballast load. The areas included were 20.97, 41.94, 62.92 and 83.89, sq. ft. while the static weights included 12,820, 25,640, 38,460, and 51,280 lbs., respectively. For a footing test a particular eccentricity

city was selected for a constant magnitude of eccentric mass and steady state conditions were obtained for various values of frequency. Four values of eccentricity were used for each footing. Sinusoidal forces were applied for frequencies ranging from approximately 6 cps. to 30 cps., subject to the limitations of the vibrator. This corresponds to force amplitude, F_D , ranging from approximately 525 lbs. to 52,000 lbs., depending upon the magnitude of the eccentric mass, the eccentricity, and frequency of oscillation. All footings were carefully instrumented with various configurations of transducers and pick ups for both test control and displacement measurement. Special instrumentation was used to measure the phase angle, δ , between the applied force and the footing displacement. Thus, for each frequency of oscillation, the force amplitude, vertical displacement amplitude, and phase angle between force and displacement were obtained.

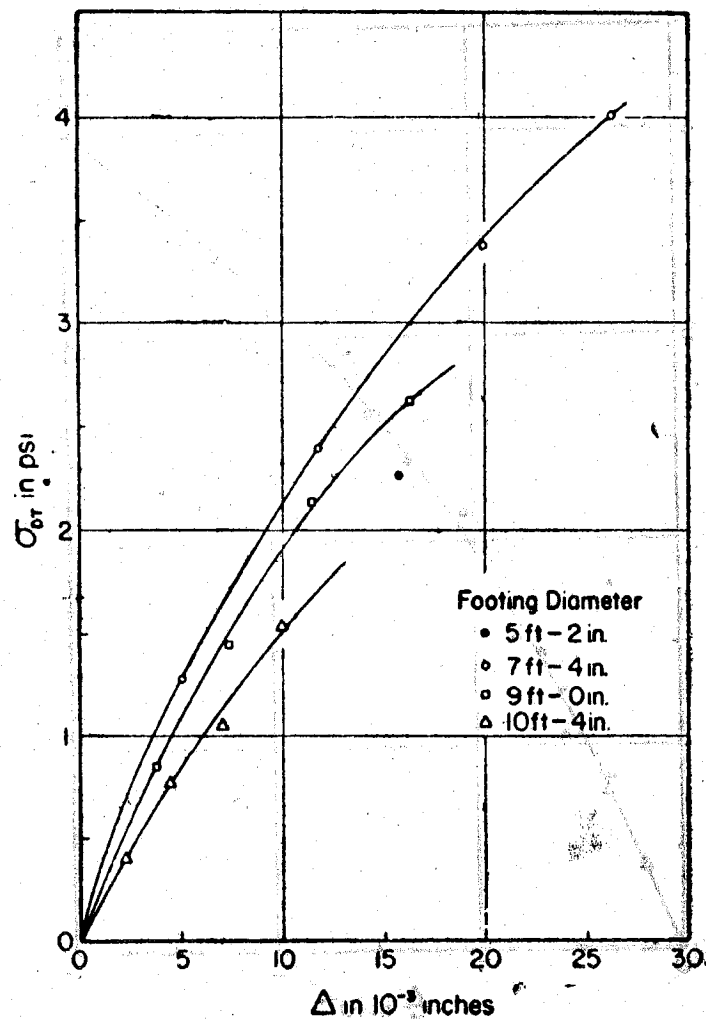


Figure 4 Transmitted Stress versus Displacement : Resonant Amplitude Response

Fig. 4 is analogous to a conventional static type of stress-deflection plot for the footing tested. In this case, the stress considered is the resonant dynamic stress amplitude transmitted

to the supporting cohesive soil and the deflection used is the resonant amplitude of footing displacement. The response given in Fig. 4 is similar to that obtained from conventional static loadings; namely, for a constant value of transmitted dynamic stress amplitude the deflection amplitude is larger for the larger size footing. The results of the single test for the 5 ft. 2 in. diameter footing do not fit in with the trends of the other 12 tests. However, the reliability of the test on the small footing is highly questionable because of improper functioning of the phase angle instrumentation, leading to doubtful values of the phase angles for this particular test. Thus, one must disregard that point on Fig. 4.

Because the footings were all supported on the same cohesive soil, the restoration parameter of the soil may be considered constant. Thus, the non-dimensional parameter σ_{DT}/q is proportional to the resonant stress amplitude transmitted, σ_{DT} . Fig. 5 is a plot of the non-

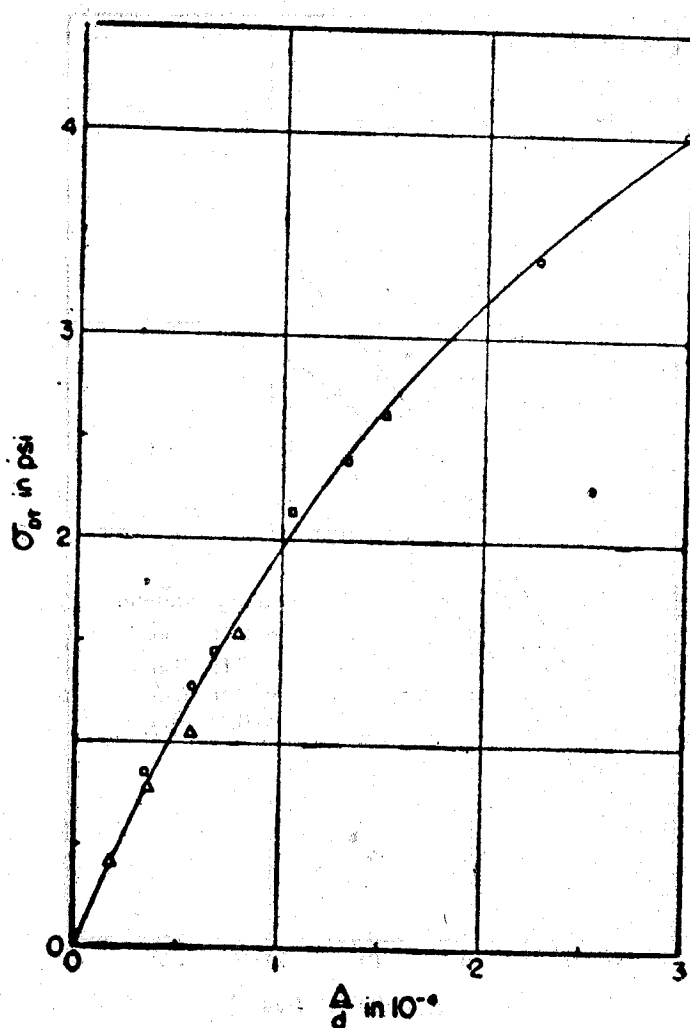


Figure 5 Transmitted Stress versus Dimensionless Displacement
Parameter : Resonance Amplitude Response

dimensional resonant amplitude parameter, Δ/d , as a function of σ_{DT} . The response of the

three large footings given in Fig. 4 seems to collapse in a single band or curve in Fig. 5 with no apparent phenomenological order. The advantage of the non-dimensional formulation is quite apparent. Since σ_{DT} is proportional to σ_{DT}/q , Fig. 5 is essentially a plot of σ_{DT}/q versus Δ/d for a normalized value of q . Although the value of the resonant transmission factor, $(T.F.)_r$, varies from 1.03 to 1.40, the lack of any apparent effect of $(T.F.)_r$ in Fig. 5 indicates that it can be considered negligible and Eq. (21) simplifies to

$$\frac{\Delta}{d} = \psi \left[\frac{\sigma_{DT}}{q} \right] \quad (22)$$

It must be emphasized that the effect of $(T.F.)_r$ is already included in σ_{DT} as indicated in Eqs. (17), (18), and (20).

The explicit form of the functional relation of Eq. (22) is presented graphically in Fig. 5. By plotting $1/\sigma_{DT}$ versus $d/\Delta \sigma_{DT}$ on log scales, as given in Fig. 6, and fitting the plot with a straight line approximation leads to an expression of the form

$$\frac{\Delta}{d} = B (\sigma_{DT})^C \quad (23)$$

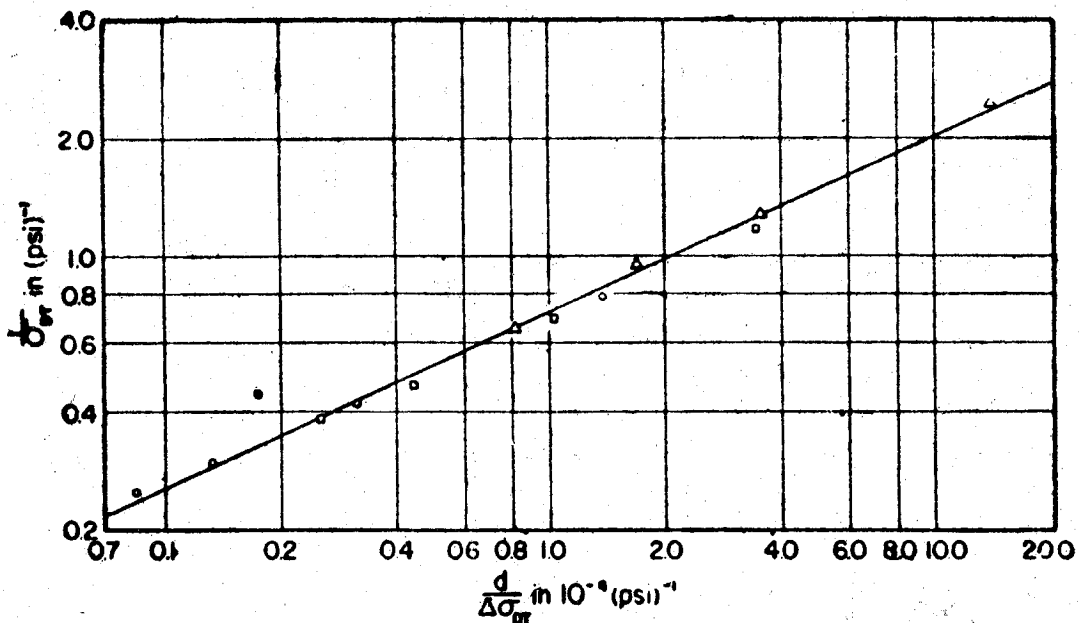


Figure 6 Resonant Amplitude Response : Measured Phase Angles

For the particular cohesive soil and footing systems tested, the values of the coefficients are $B = 4.81 \times 10^{-5}$ and $C = 1.21$ with normalized value of $q = 1$ psi.

In order to use the results given in Figs. 5 and 6 or Eq. (23) for a particular vibratory loading on a footing with the static stress level considered and supported on the cohesive soil tested, it is necessary to know the value of the resonant transmission factor in order to

calculate the value of σ_{DT} . However, the resonant transmission factor is a function of the soil-foundation system and the manner of loading.

From the conventional analysis of the forced vibration of a linear damped spring-mass system, it can be shown that the resonant value of the transmission factor can be written

$$[T.F.]_{r-L} = \sqrt{1 + \left(\frac{\Delta}{\epsilon}\right)^2} \quad (24)$$

where ϵ is the eccentricity factor defined as

$$\epsilon = \frac{M_0 e}{M} \quad (25)$$

with M_0 the eccentric mass, e the eccentricity, and M the total mass of the footing-machine system. Since Δ is an expression of the soil-foundation system and ϵ relates to the footing-machine loading system, Eq. (24) may be related to the actual resonant transmission factor associated with the prototype dynamic soil-foundation system. Comparison of the resonant

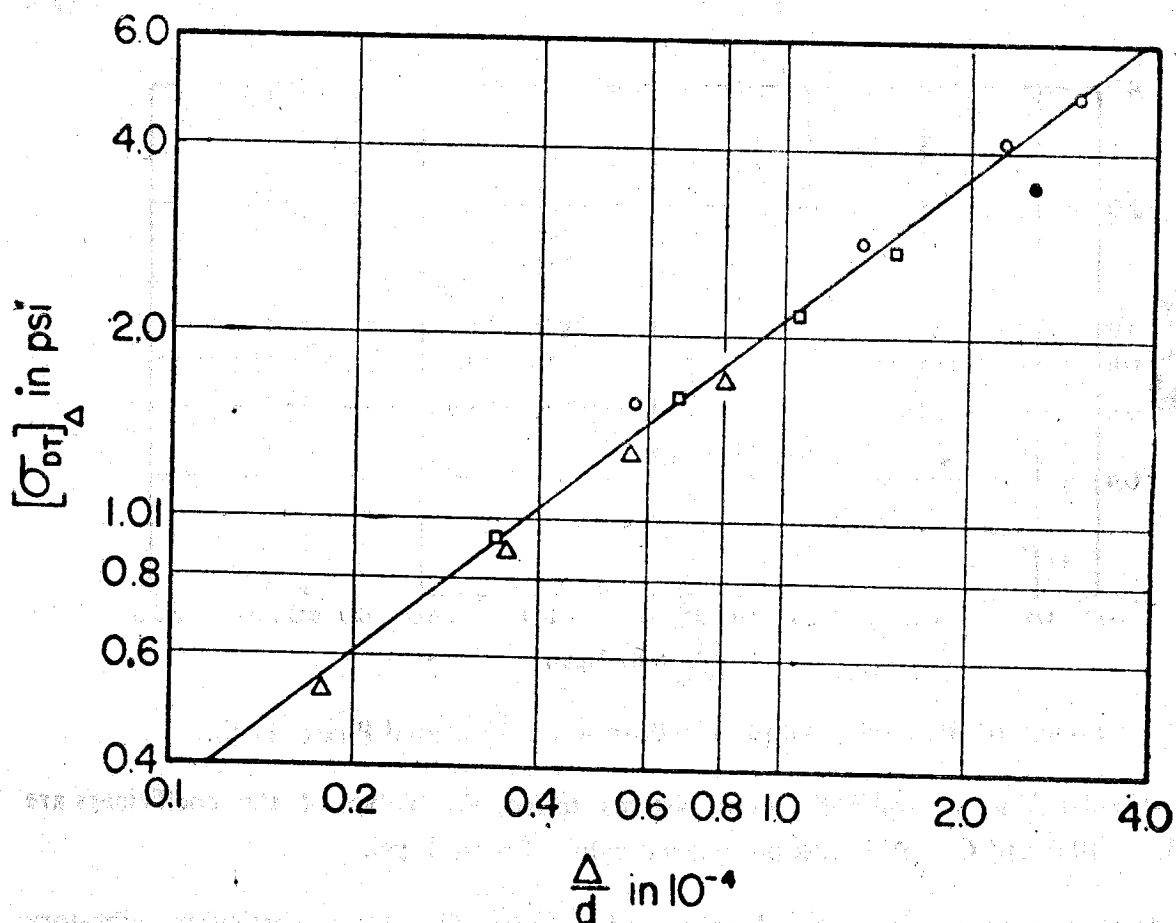


Figure 7 Resonant Amplitude Response : Transmission Factor By Equation 24

transmission factors determined by Eqs. (17) and (24) indicate that those determined by Eq. (24) are approximately 89 per cent higher than those given by Eq. (17). The values determined with Eq. (24) range from 1.28 to 1.74 while those determined by Eq. (17) range from 1.03 to 1.40. If the resonant transmission factors calculated with Eq. (24) are used in Eq. (20) to determine the transmitted dynamic stress amplitudes, σ_{DT} , the results given in Fig. 7 are obtained. Approximation of the results of Fig. 7 with a straight line representation leads to an equation of the form of Eq. (23) with the values of the coefficients $B = 3.79 \times 10^{-5}$ and $C = 1.287$. In Fig. 7, the response of the 5 ft. 2 in. diameter footing is more compatible with the results of the other footing tests. This would seem to indicate that the phase angle measurements for the small footing were indeed in error.

For the prototype study conducted, the response can be represented by Fig. 7 and Eq. (24). It can also be represented by Figs 5 and 6 or Eq. (23) along with the values of $(T.F.)_r$ determined from the phase angle response of the soil-foundation system. It is felt that these analyses and representations shed insight on the estimation of resonant displacement amplitude response of machine foundations supported on cohesive soil and subjected to steady state vibratory loading. The effects of footing size and total mass are included; however, the possible effects of the static stress level are not necessarily included as the static stress was maintained constant for the present study. Additional aspects such as the effects of resonant frequency, static stress level, and response at frequencies other than resonance remain to be investigated.

CONCLUSIONS

Resonant vertical displacement amplitude response of prototype circular footings supported on cohesive soil and subjected to vertical sinusoidal loading of a nature prevalent in machine foundations can be presented using the methods of dimensional analysis in conjunction with kinematic and force parameters in phase diagram representation. The response is nonlinear but can be presented in terms of a non-dimensional resonant amplitude parameter, dynamic stress amplitude transmitted to the supporting soil, and transmission factor of the soil-foundation system in both graphic and analytic form. The physical variables include the size and mass of the footing, applied dynamic force, eccentricity factor, displacement and energy dissipation. Size effects can be conveniently handled in non-dimensional form. Static stress level was maintained constant at 4.25 psi with footing diameters ranging from 5 ft. 2 in. to 10 ft. 4 in., total weights from 12,820 lbs. to 51,820 lbs., and applied force amplitudes between 525 lbs. and 52,000 lbs. The results can shed insight into other studies of resonant amplitude response of machine foundations.

FOOTING RESPONSE UNDER VIBRATORY LOADING

Robert L. Kondner* and Bruce B. Schimming**

SYNOPSIS

The dynamic response of a soil-footing system subjected to vertical vibratory loading is analyzed using the equation of motion with the kinematic and force parameters represented in phase diagram form. Large scale prototype circular footing tests on cohesive soil are analyzed. Dissipation stress function amplitude is given as a function of the strain rate amplitude and the energy storage or restoring stress amplitude is presented as a function of a nondimensional displacement amplitude. Dissipation and restoring response are both nonlinear. The physical variables considered include size and mass of the footing, static stress level, footing displacement, damping of the system, applied dynamic force, phase angle and frequency of loading. The response includes diameters ranging from 62 inches to 124 inches, weights from 12850 lbs. to 51280 lbs., applied force amplitudes between 525 lbs. and 52000 lbs., and frequencies up to the resonant values.

INTRODUCTION

The degree of complexity of many of the problems currently confronting the field of soil dynamics is such that the soil response under various loading conditions is extremely difficult to adequately estimate. Theoretical developments in the soil dynamics field, in general, have been highly restricted with regard to their applicability to represent actual field conditions because of general lack of basic knowledge of the response behavior of soils and soil-structure systems under a variety of loading conditions. This difficulty is due to the complexity of soil as a structural material and also to the complicated interaction of the soil and the structure being supported. Dynamic studies in soil mechanics seem to fall into two categories; namely, the response of soil-structure systems and the determination of dynamic soil properties. Present knowledge of soil properties indicates that the general forms of stress-strain-time relations will probably be very complicated, nonlinear relations which may take the form of integral equations. In addition, nonlinearities may arise because of the soil-structure interaction as well as the development of finite deformations.

*Associate Professor of Civil Engineering, Technological Institute, Northwestern University, Evanston, Illinois, U.S.A.

**Assistant Professor, University of Notre Dame, Notre Dame, Indiana, U.S.A., formerly Instructor, Northwestern University.

The purpose of this paper is the analysis of the response of a full scale soil-footing system using the equation of motion directly, with the kinematic and force parameters represented in phase diagram form. Dissipation stress function amplitude and restoring stress function amplitude relations are given for field situations.

There are a multitude of transient and steady state dynamic problems of practical importance involving soils and soil-foundation systems which can be represented by the differential equation of motion \

$$B \ddot{x} + R_1 + R_2 = F_d(t) \quad (1)$$

where :

- \ddot{x} = acceleration of the dynamic system
- B = a function of the mass and distribution of mass of the dynamic system
- R_1 = energy dissipation function
- R_2 = restoring function of the system
- $F_d(t)$ = applied dynamic forcing function which is a function of time,

and the dot indicates differentiation with respect to time. Although the form of Eq. (1) is one dimensional, it can be easily written in functional form in several dimensions. The variable x is considered to be a generalized coordinate and hence symbolizes a variety of motions including a rotation, θ , about some axis.

In order to attempt to develop solutions to Eq. (1), one must know the explicit form of the function B as well as the forms of the energy dissipation function R_1 and the energy storage or restoring function R_2 . The functions R_1 and R_2 are manifestations of the stress-strain-time response of the particular soil under consideration as well as the geometry involved and, hence, in general, unknown functions. It is important to note that the functions R_1 and R_2 , as given in Eq. (1), may be quite general nonlinear functions and include geometry and relative mass effects. In addition, the functional B is a function of the interaction of the particular soil-structure (soil-foundation) system under consideration; that is, the soil type, type and geometry of the structure, and the type as well as magnitude of the loading. Thus, realistic theoretical solutions to Eq. (1), as well as other systems of equations applicable to various static and dynamic phenomena in soil mechanics, require a knowledge of stress-strain-time response of soils. No such relations are available at present.

Theoretical solutions of Eq. (1) have been given for highly idealized, simplified, assumed forms of R_1 , R_2 and B . However, in general, these solutions are highly restricted with regard to their applicability to represent actual field conditions, and they have failed to agree in many respects with the results of experimental studies. In addition, the most extensive experimental studies are on models or relatively small footings with prototype investiga-

tions quite limited in scope. This is clearly indicated in the literature on soil dynamics.

Since the present paper is concerned with various aspects of the determination of the functions R_1 and R_2 , the basic approach lies in the controlled utilization of the differential equation of motion itself. By testing soil-footing systems with a controlled or prescribed forcing function of time, $F_d(t)$, and making appropriate measurements, it is possible to determine explicit values of R_1 and R_2 in Eq. (1). It would be desirable that these functionals be expressed in the form of stresses in order to obtain maximum generality and a possible correlation between various static and dynamic phenomena from both the load-deformation and stability viewpoints. By testing soil specimens in the laboratory with similarly controlled or prescribed forcing functions, it may be possible also to use the differential equation of motion to obtain the energy dissipation and restoring functions and, hence, form a possible correlation between the soil response properties, as determined by the two methods (laboratory soil test and prototype foundation test). Such a correlation might allow extrapolation of the prototype test results on specific soils to other soil types. An investigation of vibratory testing of soil specimens in the laboratory has been undertaken by the senior author with the initial phase given by Kondner (1961, 1962) and more recent results reported by Kondner, Krizek, and Haas (1963).

Another method of greatly expanding the range of practical usefulness of the prototype test programs is to expand the range of variables by conducting simple small scale model tests, designed and tested using nondimensional techniques. To insure realistic model representation, similitude of model and prototype, the actual test results from the prototype studies can be a control and check on the model study. Such a model-prototype feedback control and check system in conjunction with nondimensional techniques might greatly enhance the reliability of model methods as one of the tools of the soil-foundation field.

THEORETICAL CONSIDERATIONS

If the steady state displacement-time records of prototype footings under vibratory loading are considered to be harmonic wave forms, the displacement, x , can be written

$$x = x_0 \cos \omega t \quad (2)$$

while the applied forcing function, F_d , is given as a harmonic function of the same frequency

$$F_d = F_D \cos (\omega t + \delta) \quad (3)$$

in which

- x = footing displacement at any time
- x_0 = displacement amplitude
- F_d = applied force at any time
- F_D = force amplitude
- ω = frequency of loading
- δ = phase angle between the force and displacement vectors

Inherent in such a harmonic consideration is the concept of linearity, since the motion in nonlinear vibration may be periodic but not harmonic. Previous research and the soil mechanics literature indicate that soil is a nonlinear material. Nevertheless, depending upon the degree of nonlinearity, it is possible to use a harmonic approximation for the response, particularly when only amplitude data are being considered.

The displacement and force given by Eqs. (2) and (3) are simple harmonic functions of time. It is often advantageous to represent a simple harmonic function in terms of a rotating vector. In Fig. 1 the amplitude of vibratory displacement, x_0 , is taken as the length of the vector and is rotated about an axis through the end of the vector and perpendicular to the plane of the paper. By uniformly rotating the vector, its projection, x , on any fixed line in the plane of the paper will change according to Eq. (2).

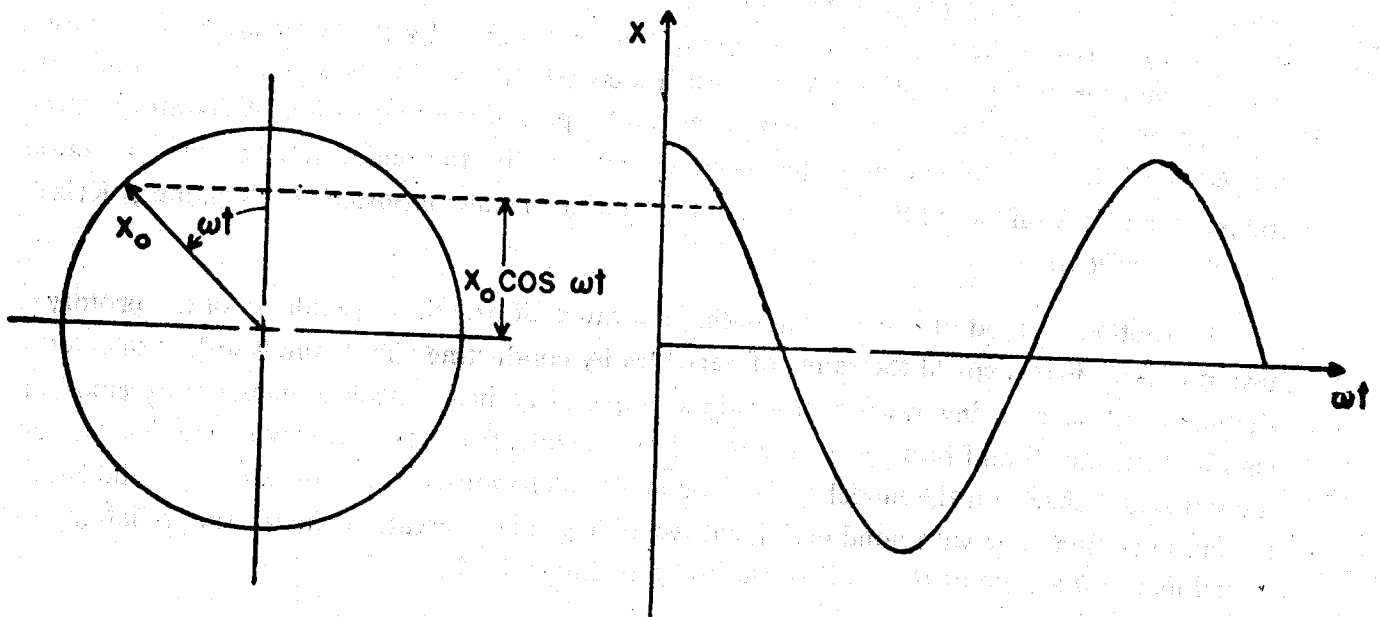


Figure 1 Rotating Vector Representation of Harmonic Motion

Utilizing constructions similar to that given in Fig. 1, it is possible to represent the various terms in Eq. (1) as rotating vectors. Consider that $R_1(t)$ and $R_2(t)$ are functions of the velocity, \dot{x} , and displacement, x , respectively. The resulting displacement is written

$$x = x_0 \cos \omega t \quad (4)$$

while the velocity, \dot{x} , and acceleration, \ddot{x} , are written as

$$\dot{x} = \dot{x}_0 \sin \omega t \quad (5)$$

$$\ddot{x} = -x_0 \omega^2 \cos \omega t \quad (6)$$

Consider the special case in which the forcing function is generated by the centrifugal force due to a rotating eccentrically mounted mass. The forcing function can be written as

$$F_d = F_D \cos(\omega t + \delta) = M_0 e \omega^2 \cos(\omega t + \delta) \quad (7)$$

in which M_0 is the eccentric mass, e is the eccentricity, and the force amplitude, F_D , is

$$F_D = M_0 e \omega^2$$

(8)

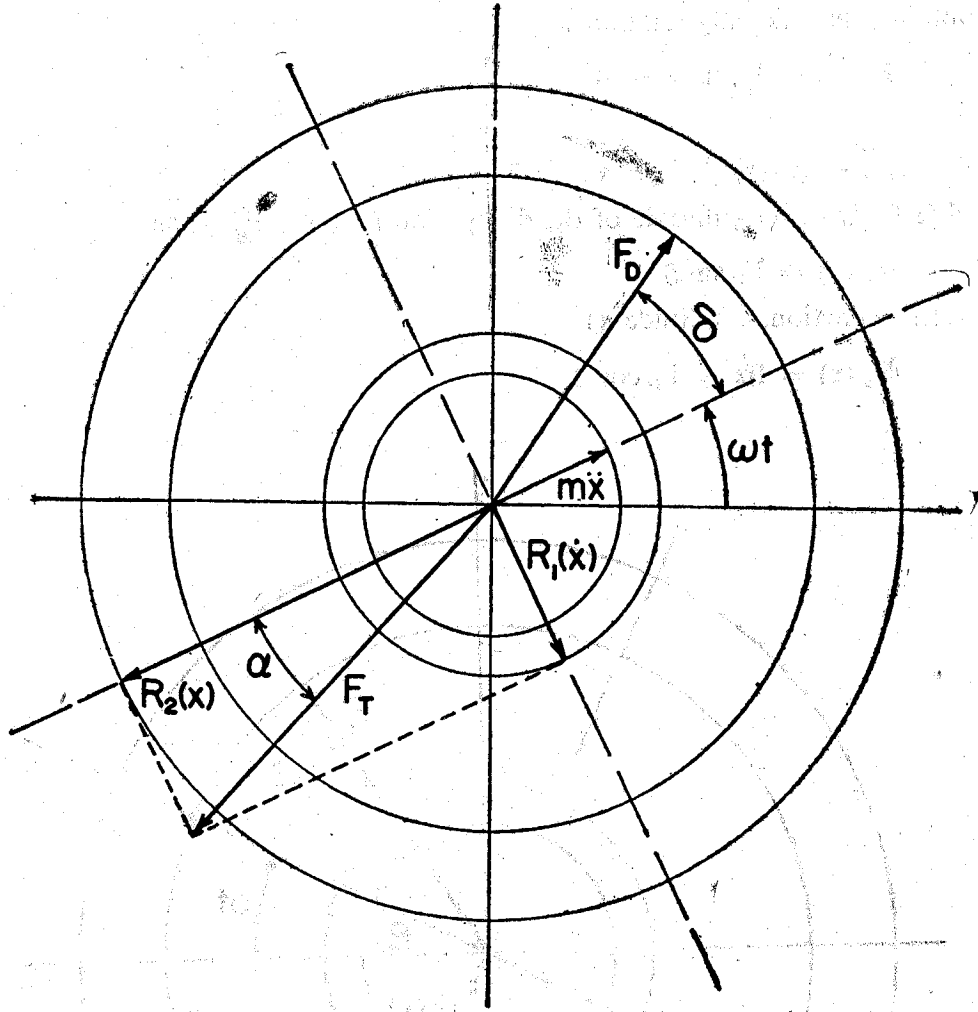


Figure 2 Phase Diagram: Kinematic Parameters and Force

Since the displacement is a cosine function, the velocity is a negative sine function and the acceleration is a negative cosine function; the velocity and acceleration are 90° and 180° , respectively, out of phase with the displacement. Fig. 2 is a vector diagram of the displacement, velocity and acceleration. The angles between the vectors are called phase angles and the diagram itself is called a phase diagram. Since all of the vectors in Fig. 2 are rotating at the same frequency, they may be considered as turning like the spokes of a wheel, preserving their relative positions in the wheel.

Using D'Alembert's principle, the inertial term $B \ddot{x}$ is a force whose direction is opposite to that of the acceleration vector. The restoring function vector $R_2(x)$ is opposite to that of the displacement and the dissipation function vector $R_1(\dot{x})$ is in the opposite direction of the velocity. Thus, the phase diagram for the force system can be constructed as given in Fig. 3

for the situation in which the forcing function F_d leads the displacement function by the phase angle δ . By resolving the forcing function into two components parallel and perpendicular to the displacement vector and then applying the equilibrium conditions at an instant of time, one obtains the following relations:

$$R_1(\dot{x}) - F_D \sin \delta = 0 \quad (9)$$

and

$$B\ddot{x} - R_2(x) + F_D \cos \delta = 0 \quad (10)$$

Eqs. (9) and (10) give the amplitude of the dissipation function $R_1(t)$ as

$$R_1(\dot{x}) = F_D \sin \delta \quad (11)$$

and the restoring function amplitude as

$$R_2(x) = B\ddot{x} + F_D \cos \delta \quad (12)$$

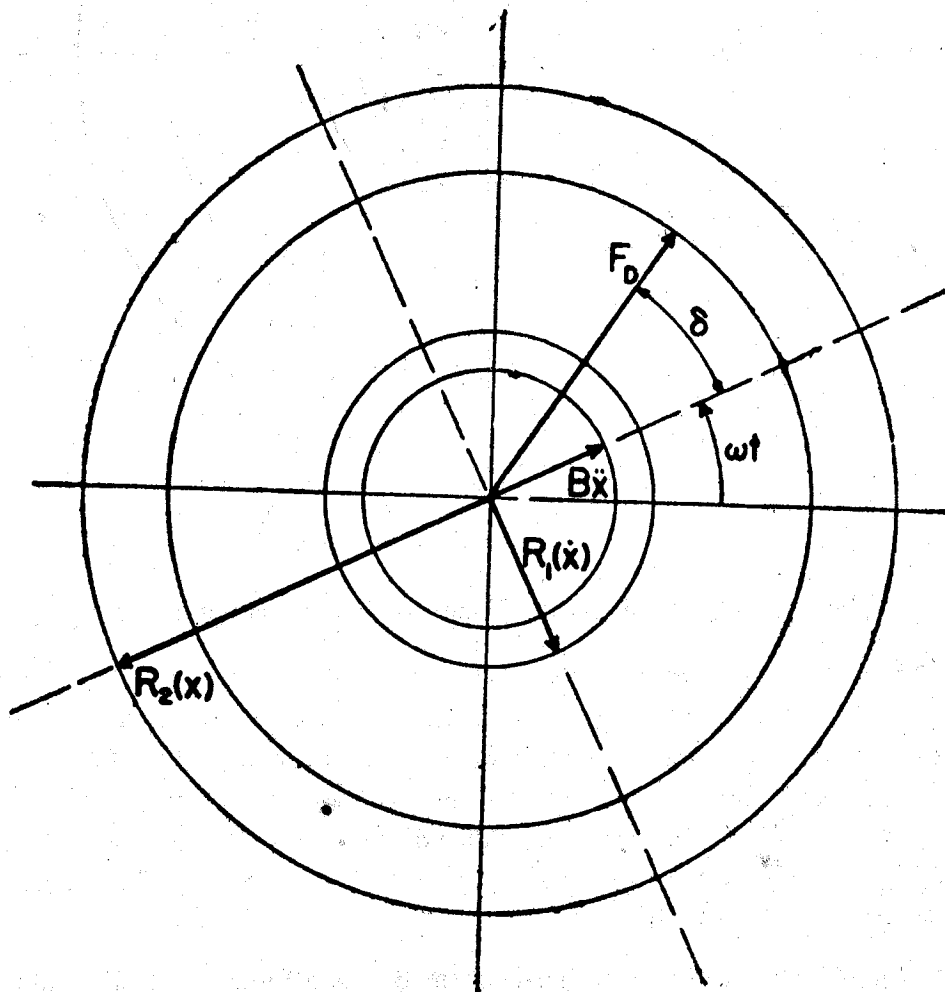


Figure 3 Phase Diagram: Force Parameters

The same relations can be obtained directly from the equation of motion. Substitution of Eqs. (6) and (3) into Eq. (1) gives

$$-B\omega^2 x_0 \cos \omega t + R_1(t) + R_2(t) = F_D \cos (\omega t + \delta) \quad (13)$$

Since $R_1(t)$ and $R_2(t)$ can be written as

$$R_1(t) = R_1(\dot{x}) \sin \omega t \quad (14)$$

and

$$R_2(t) = -R_2(x) \cos \omega t, \quad (15)$$

substitution into Eq. (13) gives

$$-B\omega^2 x_0 \cos \omega t + R_1(\dot{x}) \sin \omega t - R_2(x) \cos \omega t = F_D \cos (\omega t + \delta) \quad (16)$$

For the condition $\omega t = \pi/2$, Eq. (16) gives

$$R_1(\dot{x}) = -F_D \sin \delta, \quad (17)$$

and for the condition $\omega t = 0$, it gives

$$R_2(x) = -[F_D \sin (90^\circ + \delta) + B \omega^2 x_0] \quad (18)$$

or

$$R_2(x) = -[F_D \cos \delta + B \omega^2 x_0] \quad (19)$$

The negative signs in Eqs. (17) and (18) indicate that the vectors $R_1(\dot{x})$ and $R_2(x)$ are in the directions opposite the velocity and displacement vectors, respectively. The above relations can also be developed for lag phase angles instead of lead phase angles. In the above development, the explicit functional form of $R_1(\dot{x})$ and $R_2(x)$ have been left open; that is, specific form have not been assumed.

By Eq. (1) by a characteristic area A , one obtains

$$\frac{B \ddot{x}}{A} + \frac{R_1(t)}{A} + \frac{R_2(t)}{A} = \frac{F_d(t)}{A} \quad (20)$$

which can be written in terms of stresses as

$$\sigma_1(t) + \sigma_1(t) + \sigma_2(t) = \sigma_d(t) \quad (21)$$

where

$$\begin{aligned} \sigma_1(t) &= \text{inertial stress as a function of time,} \\ \sigma_1(t) &= \text{dissipation stress as a function of time,} \\ \sigma_2(t) &= \text{restoring stress as a function of time,} \\ \sigma_d(t) &= \text{dynamic stressing function of time.} \end{aligned}$$

Dividing the dissipation and restoring functions of Eqs. (14) and (15), respectively, by the characteristic area A , one obtains

$$\sigma_1(t) = \sigma_1(\dot{x}) \sin \omega t \quad (22)$$

and

$$\sigma_2(t) = -\sigma_2(x) \cos \omega t \quad (23)$$

where $\sigma_1(\dot{x})$ and $\sigma_2(x)$ are the dissipation stress amplitude and restoring stress amplitude, respectively. These amplitudes can be written

$$\sigma_1(\dot{x}) = \frac{R_1(\dot{x})}{A} \quad (24)$$

and

$$\sigma_2(x) = \frac{R_2(x)}{A} \quad (25)$$

where $R_1(\dot{x})$ and $R_2(x)$ are given by Eqs. (11) and (12), respectively.

PROTOTYPE TEST RESULTS

The senior author has been involved in the analysis of the results of a number of prototype footing tests conducted using vertical sinusoidal forces generated by the centrifugal force due to a rotating eccentrically mounted mass. The test results analyzed in this paper were obtained from reinforced concrete circular footings 62 inches, 88 inches, 108 inches and 124 inches in diameter resting on the surface of a relatively uniform silty clay. Unfortunately, extensive soil test data are not available for the test area. Each footing was loaded symmetrically with ballast secured to the footing to a static pressure of 4.25 psi. This static pressure included the weight of the footing, weight of the vibrator and ballast load. Sinusoidal forces were applied for frequencies ranging from approximately 6 cps to 30 cps, subject to the limitations of the vibrator. This corresponded to force amplitudes, F_0 , ranging from approximately 525 lbs. to 52,000 lbs., depending upon the magnitude of the eccentric mass, the eccentricity, and frequency of oscillation. All footings were carefully instrumented with various configurations of transducers and pickups for both test control and displacement measurement. Special instrumentation was used to measure the phase angle, δ , between the applied force and the footing displacement. For a footing test, a particular eccentricity was selected for a constant magnitude of eccentric mass and steady state conditions were obtained for various values of frequency. Four values of eccentricity were used for each footing. Thus, for each frequency of oscillation, the force amplitude, vertical displacement amplitude, and phase angle between force and displacement were obtained.

Fig. 4 is a graphical representation of the amplitude of the energy dissipation stress, $\sigma_1(\dot{x})$, as a function of the strain rate amplitude for the experimental program with the static stress level of 4.25 psi. The dissipation stress amplitude, $\sigma_1(\dot{x})$, was calculated by dividing the dissipation function amplitude of Eq. (11) by the footing area as indicated in Eq. (24) while the strain rate amplitude is the product of the displacement amplitude and the frequency of oscillation.

The amplitude of the restoring function is represented in Fig. 5 by the restoring stress amplitude as a function of the nondimensional displacement amplitude, x_0/d , where d is the diameter of the footing. The restoring stress amplitude, $\sigma_2(x)$, is obtained by dividing the restoring function amplitude of Eq. (12) by the footing area as indicated in Eq. (25).

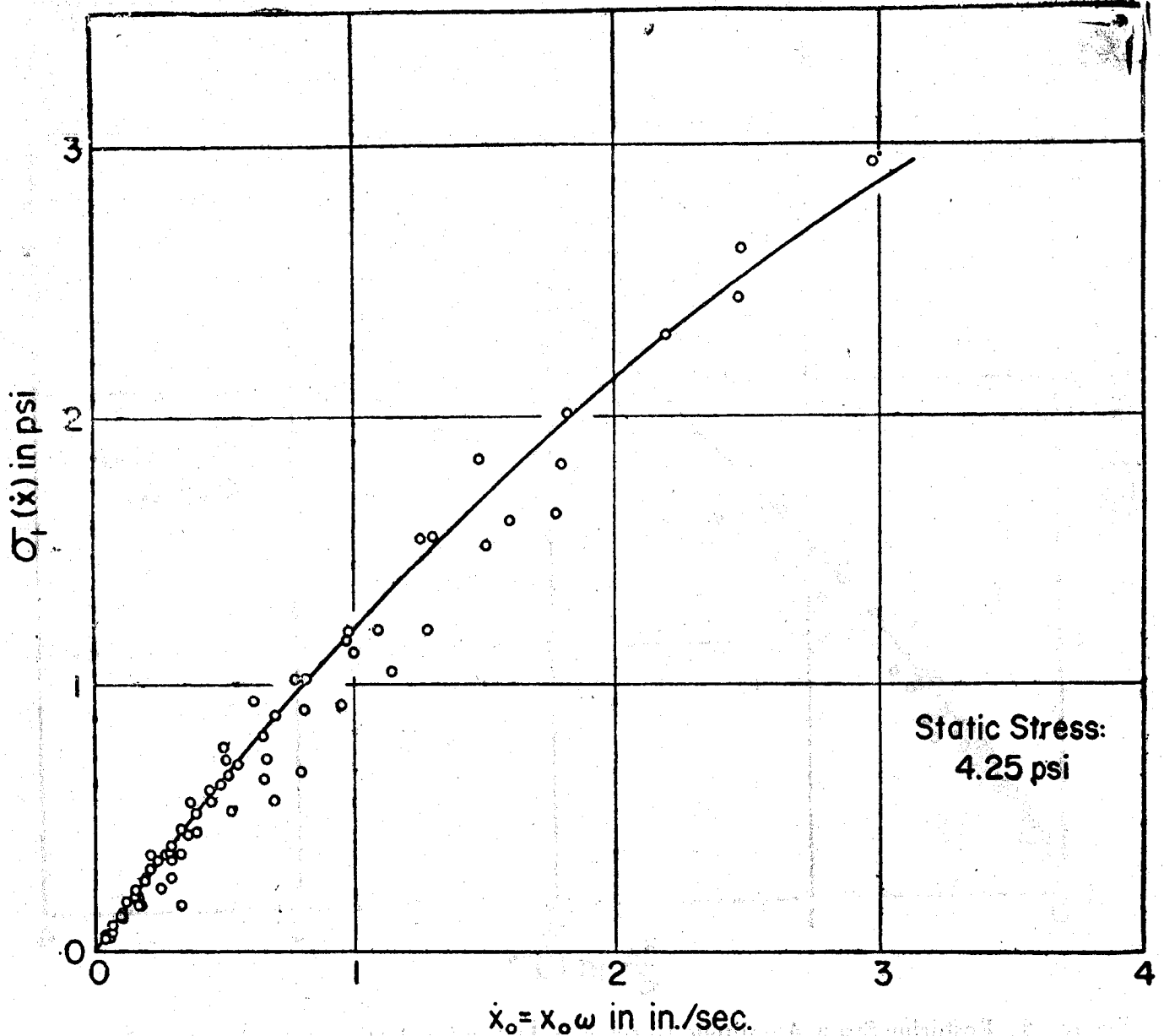


Figure 4 Dissipation Stress Amplitude versus Strain Rate Amplitude: Prototype Tests

Figs. 4 and 5 include the amplitude-frequency-phase angle data with increasing frequency up to resonant frequency. For frequencies greater than resonant frequency, both the dissipation stress amplitude and restoring stress amplitude decrease rapidly and fall below the response given in Figs. 4 and 5. It is interesting to note that Figs. 4 and 5 include the effects of varying area, static weight, frequency, eccentric setting, eccentric mass and displacement amplitude. The areas included are 20.97, 41.94, 62.92, and 83.89 sq. ft.; while the static weights included 12,820, 25,640, 38,460, and 51,280 lbs., respectively.

Although a point by point linear approximation was used by virtue of the assumed

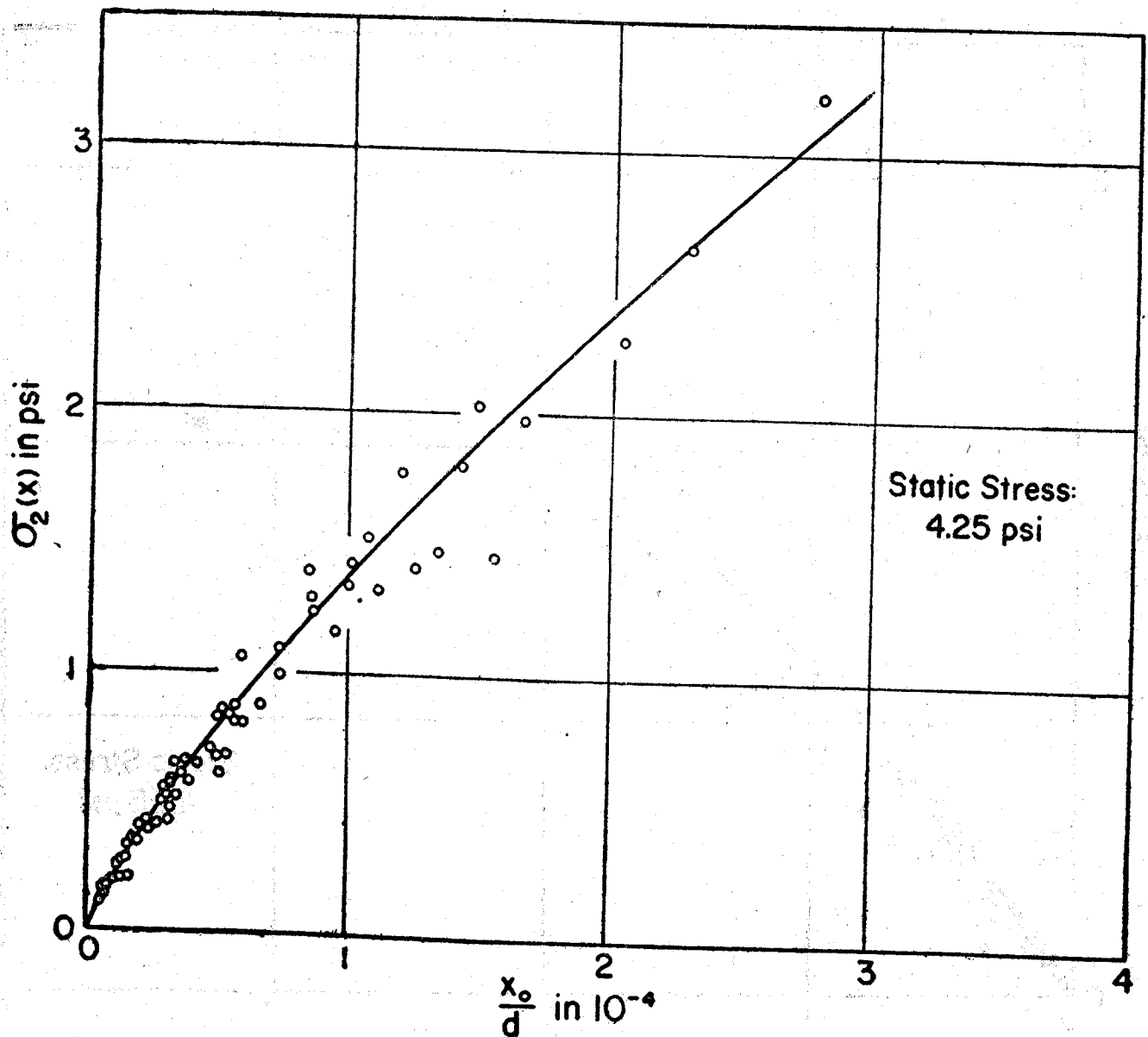


Figure 5 Restoring Stress Amplitude versus Non-Dimensional Displacement: Prototype Tests

harmonic wave form and subsequent representation with phase diagrams, the prototype footing response of Figs. 4 and 5 is definitely nonlinear. Thus, linear approximations may be useful in studying various aspects of soil-foundation response. It must be emphasized that although the present study is relatively extensive for a prototype investigation, it is quite limited in terms of the many factors that influence dynamic response of soil-foundation systems. The loading was restricted to sinusoidal and may be associated with that of interest in problems of machine vibration. Further analysis must be conducted to study the effects of size of footing, mass of the system, mode of vibration, magnitude of displacement, static stress level, magnitude and type of loading, frequency, resonant frequency, and the

characteristics of the soil on which the foundation is supported. It is felt that some of these effects are responsible for the scatter in Figs. 4 and 5; hence, the necessity for a more detailed analysis.

CONCLUSIONS

Prototype response of circular footings subjected to vertical vibratory loading can be conveniently analyzed with an amplitude linear approximation of assumed harmonic motion using the equation of motion and kinematic as well as force parameters in phase diagram form. The energy storage or restoring stress amplitude can be represented as a function of a nondimensional displacement amplitude and the dissipation stress function amplitude can be related to the strain rate amplitude. Both the dissipation and restoring aspects of the cohesive soil-footing response are nonlinear. The response includes diameters ranging from 62 to 124 inches, weights from 12,820 to 51,280 lbs., applied force amplitudes between 525 to 52,000 lbs., and frequencies up to the resonant values.

REFERENCES

- Kondner, R. L., (1961), "Vibratory Simple Shear of a Clay," Proc. Highway Research Board (U.S.A.) Vol. 40, pp. 647-662.
- Kondner, R. L., (1962), "Vibratory Characteristics of Cohesive Soils in Uniaxial Compression," Proc. Second Symposium on Earthquake Engineering, Roorkee, (India), pp. 109-129.
- Kondner, R. L., R. J. Krizek, and H. J. Hass, (1963), "Dynamic Clay Properties by Vibratory Compression," ASCE, Symposium on Dynamic Response of Materials and Structures, Annual Meeting, San Francisco (U.S.A.).

THE HISTORY OF THE UNITED STATES

The history of the United States is a story of growth and change. It begins with the first settlers and continues through the years of exploration, settlement, and the struggle for independence.

The early years of the United States were marked by a period of rapid expansion. The country grew from a small colony on the eastern coast to a vast nation stretching across the continent. This growth was driven by a combination of factors, including the desire for land, the search for new markets, and the need for resources.

The history of the United States is also a story of conflict and compromise. From the American Revolution to the Civil War, the country has been shaped by a series of struggles over its identity, its values, and its future. These conflicts have led to the development of a unique political system and a sense of national unity.

THE VIBRATIONS OF A CLAMPED RECTANGULAR PLATE WITH CONCENTRATED MASS, SPRING AND DASHPOT

K.T. Sundara Raja Iyengar* and K.S. Jagadish*

SYNOPSIS

An approximate analytical method has been given for the determination of natural frequencies of a composite system consisting of an isotropic rectangular plate with a concentrated mass, spring and dashpot attached at any point of the plate, the plate being clamped at all the edges. This method makes use of a double series expansion in terms of the beam function. Numerical examples are given for a square plate with (a) concentrated mass at the centre and (b) a spring at the centre. This method is applicable to many other edge conditions and combinations of mass, spring and dashpot.

Nomenclature

2a, 2b	sides of the rectangular plate
h	plate thickness
D	flexural rigidity of the plate
E	Young's modulus of the plate material
ν	Poisson's ratio
K_p	spring constant of the plate
K_s	constant of the plate per unit area
ρ	mass of the plate per unit area
M_p	total mass of the plate
M	concentrated mass
c	dashpot strength
γ	b/a ratio
μ	exponential decay constant
p	circular frequency of the system
$W(x,y,t)$	deflection of the plate
X_m, Y_n	beam functions
λ	the frequency parameter

*Department of Civil Engineering, Indian Institute of Science, Bangalore-12

1. Introduction.

In engineering instrumentation or in structural analysis, problems often arise where the natural frequencies of lateral vibrations of a rectangular plate of appreciable mass which carries a concentrated mass are important, especially when the attached masses are comparable in magnitude to the mass of the plate itself. Under such circumstances the natural frequencies of the plate-mass system may be considerably different from those of the plate without masses. For a vibrating beam with concentrated mass, spring and dashpot an analytical solution has been given by Dana Young (1948). This method makes use of a series expansion in terms of the set of orthogonal functions which represent the normal modes of vibration of the beam alone. This method is very general in character and may be applied when the beam has any type of end supports. This method has been extended by Das and Navaratna (1963) to isotropic rectangular plates with attached mass, spring and dashpot. They have considered a rectangular plate simply supported along two parallel edges and supported in any manner along the other two parallel edges. A Fourier series expansion in terms of the corresponding plate-eigenfunctions has been utilised to represent the modal form of the plate system. An independent analysis for the problem of vibration of a plate with attached mass has been given by Thein Wah (1961). Even here the plate is simply supported on two opposite edges. An extension of Young's procedure is possible only for plates treated by the above authors where the two opposite edges are simply supported. Only in this case a series expansion in terms of the plate eigenfunctions is possible. For other types of boundary conditions such an expansion is not possible as the plate eigenfunctions are not known. This paper is devoted to an analytical solution for such plates.

A fourier series procedure has been made use of in solving the vibrations of a clamped rectangular plate with concentrated mass, spring and dashpot. It leads to the same results as given by the Galerkin method when the same functions are used. The procedure may be applied for any combination of clamped and simply supported edges. When there are free edges it is not possible to use this method and the Rayleigh-Ritz method may have to be used.

2. The equation for the composite system.

Let the mass, spring and dashpot be attached to the plate at a point (x_1, y_1) (Fig. 1.). During vibration the plate may be considered to be under forced vibration due to the force of interaction between the plate and the mass-spring-dashpot system. Then the motion of the plate is described by

$$D \nabla^4 W + \rho \frac{\partial^2 W}{\partial t^2} = f(x, y) e^{(-\mu + ip)t} \quad (1)$$

Where μ is the exponential decay constant and $f(x, y) e^{(-\mu + ip)t}$ represents the force of interaction.

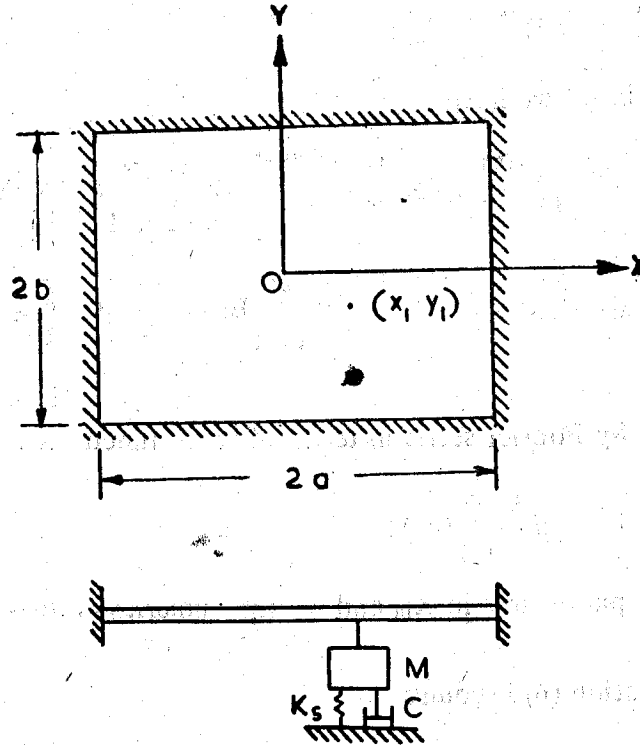


Figure 1

The differential equation for the mass-spring-dashpot system can be written as

$$M \frac{d^2 \bar{W}}{dt^2} + c \frac{d \bar{W}}{dt} + K_s \bar{W} = -F_0 e^{(-\mu + ip)t} \quad (2)$$

Where $\bar{W} = W(x_1, y_1, t)$

$f(x, y) = \delta(x_1, y_1) F_0$; $\delta(x_1, y_1)$ being the Dirac-delta function in two dimensions, c and K_s are the dashpot strength and the spring constant respectively.

Combining (1) and (2) we may write

$$\nabla^4 W + \frac{\rho}{D} \frac{\partial^2 W}{\partial t^2} + \frac{\delta(x_1, y_1)}{D} \left[M \ddot{\bar{W}} + c \dot{\bar{W}} + K_s \bar{W} \right] = 0 \quad (3)$$

The solution may now be assumed in the form

$$W = \sum_{m=1}^{\infty} \sum_{n=1}^{\infty} B_{mn} X_m Y_n e^{(-\mu + ip)t} \quad (4)$$

where X_m, Y_n are the eigenfunctions of a clamped beam. We now expand $\delta(x_1, y_1)$ by a fourier series—

$$\delta(x_1, y_1) = \sum_{m=1}^{\infty} \sum_{n=1}^{\infty} A_{mn} X_m Y_n \quad (5)$$

where $A_{mn} = \frac{1}{4ab} X_m(x_1) Y_n(y_1)$

Substituting (5) and (4) in (3) we have

$$\begin{aligned} & \sum_{m=1}^{\infty} \sum_{n=1}^{\infty} B_{mn} \left\{ a_m^4 + \beta_n^4 + \frac{e(ip-\mu)^2}{D} \right\} X_m Y_n e^{(-\mu+ip)t} + 2 \sum_{m=1}^{\infty} \sum_{n=1}^{\infty} B_{mn} X_m'' Y_n'' e^{(-\mu+ip)t} \\ & + \frac{1}{4Dab} \sum_{m=1}^{\infty} \sum_{n=1}^{\infty} X_m(x_1) Y_n(y_1) X_m Y_n e^{(-\mu+ip)t} \left[\sum_{i=1}^{\infty} \sum_{j=1}^{\infty} B_{ij} X_i(x_1) Y_j(y_1) \left\{ M(ip-\mu)^2 + c(ip-\mu) + K_s \right\} \right] \\ & = 0 \end{aligned} \quad (6)$$

Expanding X_m'' and Y_n'' by Fourier series in terms of beam functions we can write

$$X_m'' = a_m^2 \sum_{i=1}^{\infty} K_i X_i; \quad Y_n'' = \beta_n^2 \sum_{j=1}^{\infty} L_j Y_j \quad (7)$$

where a_m and β_n are the parameters in X_m and Y_n the numerical values of which will be given later.

Using (7) the equation (6) becomes

$$\begin{aligned} & \sum_{m=1}^{\infty} \sum_{n=1}^{\infty} \left[B_{mn} \left\{ a_m^4 + \beta_n^4 + \frac{\rho(ip-\mu)^2}{D} \right\} + 2 \sum_{i=1}^{\infty} \sum_{j=1}^{\infty} B_{ij} a_i^2 \beta_j^2 K_m^i L_n^j \right] X_m Y_n e^{(-\mu+ip)t} \\ & + \frac{1}{4Dab} \sum_{m=1}^{\infty} \sum_{n=1}^{\infty} X_m(x_1) Y_n(y_1) X_m Y_n e^{(-\mu+ip)t} \left[\sum_{i=1}^{\infty} \sum_{j=1}^{\infty} B_{ij} X_i(x_1) Y_j(y_1) \left\{ M(ip-\mu)^2 + c(ip-\mu) + K_s \right\} \right] = 0 \end{aligned} \quad (8)$$

Putting

$$C_{mn}^{mn} = a^2 b^2 (a_m^4 + \beta_n^4 + 2a_m^2 \beta_n^2 K_m^m L_n^n)$$

$$C_{ij}^{mn} = 2a^2 b^2 a_i^2 \beta_j^2 K_m^i L_n^j, \quad i \neq m, \text{ or } j \neq n$$

$$E_{ij}^{mn} = X_m(x_1) Y_n(y_1) X_i(x_1) Y_j(y_1)$$

and collecting the coefficient of

each $X_m Y_n e^{(-\mu+ip)t}$ in (8) and equating to zero we get

$$\sum_{i=1}^{\infty} \sum_{j=1}^{\infty} B_{ij} \left[C_{ij}^{mn} + \frac{\rho(\mu^2 - p^2) a^2 b^2}{D} \delta_{ij}^{mn} + \frac{E_{ij}^{mn} ab}{4D} \left\{ M(\mu^2 - p^2) + K_s - c\mu \right\} \right] = 0 \quad (9)$$

$$m = 1, 2, 3, \dots$$

$$n = 1, 2, 3, \dots$$

and

$$\sum_{i=1}^{\infty} \sum_{j=1}^{\infty} B_{ij} \left[\frac{2 \mu p \rho a^2 b^2}{D} \delta_{ij}^{mn} + \frac{E_{ij}^{mn} ab}{4D} (2 \mu p M - c \rho) \right] = 0 \quad (10)$$

$$m = 1, 2, 3, \dots$$

$$n = 1, 2, 3, \dots$$

Thus we get two infinite sets of homogeneous equations in the unknowns B_{ij} . The non-dimensional parameters involving μ and p can be found from the condition that the two infinite determinants of coefficients shall vanish for non-trivial solutions.

3. Plate with a single concentrated mass M .

We get this case by putting $K_s = c = \mu = 0$ in the above equations. The set of equations (10) vanishes identically and the set (9) reduces to

$$\sum_{i=1}^{\infty} \sum_{j=1}^{\infty} E_{ij} \left[C_{ij}^{mn} - \lambda (\delta_{ij}^{mn} + \frac{M}{M_p} E_{ij}^{mn}) \right] = 0 \quad (11)$$

$$m = 1, 2, 3, \dots$$

$$n = 1, 2, 3, \dots$$

Numerical work has been carried out for the case of a square clamped plate with a concentrated mass at centre. Considering only symmetric vibrations, the beam functions selected are

$$X_m = \frac{\cosh a_m x}{\cosh a_m a} - \frac{\cos a_m x}{\cos a_m a}$$

$$Y_n = \frac{\cosh \beta_n y}{\cosh \beta_n b} - \frac{\cos \beta_n y}{\cos \beta_n b} \quad (12)$$

The values of $a_m a$ and $\beta_n b$ are given in the Table-1, below.

TABLE 1

m	$a_m a = \beta_m b$
1	2.3650204
2	5.4978039
3	8.6393798
$m > 3$	$(4m-1) \frac{\pi}{4}$

Taking third order determinants, approximations to the first three symmetric modes have been given. The convergence has been studied by allowing the first order determinant, the second order determinant and the third order determinant to vanish successively. These calculations have been carried out for several values of M/M_p ratio and the results have been given in the figures 2 and 3. It was found that the convergence of the values for λ for the first mode is good. To obtain better values one will have to consider higher order deter-

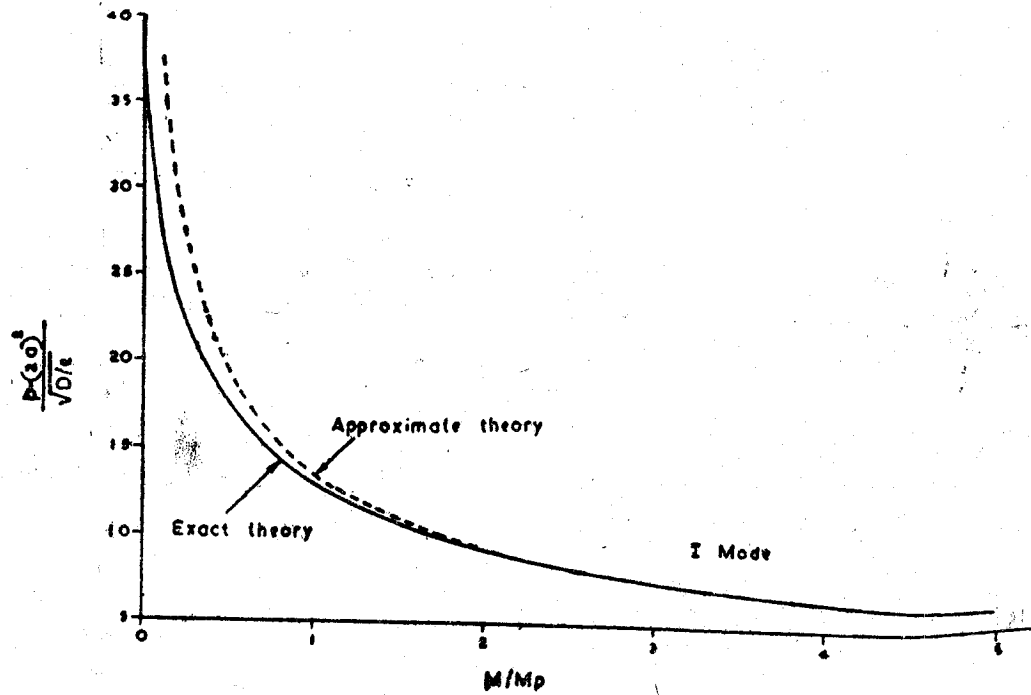


Figure 2

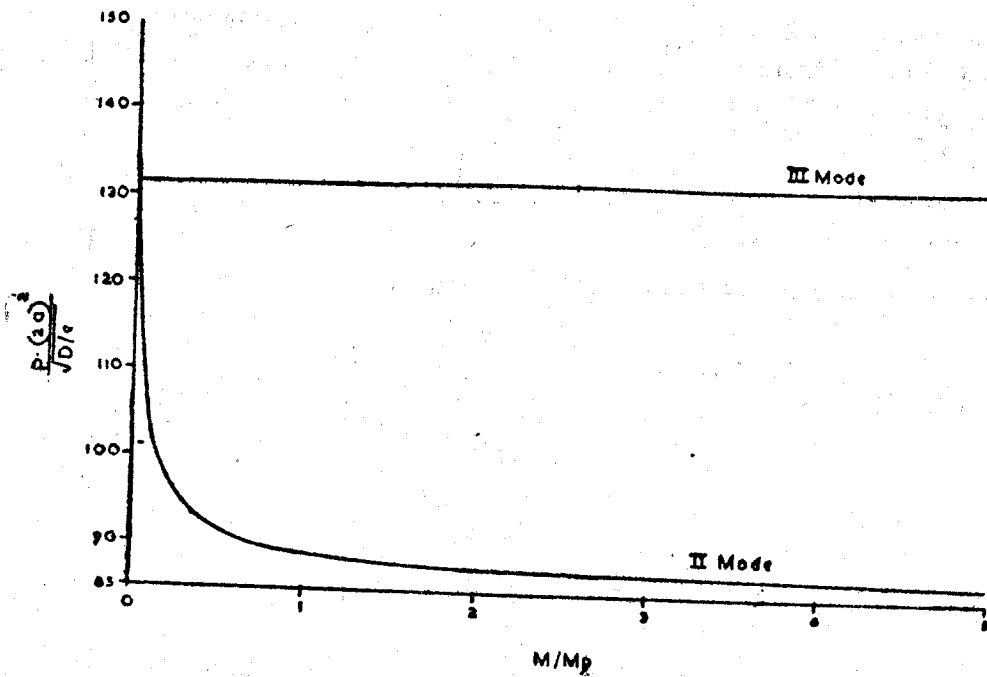


Figure 3

minants. It was also found that for $M/M_p = 0.0022$ values of λ for the second and third modes are equal. This happens because of the presence of a nodal point at the centre in the second mode of an ordinary plate without concentrated mass. The presence of mass leaves

the frequency of this mode unaffected while that of the third mode is reduced. Hence for values of $M/M_p > 0.0022$ the order of the modes get interchanged.

When the M/M_p ratio is very large it is customary to approximate the system by a single degree of freedom system for the first mode of vibration. In the approximation the plate is replaced by an equivalent spring having a spring constant K_p . This spring constant (Timoshenko Krieger 1959) K_p has a Value of $D/0.0224 a^2$ for a square plate of side $2a$. Using this we may write down the square of the circular frequency of the system as

$$p^2 = K_p/M = D/0.0224 Ma^2$$

This may be rewritten as

$$\frac{p \cdot (2a)^2}{\sqrt{D/\rho}} = \frac{13.4}{\sqrt{M/M_p}}$$

The variation of this frequency parameter has been presented in Fig. 2. in dotted lines. It may be noticed that for values of M/M_p greater than unity this approximate theory differs from the exact theory by less than 5 percent. The two frequencies become indistinguishable for M/M_p greater than 2.25.

4. Plate with a spring.

The solution for this case is obtained by putting c , μ and M equal to zero in the set of equations (9) and (10). The set (10) vanishes identically and the set (9) reduces to

$$\sum_{i=1}^{\infty} \sum_{j=1}^{\infty} B_{ij} \left[C_{ij}^{mn} - \frac{\rho p^2 a^2 b^2}{D} \delta_{ij}^{mn} + \frac{E_{ij}^{mn} ab}{4D} K_s \right] = 0 \quad (13)$$

$$m = 1, 2, 3, \dots$$

$$n = 1, 2, 3, \dots$$

Again putting $K_p = \frac{D}{0.0224 a^2}$ this set can be written as

$$\sum_{i=1}^{\infty} \sum_{j=1}^{\infty} B_{ij} \left[C_{ij}^{mn} - \frac{\rho p^2 a^2 b^2}{D} \delta_{ij}^{mn} + E_{ij}^{mn} \frac{b}{a} \cdot \frac{K_s}{K_p} \cdot \frac{1}{0.0896} \right] = 0 \quad (14)$$

$$m = 1, 2, 3, \dots$$

$$n = 1, 2, 3, \dots$$

Here again we obtain an infinite determinant and the approximation to λ are determined as described in Art. 3. The numerical calculations have been carried out for a square plate with a spring at the centre, considering symmetric vibrations just as in Art. 3. The results are given in Fig. 4. It may be noticed that the centre of the plate happens to be a nodal point for the second mode.

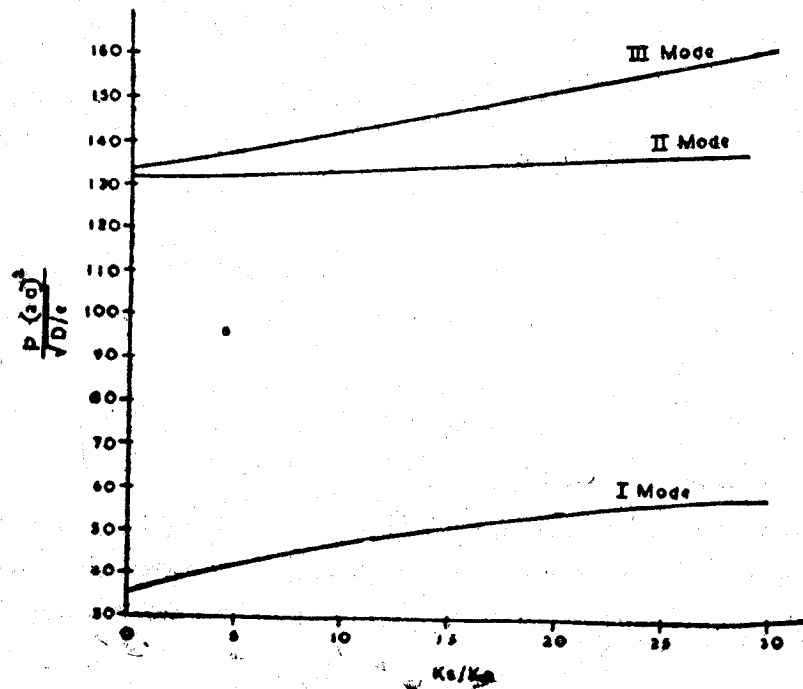


Figure 4

5. Plate with a dashpot

We obtain this case by putting M and K_s equal to zero. The following non-dimensional parameters have been introduced for convenience.

$$\lambda_1 = \frac{\rho(\mu^2 - p^2) a^2 b^2}{D}, \quad X = \frac{c \mu a b}{4D}$$

$$\bar{\lambda}_1 = \frac{2\mu p \rho a^2 b^2}{D}, \quad \bar{X} = \frac{c p a b}{4D} \quad (15)$$

We now obtain the infinite sets of homogeneous equations from (9) and (10)

$$\sum_{i=1}^{\infty} \sum_{j=1}^{\infty} B_{ij} \left[C_{ij}^{mn} + \lambda_1 \delta_{ij}^{mn} - X E_{ij}^{mn} \right] = 0 \quad (16)$$

$$m = 1, 2, 3, \dots$$

$$n = 1, 2, 3, \dots$$

and

$$\sum_{i=1}^{\infty} \sum_{j=1}^{\infty} B_{ij} \left[\bar{\lambda}_1 \delta_{ij}^{mn} - \bar{X} E_{ij}^{mn} \right] = 0 \quad (17)$$

$$m = 1, 2, 3, \dots$$

$$n = 1, 2, 3, \dots$$

From the relations (15) we have

$$\frac{\rho (\mu + ip)^2 a^2 b^2}{D} = \lambda_1 + i \bar{\lambda}_1 \quad (18)$$

and

$$(\mu + ip)^2 = \frac{16 D^2}{c^2 a^2 b^2} (X + i \bar{X})^2 \quad (19)$$

Using (19) in (18) we get

$$\lambda_1 = \frac{16 \rho D}{c^2} (X^2 - \bar{X}^2) \quad (20)$$

$$\bar{\lambda}_1 = \frac{32 \rho D}{c^2} X \bar{X} \quad (21)$$

The values of $\bar{\lambda}_1$, λ_1 , X and \bar{X} must now be determined such that the determinants corresponding to (16) and (17) vanish and the relations (20) and (21) are satisfied. The numerical labour in such a determination is quite involved and would require the use of a digital computer.

REFERENCES

- Das, Y.C. and D.R. Navaratna (1963), "Vibrations of a Rectangular Plate with Concentrated Mass, Spring and Dashpot", *Journal of Applied Mechanics*, Vol. 30, March 1963, P.31.
- Timoshenko, S.P. and W. Krieger (1959), "Theory of Plates and Shells", McGraw-Hill, New York, 1959, P.206.
- Wah, T. (1961), "Natural Frequencies of Plate-mass Systems", *Proceedings, Seventh Congress on Theoretical and Applied Mechanics*, Bombay, Dec. 1961, P. 157.
- Young, D. (1948), "Vibration of a Beam with Concentrated Mass, Spring and Dashpot", *Journal of Applied Mechanics*, Vol. 15, March 1948, P. 265.

DESIGN OF DISPLACEMENT PICKUPS

A.R. Chandrasekaran* and B.L. Mehrotra**

SYNOPSIS

This paper deals with the design and fabrication of a seismic displacement pickup.

INTRODUCTION

Vibration pickups are required in connection with instrumentation of various research projects currently planned to be executed at the Earthquake Engineering Laboratory at Roorkee. The principles of design of such pickups are well known. These pickups are now commercially available in foreign countries. Taking into account the following factors, namely, availability of materials locally, ease of fabrication in large numbers, simple auxiliary instrumentation and ease of calibration, a pickup has been designed and fabricated at the Earthquake Engineering Laboratory at Roorkee. This paper describes the details of the pickup.

PRINCIPLES OF DESIGN

In the variety of applications where pickups would be used, more often than not, a fixed reference would not be available for measurement of absolute motion. Therefore a seismic type pickup is chosen in which the relative motion between the mass and the support could be made proportional to the motion of the support (for a particular range of frequencies).

From the equation of motion of a seismic pickup, it can be shown that (Myklestad, 1956)

$$Z = y_0 \eta^2 \mu \sin(\omega t + \alpha)$$

where Z = relative displacement between the mass and the support

y_0 = maximum amplitude of the support which is assumed to move sinusoidally

η = ratio of forcing frequency to the natural frequency of the system

μ = dynamic magnification factor

$$= \frac{1}{[(1-\eta^2)^2 + (2\eta \zeta)^2]^{\frac{1}{2}}}$$

* Reader in Civil Engineering, School of Research and Training in Earthquake Engineering, University of Roorkee, Roorkee

** Senior Fellow, (Ministry of Education, Govt. of India) University of Roorkee, Roorkee.

- ζ = damping in the system expressed as a fraction of critical damping
 ω = forced frequency of the support
 t = time
 α = phase difference between relative motion Z and base motion y

Figures 1 and 2 show respectively the frequency response and phase response curves. It can be observed that $|Z|$ is almost equal to y_0 for η greater than 4.00 and ζ between 0.00 and 0.70.

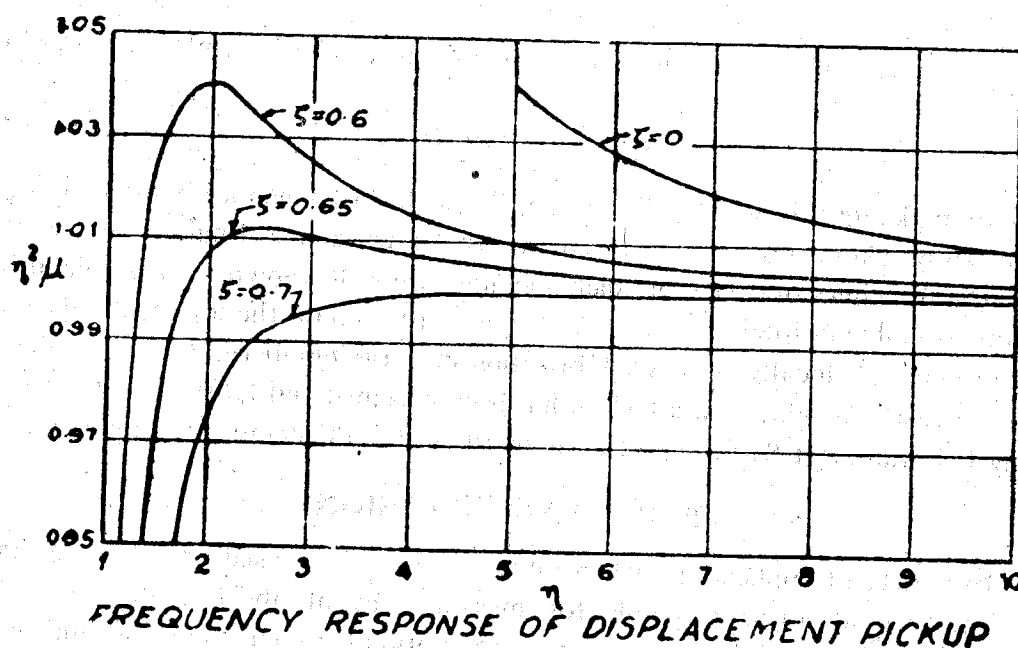


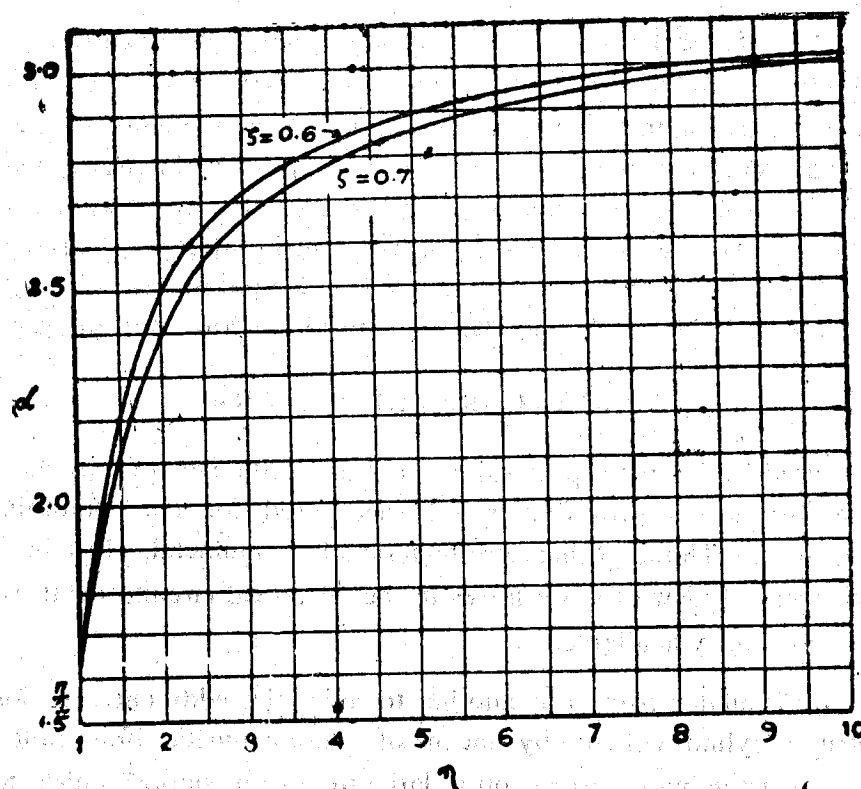
Figure 1

Displacement pickups cannot have flat frequency response below their natural frequency. The size and weight of the pickup increases with decrease in natural frequency of the pickup. Therefore the natural frequency has to be chosen as a compromise between the size of the pickup and the low frequency response. The natural frequency that is adopted is 4.5 c.p.s.

If the damping is zero, there would be no phase distortion. However, zero damping is not advisable, as the pickups would pass through resonance every time it operates. If η is large, phase distortion is negligible for damping, (ζ), between 0.00 and 0.70. A damping of 0.15 has been adopted in this case.

MEASUREMENT OF RELATIVE DISPLACEMENT

Of the various methods of measurement, 'Electrical Gauging' in which the mechanical quantity is converted into an equivalent electrical quantity, is best suited for vibration pickups. The various methods of measuring relative displacement have been discussed in detail by Mehrotra (1964), where it is concluded that linear variable differential transformer (L.V.D.T.) type is most suitable for displacement pickups.



PHASE RESPONSE OF DISPLACEMENT PICKUP

Figure 2

PRINCIPLE OF L.V.D.T.

The output of L.V.D.T. depends upon the mutual inductance between a primary and secondary coil. The basic components are shown in fig. 3. It consists of a core of magnetic

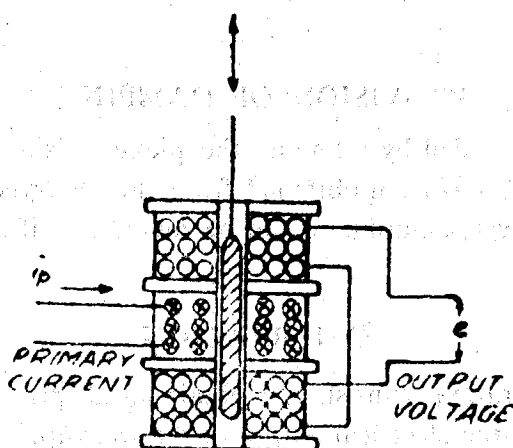


Figure 3

material, a primary coil and two secondary coils. The centre coil is energised with alternating

current. This causes a magnetic flux to be produced, linking the centre coil (primary) with each of the others (secondaries). The secondaries are connected such that the voltages induced in them by mutual inductance oppose each other. As the core is moved up or down, the inductance and induced voltage of one secondary coil are increased while those of the other are decreased. The output voltage is the difference between two induced voltages. For some core position, the voltages balance and the combined output of the secondary combination is very very small. This position is called the balance point. In this type of transducer, the output voltage is proportional to the displacement of the core over an appreciable range.

L.V.D.T. CORE PREPARATION

The core used in the pickup consists of a large number of circular discs of $15/32$ " diameter. These discs are cut out of a metal sheet used for core stampings in the audio frequency transformers. Though other core materials like Mumetal, dustcore etc., are more efficient from the point of view of lesser losses in the electrical circuit, metal sheets have been used because they are easily available.

The discs are insulated from one another to minimize eddy current loss and are kept in position to form a cylindrical core by means of a nonmagnetic brass bolt passing tightly through them. This assembly is turned on a lathe to give a smooth finish to the core. As the desired small size of the pickup and a particular ratio of length to diameter of the effective core does not allow a larger effective core size, additional brass and lead attachments had to be provided to bring the core weight to 0.24 lbs. so as to get the desired natural frequency.

DETAILS OF SPRING

A helical spring of rectangular cross section was found to give the least value of spring constant in conjunction with small size. The designed spring is also given a hardening treatment to increase its ductility.

PROVISION OF DAMPING

Damping has been provided by filling up the pickup casing with thin transformer oil. A damping value (ζ) of 0.15 has been obtained from the observed frequency response curve for forced vibration. However, damping could be increased, if necessary, by using a more viscous oil.

CALIBRATION

The process of calibration consists in obtaining a proper relationship between the quantity to be measured and the electrical output of the pickup. In this case, the electrical output is a voltage and the mechanical input is a displacement.

The fabricated pickup has been calibrated for the following conditions :

(i) Static Calibration—"Pickup Open"

- (ii) Dynamic Calibration—"Pickup Open"
that is undamped
- (iii) Dynamic Calibration—"Pickup Closed"
that is damped.

Figures 4 to 7 give the calibration curves

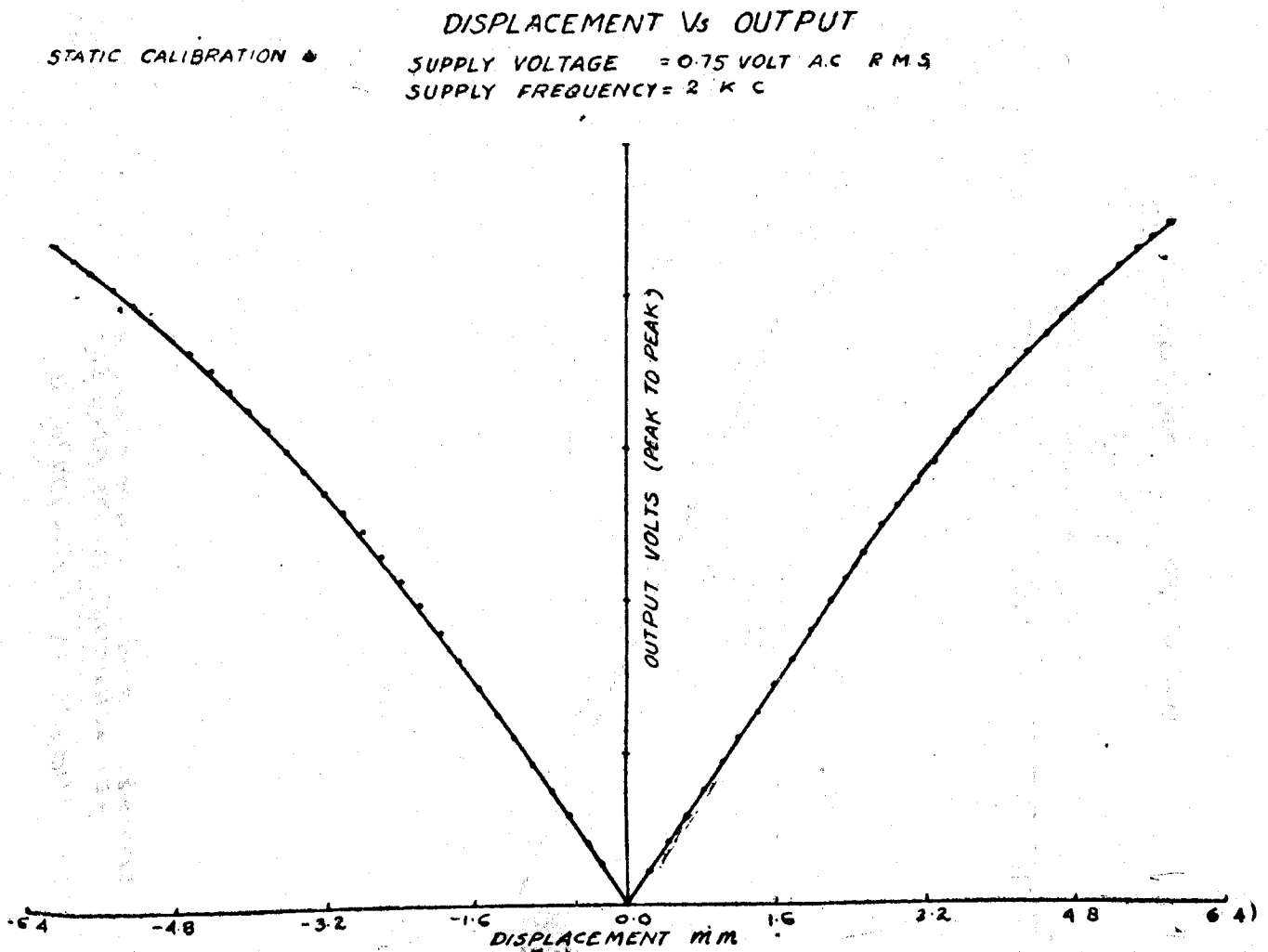


Figure 4

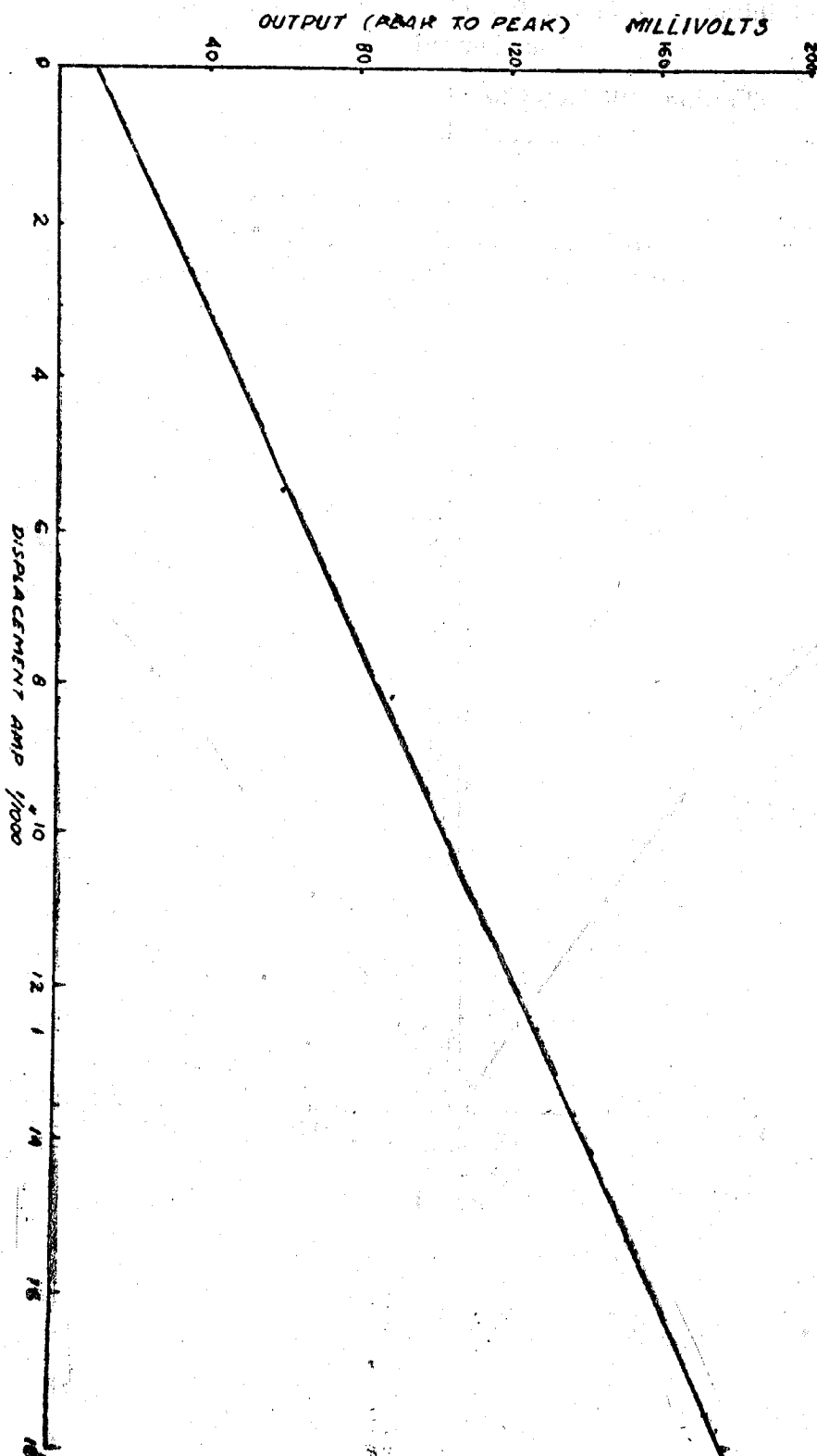
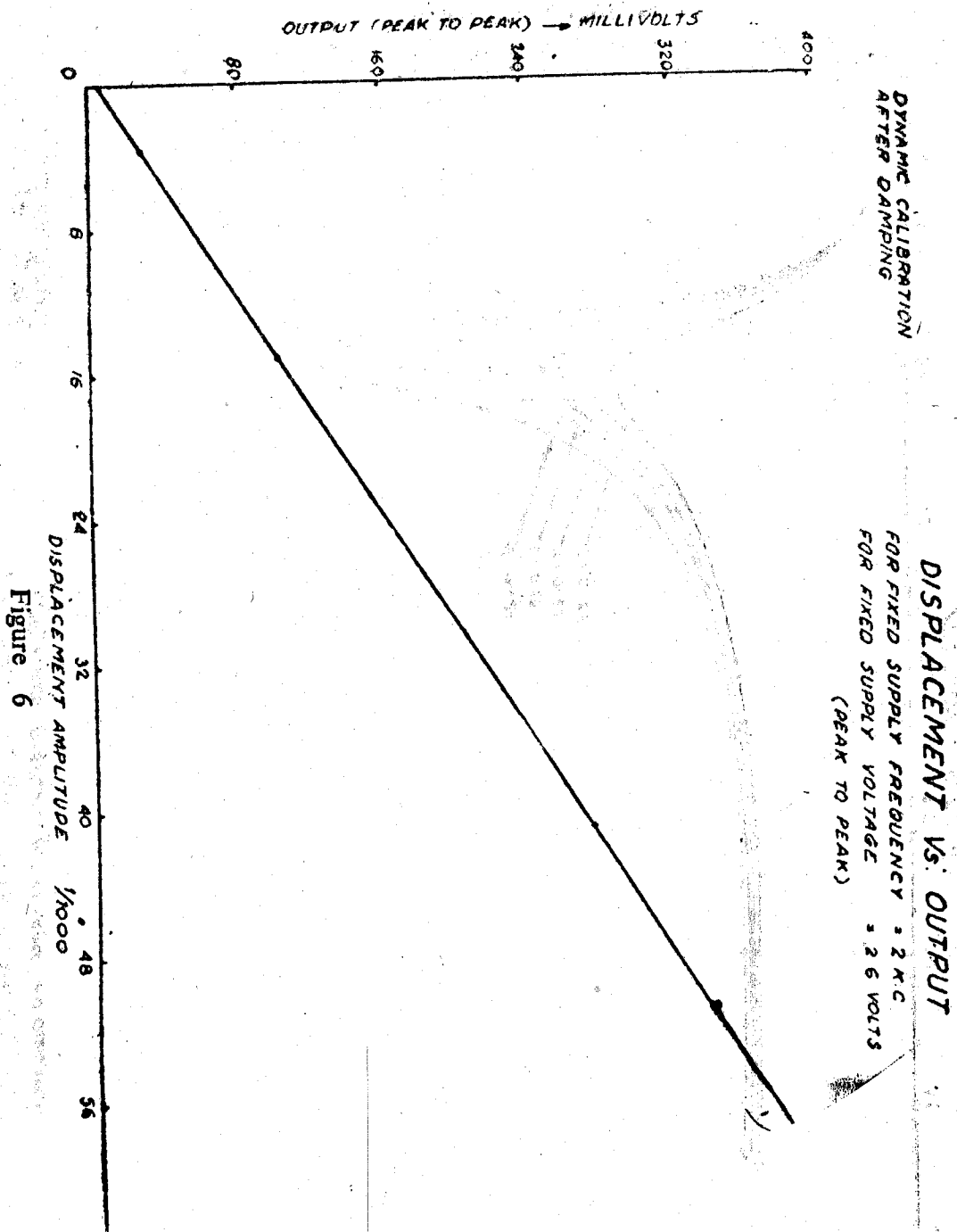


Figure 5

Note:—Voltage measured peak to peak



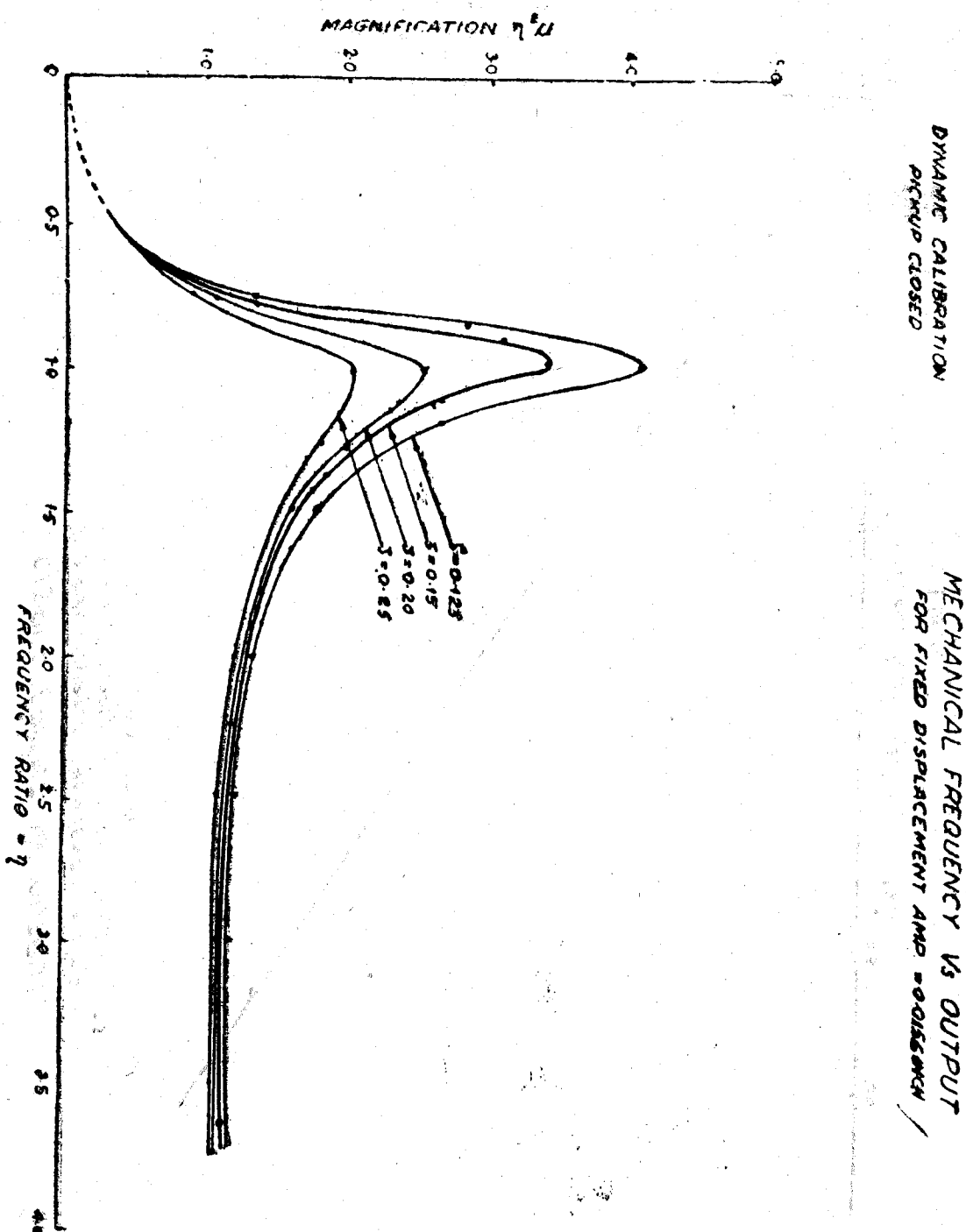
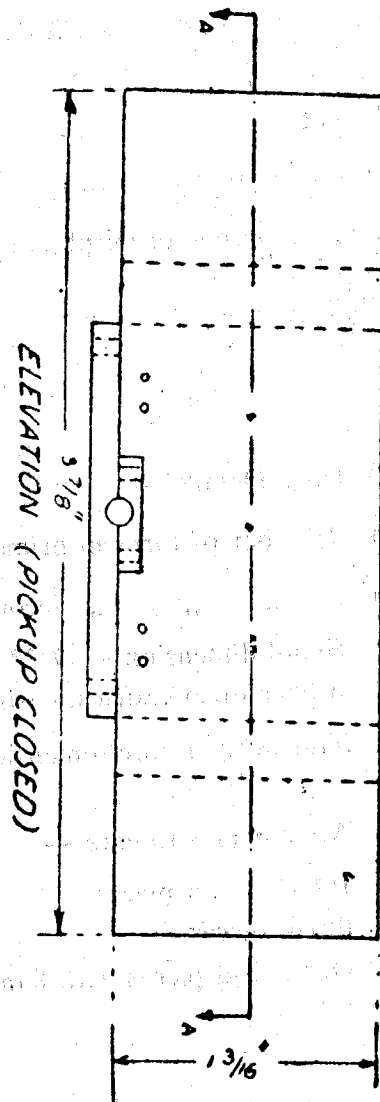


Figure 7

L.V.D.T. TYPE SEISMIC DISPLACEMENT PICKUP



(ATTACHMENTS)

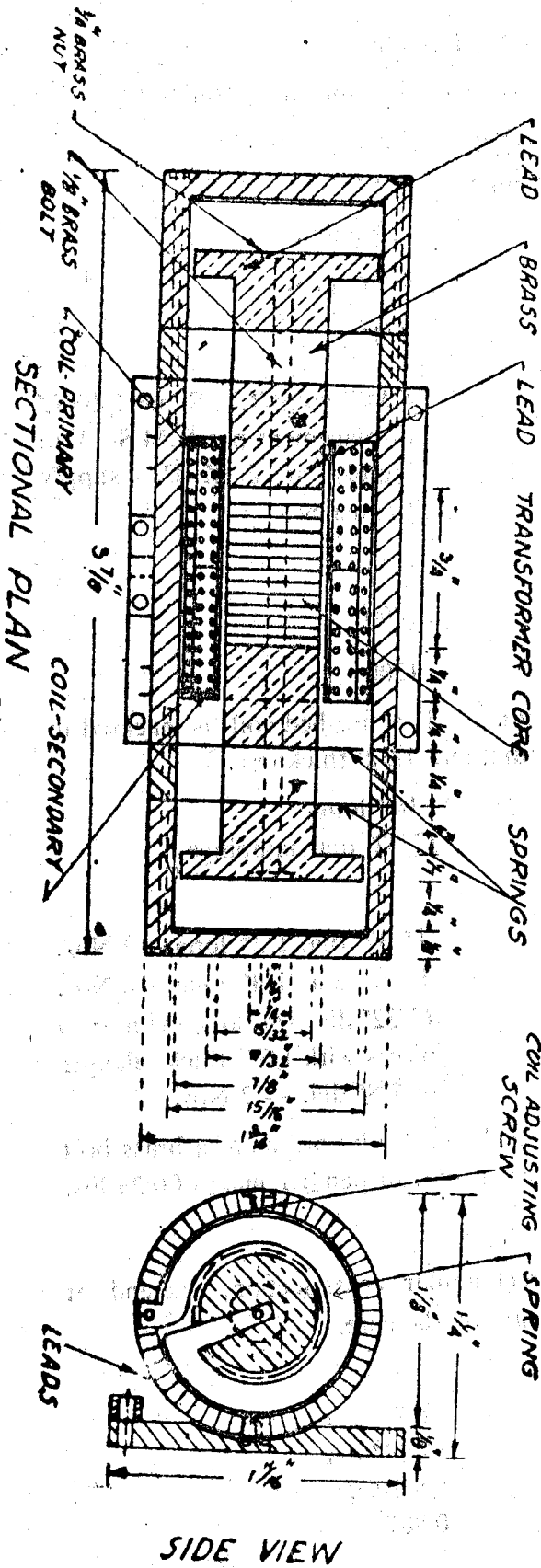


Figure 8

SPECIFICATIONS OF THE PICKUP

Figure 8 gives details of the pickup. The detailed specifications are as follows :

- (i) The overall size of the Pickup is —(a) length — $3\frac{1}{8}"$
 (b) diameter — $1\frac{3}{16}"$
- (ii) Weight ... 0.505 lbs.
- (iii) Natural frequency ... 4.5 c. p. s.
- (iv) Max. Amplitude of Displacement ... $1/4"$
- (v) Calibration factor ... 4 Millivolts R.M.S. per $1/1000"$ displacement per R.M.S. Volt supply at 2 K. C. supply frequency.
- (vi) L.V.D.T. Details —
- (a) Number of turns in primary... 400
- (b) " " " Secondary 1200
- (c) Spool dimensions— $17/32"$ bore,, $1\frac{1}{4}"$ long. The finished coil is encased in a bakelite cylindrical casing of $15/16"$ dia. and $1/32"$ thickness.
- (d) Transformer core dimensions $3/4"$ long.
 $15/32"$ dia stampings
- (e) Attachments to core —
- | | |
|--------------------------------|-----------------------------------------------------------------------------------------------|
| Interior lead pieces | $15/32"$ dia: $1/2"$ long —2 Nos. |
| Brass pieces | $15/32"$ dia. $1/4"$ long —2 Nos. |
| Outer lead pieces with flanges | $15/32"$ dia $1/4"$ long cylindrical pieces with $1/7"$ thick flanges of $7/8"$ dia. — 2 Nos. |

The core stampings and all the attachments being tied together by means of a brass bolt of $1/8"$ dia. with $1/4"$ dia. nuts at either ends. This makes a total suspended mass of 0.24 lbs.

(vii) Spring Details—

The core is suspended on four helical springs of rectangular cross section, one end of which is fixed to the casing and the other, fixed to the centre of the core.

The spring dimensions are—

Outer diameter	$7/8"$ dia
Inner diameter	$47/72"$ dia
Thickness of spring	$5.5/1000"$
Number of turns	0.887

(viii) Housing details:—

The entire assembly with the coil is housed in a cylindrical sleeve of 15/16" inner diameter and 1/8" thick walls. The sleeve is made into five parts as shown in figure 8 so as to allow for proper placing of springs and to allow for ease in repairs. Adequate keys and screws are provided to make the assembly leak proof. A coil-adjustment screw is provided which when tied fixes the coil at a desired balanced position.

(ix) Damping—

Two holes are provided for filling thin transformer oil which provides viscous damping value of 0.15.

Rubber stops at the end walls are provided to absorb shocks and prevent damage to the springs.

PERFORMANCE OF THE PICKUP

The linear behaviour of the transfer characteristics with respect to more or less all the involved parameters as seen from the characteristic curves indicates that the pickup performs satisfactorily. The auxiliary instrumentation necessary for recording the output is an audio frequency oscillator, an A.C. Amplifier, a phase sensitive demodulator and an oscilloscope. These equipments are of standard variety and should be available in any instrumentation laboratory. Knowing the natural frequency of the pickup, the calibration could always be checked even in the sealed condition, by giving a known tilt to the pickup.

ACKNOWLEDGEMENT

Dr. Jai Krishna, Professor and Director of Earthquake School, Roorkee gave active encouragement to this research project. Mr. A.P. Sharma and Mr. L. Chand of Earthquake School are responsible for the fabrication of the pickup.

REFERENCES

- Mehrotra, B.L., (1964) "Study of Displacement Pickups", M. E. Thesis, University of Roorkee, Roorkee.
- Myklestad, N.O., (1956) "Fundamentals of Vibration Analysis", McGraw Hill Book Co., New York, N.Y.

STUDY OF SHEAR BEAMS UNDER DYNAMIC LOADS

A. R. Chandrasekaran*

SYNOPSIS

Beams in which deformations due to a load are essentially due to shearing action are known as 'Shear Beams'. In practice, cantilever beams of very large cross sectional area and of small length have predominantly shear deformation. Such type of structures, however, would have very high natural frequency and therefore would be very little affected by ground motion.

The equation of motion of a shear structure is of second degree and so is the equation of motion of multistoreyed framed structure. Therefore, there is a possibility that cantilever shear beams could be theoretical models of multistoreyed structures. In this paper, it is proposed to study shear beams and compare them with multistoreyed frames.

1. Basic Equations of the Problem

The following assumptions are made in solving the problem: The material of which the beam is made is homogeneous, isotropic and behaves elastically. The deformations are in shear only.

Considering the equilibrium of elastic and inertia forces, (adopting the procedure outlined by Rogers (1959)).

$$V = -\sigma'AG \frac{\partial y}{\partial x} \quad 1.1^\dagger$$

$$\frac{\partial V}{\partial x} = -\rho A \frac{\partial^2 y}{\partial t^2} + w(x, t) \quad 1.2$$

From 1.1 and 1.2

$$-\frac{\partial}{\partial x} \left(\sigma'AG \frac{\partial y}{\partial x} \right) = -\rho A \frac{\partial^2 y}{\partial t^2} + w(x, t) \quad 1.3$$

* Reader in Civil Engineering, School of Research and Training in Earthquake Engineering, University of Roorkee, Roorkee (India).

† The letter symbols adopted for use in this paper are defined and are listed alphabetically in the Appendix.

FREE VIBRATION

For the free vibration problem, $w(x,t)$ will be equal to zero. If a harmonic solution in time, with circular frequency p , is assumed, then equation 1.3 reduces to

$$\frac{d}{dx} \left(\sigma' A G \frac{dy}{dx} \right) + \rho A p^2 y = 0 \quad 1.4$$

The solution of equation 1.4 would give the frequencies p_r and corresponding mode shapes $\phi_r(x)$. Since a beam has infinite degrees of freedom, there will be infinite frequencies.

In general, the free vibration solution has the form

$$y(x,t) = \sum_{r=1}^{\infty} \phi_r(x) \cdot D_r \cdot \sin(p_r t + \phi_r) \quad 1.5$$

GROUND MOTION EXCITATION

For ground motion excitation,

$$w(x,t) = \rho(x) \cdot A(x) \cdot a(t) \quad 1.6$$

Substituting 1.6 in 1.3 and if Z represents relative displacement, with respect to the base, at any section x , then

$$-\frac{\partial}{\partial x} \left(\sigma' A G \frac{\partial Z}{\partial x} \right) = -\rho(x) \cdot A(x) \cdot \frac{\partial^2 Z}{\partial t^2} + \rho(x) \cdot A(x) \cdot a(t) \quad 1.7$$

$$\text{Let } Z(x,t) = \sum_{r=1}^{\infty} \phi_r(x) \xi_r(t) \quad 1.8$$

Substituting 1.8 in 1.7

$$-\sum_{r=1}^{\infty} \xi_r(t) \left\{ \frac{d}{dx} \left(\sigma' A G \frac{d\phi_r}{dx} \right) \right\} = -\sum_{r=1}^{\infty} m(x) \cdot \ddot{\xi}_r(t) \cdot \phi_r(x) + m(x) \cdot a(t) \quad 1.9$$

where $m(x)$ has been taken equal to $\rho(x) \cdot A(x)$.

From 1.4 and 1.8,

$$\sum_{r=1}^{\infty} \left\{ \frac{d}{dx} \left(\sigma' A G \frac{d\phi_r}{dx} \right) \right\} \xi_r(t) = -\sum_{r=1}^{\infty} m(x) \cdot p_r^2 \cdot \phi_r(x) \cdot \xi_r(t) \quad 1.10$$

combining 1.9 and 1.10,

$$\sum_{r=1}^{\infty} (\ddot{\xi}_r + p_r^2 \xi_r) \cdot m(x) \cdot \phi_r(x) = m(x) \cdot a(t) \quad 1.11$$

Expressing the right hand side of 1.11, in terms of mode functions, $\phi_r(x)$, and making use of the relationship of orthogonality of modes, namely

$$\int_0^H m(x) \cdot \phi_r(x) \cdot \phi_s(x) \cdot dx = 0 \text{ for } r \neq s \text{ and}$$

$$m(x) \cdot a(t) = \sum_{r=1}^{\infty} a(t) \cdot m(x) \cdot \phi_r(x) \cdot \frac{\int_0^H \phi_r(x) \cdot m(x) \cdot dx}{\int_0^H (\phi_r(x))^2 \cdot m(x) \cdot dx} \quad 1.12$$

from 1.11 and 1.12

$$\ddot{\xi}_r + p_r^2 \xi_r = a(t) \cdot \frac{\int_0^H \phi_r(x) \cdot m(x) \cdot dx}{\int_0^H (\phi_r(x))^2 \cdot m(x) \cdot dx} \quad 1.13$$

The solution of 1.13 is

$$\xi_r = -\frac{1}{p_r} \int_0^t a(t) \cdot \frac{\int_0^H \phi_r(x) \cdot m(x) \cdot dx}{\int_0^H (\phi_r(x))^2 \cdot m(x) \cdot dx} \cdot \sin p_r(t-\tau) \cdot d\tau \quad 1.14$$

from 1.8 and 1.14

$$Z(x, t) = -\sum_{r=1}^{\infty} \frac{\phi_r(x)}{p_r} \cdot \frac{\int_0^H \phi_r(x) \cdot m(x) \cdot dx}{\int_0^H (\phi_r(x))^2 \cdot m(x) \cdot dx} \int_0^t a(t) \cdot \sin p_r(t-\tau) \cdot d\tau \quad 1.15$$

If there is damping in the system such that mode superposition is still applicable, then

$$Z(x, t) = -\sum_{r=1}^{\infty} \frac{\phi_r(x)}{p_{dr}} \cdot \frac{\int_0^H \phi_r(x) \cdot m(x) \cdot dx}{\int_0^H (\phi_r(x))^2 \cdot m(x) \cdot dx} \int_0^t a(t) \cdot e^{-\zeta_r p_r(t-\tau)} \sin p_{dr}(t-\tau) \cdot d\tau \quad 1.16$$

From 1.16, the maximum relative displacement at any section x , due to r^{th} mode of vibration could be expressed as

$$|Z_x^{(r)}| = -B_x^{(r)} \cdot \frac{1}{p_r} \cdot (S_v)_r \quad 1.17$$

From 1.1, the shear force, V , at any section x is,

$$V_x^{(r)} = \sigma' AG \frac{dZ_x^{(r)}}{dx} \quad 1.18$$

The bending moment, MT , at any section x , is

$$MT_x^{(r)} = \int_0^h V_x^{(r)} \cdot dx \quad 1.19$$

where h is measured from the free end.

2. Theoretical Solution

To find the effect of ground motion on a shear beam, its frequencies and mode shapes are to be determined. In certain cases, where the properties of the beam vary in a regular fashion along the beam, theoretical solutions are possible (Conway, 1948). Some of these cases are discussed below. Where theoretical solutions are cumbersome or impossible, numerical methods could be adopted with success.

Let the area of cross section 'A' be a function of the length of the beam, that is

$$A = f(x) \quad 2.1$$

Substituting 2.1 in 1.4

$$\frac{d^2 y}{dx^2} + \frac{f'(x)}{f(x)} \frac{dy}{dx} + \gamma^2 y = 0 \quad 2.2$$

where prime denotes differentiation and

$$\gamma^2 = \frac{\rho p^2}{\sigma' G} \quad 2.2a$$

UNIFORM BEAM

Here $f(x)$ is constant. Hence 2.2 reduces to

$$\frac{d^2 y}{dx^2} + \gamma^2 y = 0 \quad 2.3$$

For a cantilever beam with boundary conditions,

$$\left. \begin{array}{l} y=0 \text{ at } x=H \\ \text{and } \frac{\partial y}{\partial x}=0 \text{ at } x=0 \end{array} \right\} \text{ for all } t \quad 2.4$$

the frequency equation is given by

$$\cos \gamma H = 0 = \cos \frac{2r-1}{2} \pi \quad 2.5$$

$$\text{that is } \gamma H = \frac{2r-1}{2} \pi \quad 2.6$$

where $r=1,2,3 \dots \infty$

from 2.2a,

$$p_r = \frac{2r-1}{2} \cdot \frac{\pi}{H} \cdot \sqrt{\frac{\sigma' G}{\rho}} \quad 2.7$$

The mode shape is given by

$$\phi_r(x) = \cos \frac{(2r-1) \cdot \pi \cdot x}{2H} \quad 2.8$$

The general free vibration solution is given by

$$y(x,t) = \sum_{r=1}^{\infty} \left\{ D_r \cdot \sin(p_r t + \theta_r) \right\} \cdot \cos \frac{(2r-1) \cdot \pi \cdot x}{2H} \quad 2.9$$

NON-UNIFORM BEAM

Consider the case when

$$A=f(x)=A_0 \left(a + \frac{bx}{H} \right)^s \quad 2.10$$

where x is measured from free end and A_0 , a , b and s are constants.

Then 1.4 could be written as

$$\frac{d^2 y}{dx^2} + \frac{s \cdot b/H}{a + b(\frac{x}{H})} \cdot \frac{dy}{dx} + \gamma^2 y = 0 \quad 2.11$$

$$\text{Let } \gamma H \left(a + \frac{b}{H} x \right) = \psi \quad 2.12$$

then from 2.11 and 2.12,

$$\frac{d^2 y}{d\psi^2} + \frac{s}{\psi} \frac{dy}{d\psi} + y = 0 \quad 2.13$$

This is Bessel equation of order q where

$$q = \frac{1-s}{2}$$

The solution of 2.13 has the form

$$y(x) = D_1 \cdot J_q(x) + D_2 \cdot Y_q(x) \quad 2.14$$

In particular, consider the case when $s=2$. This corresponds to the case of linearly tapering beam, then

$$q = \frac{1-s}{2} = -\frac{1}{2}$$

$$\text{and } y(\psi) = D_1 \cdot J_{-\frac{1}{2}}(\psi) + D_2 \cdot J_{\frac{1}{2}}(\psi) \quad 2.15$$

$$= \frac{1}{\psi} (D'_1 \cos \psi + D'_2 \sin \psi) \quad 2.16$$

The boundary conditions for a cantilever beam are, for all t ,
at free end,

$$\{x=0; \psi=(\gamma H)^{a/b}\}$$

$$\frac{\partial y}{\partial x} = 0; \quad \frac{\partial y}{\partial \psi} = 0 \quad 2.17a$$

at built in end

$$\{x=H; \psi=\gamma H (1+a/b)\}$$

$$y=0$$

$$2.17b$$

Using boundary conditions and solving for arbitrary constants D_1' and D_2' , a frequency equation is obtained which is of the form

$$\tan \gamma H = -\gamma H \left(\frac{a}{b} \right) \quad 2.18$$

This is a transcendental equation and can be solved graphically.

For other cases of non-uniform beams, not covered by equation 2.10, the solution is cumbersome and numerical methods may be adopted.

3. Numerical Solution

If the variation of area $f(x)$ along the length of the beam is a complicated function, then the theoretical solution of equation 1.4 is practically ruled out. It is therefore desirable to adopt numerical techniques in solving such problems. If, however, a high speed computer is available, even simpler problems are better solved by numerical methods.

The method consists in replacing a continuous system with a discrete system by concentrating the mass distribution into an equivalent set of discrete point masses embedded in an ideal massless substance possessing the same elastic properties as the body simulated.

ERROR ANALYSIS OF THE NUMERICAL APPROACH

Errors are due to approximating an infinite degree of freedom system to a finite degree of freedom system and not due to the numerical technique involved. One type of error involves the number of masses used. The other type involves the determination of equivalent masses and stiffnesses.

To make an error analysis one should know the exact value of items under investigation. The errors in frequency would be investigated here for uniform cantilever shear beams for which exact theoretical solutions are available.

ERRORS IN FINDING EQUIVALENT MASSES

There are generally two procedures adopted in finding out equivalent masses. In one case, the mass of a segment is divided equally and concentrated at the ends (Fig. 3.1). In the other case, the mass is concentrated at the centre of a segment (Fig 3.2).

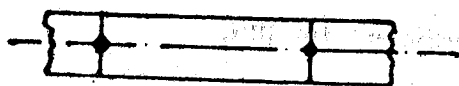


FIG 3.1

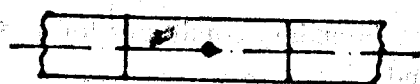


FIG 3.2

It has been shown (Duncan—1952) that for a uniform shear beam, if the mass points are located at midpoints of equal segments, the error in frequency varies inversely as the square of number of segments whereas if the masses are placed at the ends, the error varies as inverse first power of number of segments.

ERRORS DUE TO NUMBER OF SEGMENTS

In the case of shear beam in addition to having an exact solution for the continuous system, we also have an exact solution for the discrete system (Karman and Biot—1940).

For the continuous system, frequency parameter

$$\lambda_r = \frac{(2r-1)^2 \cdot \pi^2}{4} \quad 3.1$$

(λ is proportional to p^2)

For the discrete case, with mass points concentrated at the middle of segments

$$\lambda_{rn} = 2n^2 \left[1 - \cos \frac{(2r-1)\pi}{2n} \right] \quad 3.2$$

$$= \frac{(2r-1)^2 \pi^2}{4} - \frac{(2r-1)^4 \pi^4}{192n^2} + \text{small terms} \quad 3.2a$$

Here n is the number of segments

$$\text{Error } \epsilon_{rn} = \frac{\lambda_r - \lambda_{rn}}{\lambda_r} \quad 3.3$$

$$= \frac{(2r-1)^2 \pi^2}{48n^2} + \text{higher inverse powers of } n \quad 3.3a$$

This shows that the error in λ (that is, p^2) for any given mode ultimately varies inversely as the square of number of segments and that proportional error for a given n increases rapidly for higher harmonics. Fig. 3.3 shows a plot of ϵ_{rn} versus number of segments for the first four modes of vibration.

In the problems attempted by numerical method, n was chosen as 100. Even if n had been chosen as 40, it is seen that error would be negligible.

In the case of non-uniform beams, if the mass is assumed to be concentrated at the centre of gravity of the segments instead of at the middle of the segments, results obtained are extremely close to the exact values. (error in frequencies is less than 0.25% in all cases considered for this investigation). Even for the assumption that the mass is concentrated at the middle of the segments, the error in frequencies was less than 0.85% in all cases considered for this investigation.

HOLZER METHOD

This technique is very suitable to solve equations of this type numerically. Consider equations 1.1 and 1.2 and assume that a harmonic solution in time with frequency p is applicable. Then, for the free vibration problem

$$V = -\sigma'AG \frac{\partial y}{\partial x} \quad 3.4$$

$$\frac{dV}{dx} = mp^2 y \quad 3.5$$

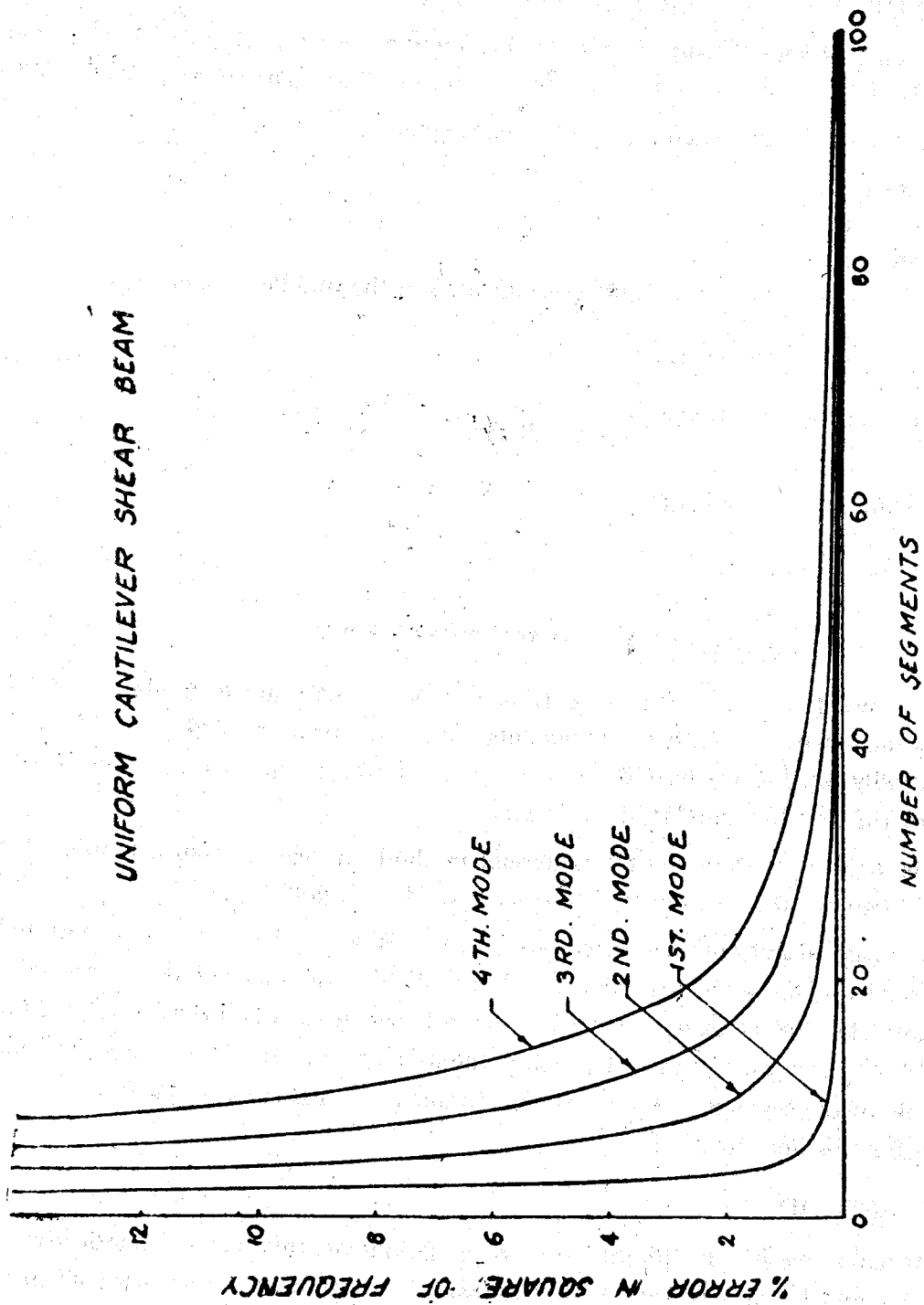


Figure 3.3

Let the beam be divided into a number of equal segments and one typical section of beam be as shown in fig. 3.4.

A finite change of shear force occurs at each mass which is equal to inertia force of mass

$$\Delta V = mp^2 y$$

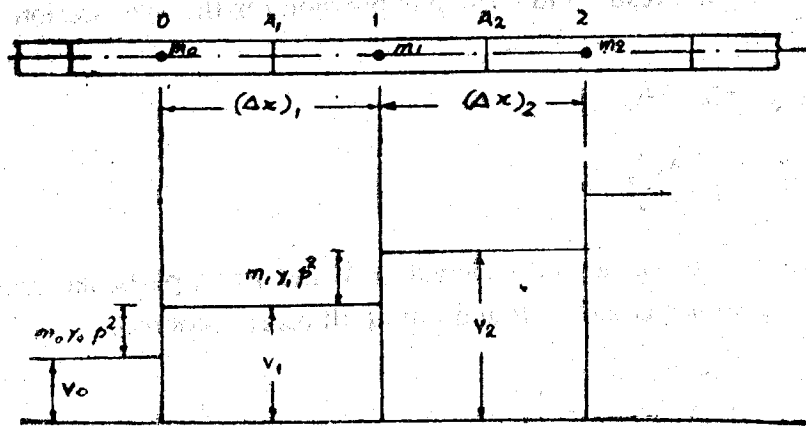


Figure 3.4

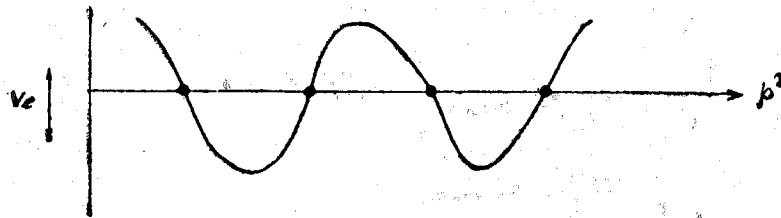


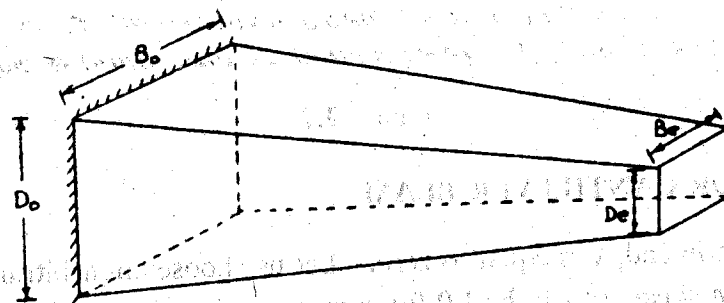
Figure 3.5

D_e/D_o = DEPTH RATIO OF THE BEAM

B_e/B_o = BREADTH RATIO OF THE BEAM

A_e/A_o = AREA RATIO OF THE BEAM

TAPER RATIO = (T.R.) = $D_e/D_o \cdot B_e/B_o \cdot \sqrt{A_e/A_o}$



VALUES OF T.R CHOSEN WERE 1.0, 0.8, 0.6, 0.4 AND 0.2

Figure 3.6

Assume that the quantities V_0 and y_0 are known at the left section. Then

$$V_1 = V_0 + m_0 p^2 y_0 \quad 3.7$$

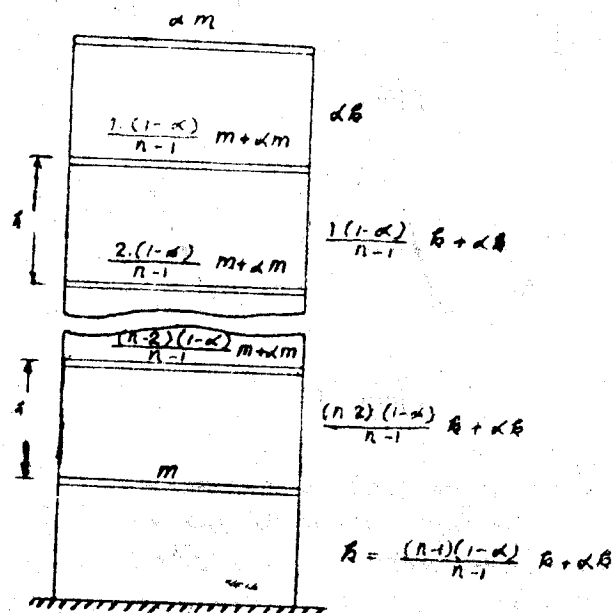
$$y_1 = y_0 - \left(\frac{V_1}{\sigma' A_1 G} \right) (\Delta x)_1 \quad 3.8$$

Generalising the result and writing expression for the n^{th} section in terms of values at $(n-1)^{\text{th}}$ section

$$V_n = V_{n-1} + m_{n-1} p^2 y_{n-1} \quad 3.9$$

$$y_n = y_{n-1} - \left(\frac{\Delta x}{\sigma' AG} \right)_n V_n \quad 3.10$$

Thus, for any frequency p , if the values V and y at a particular section is known, then the corresponding values could be found out at all other sections.



BUILDING MODEL WHERE MASS AND SPRING CONSTANT ARE ASSUMED TO VARY LINEARLY OVER HEIGHT OF BUILDING.

Figure 3.7

PROCEDURE FOR CANTILEVER BEAM

At the built in end, y is equal to zero. Let us choose an arbitrary value for p , say p' . First assume that a shear (it can be 1.0 for convenience) exists at the built-in-end and then evaluate the shear V_e at the free end. If the value of p' is such as to coincide with one of the natural frequencies of the system, then V_e should be zero.

In general, it would not be possible to guess the value of p correctly. However, various values could be arbitrarily assigned to p and then V_e evaluated. A plot of p^2 versus V_e would have a general appearance as in fig. 3.5. The correct value of p^2 are those which correspond to the intersection of the curve with the p^2 axis.

4. Specification of the Problems

Linearly tapering beams of the type shown in fig. 3.6 have been considered for dynamic analysis.

In all cases, the frequencies and responses of the beam like relative displacement with respect to the base, shear and moment at all sections due to ground motion have been calculated by the numerical method outlined above.

5. Discussion of Results

In practice; no beam would have predominantly shear deformations. However, shear beams could be theoretical models of multistoreyed framed structures as the equations of motion governing the behaviour of the two systems are analogous.

UNIFORM CASE

For a uniform multistoreyed framed structure, the frequency of vibration in the r^{th} mode is (Chandrasekaran-1963)

$$p_r = 2 \sqrt{k/m} \cdot \sin \frac{2r-1}{2n+1} \cdot \pi/2 \quad 5.1$$

For a uniform shear beam,

$$\text{the mass of the beam} = \rho A H \quad 5.2$$

considering the beam to be divided into n equal parts

$$\text{equivalent mass of element} = \frac{\rho A H}{n} \quad 5.3$$

$$\text{the spring constant of the beam} = \frac{A \sigma' G}{H} \quad 5.4$$

$$\text{equivalent spring constant element} = \frac{n A \sigma' G}{H} \quad 5.5$$

Substituting 5.3 and 5.5 in 5.1, and observing that as n is very large for the shear beam,

$$\sin \frac{2r-1}{2n+1} \frac{\pi}{2} \approx \frac{2r-1}{2n+1} \frac{\pi}{2}, \quad \text{then}$$

$$p_r = 2 \sqrt{\frac{n A \sigma' G}{H}} \times \frac{n}{\rho A H} \times \frac{2r-1}{2n+1} \frac{\pi}{2} \quad 5.6$$

$$= \frac{(2r-1)}{2} \times \frac{\pi}{H} \times \sqrt{\frac{\sigma' G}{\rho}} \quad 5.6a$$

Equation 5.6a is same as equation 2.7

NON-UNIFORM CASE

From 5.3, the variation of mass along the height for M.S.F.S. (multistoreyed framed

structure) should correspond to variation of ρA along the height for C.S.B. (cantilever shear beam). Similarly, from 5.5, the variation of spring constant along the height for M.S.F.S. should correspond to variation of $\sigma' G$ along the height for a C.S.B.

Consider building models for which the mass and stiffness varies linearly along the height and the linear variation is represented by parameter α (Refer fig. 3.7). If it is assumed that for an equivalent shear beam ρ and $\sigma' G$ remain constant over the height of the beam, then the variation of A should correspond to α . Since the variation of A is represented by $(T.R.)^2$, (refer fig. 3.6), α corresponds to $(T.R.)^2$.

COMPARISON OF M.S.F.S. AND C.S.B. FOR LINEARLY TAPERING CASES

Dynamic analysis has been carried out for M.S.F.S. (Chandrasekaran-1963). The natural frequencies of vibration and responses of the system like relative displacement with respect to the base, shear and moment at all sections due to ground motion have been calculated.

Also, dynamic analysis of C.S.B. has been carried out for various taper ratios. The various quantities could be expressed as follows:—

	M.S.F.S.	C.S.B.
Natural frequency in the r^{th} mode of vibration, p_r	$C_{1(r)} \cdot \sqrt{\frac{k}{m}}$	$C'_{1(r)} \cdot \frac{1}{H} \cdot \sqrt{\frac{\sigma' G}{E}} \cdot \sqrt{\frac{E}{\rho}}$
Relative Displacement at any section i , in the r^{th} mode of vibration, $Z_{1(r)}$	$C_{2(r)} \cdot \sqrt{\frac{m}{k}} \cdot S_v$	$C'_{21(r)} \cdot \sqrt{\frac{E}{\sigma' G}} \cdot \sqrt{\frac{\rho}{E}} \cdot H \cdot S_v$
Shear at any section i in the r^{th} mode of vibration, $V_{1(r)}$	$C_{31(r)} \cdot \sqrt{km} \cdot S_v$	$C'_{31(r)} \cdot \sqrt{\frac{\sigma' G}{E}} \cdot \sqrt{\frac{\rho}{E}} \cdot EA \cdot S_v$
Moment at any section i in the r^{th} mode of vibration, $MT_{1(r)}$	$C_{41(r)} \cdot \sqrt{km} \cdot h \cdot S_v$	$C'_{41(r)} \cdot \sqrt{\frac{\sigma' G}{E}} \cdot \sqrt{\frac{\rho}{E}} \cdot EA \cdot HS_v$

The following quantities of M.S.F.S. (multistoreyed framed structure) and C.S.B. (cantilever shear beam) are analogous to each other.

M.S.F.S.

m

k

α

C.S.B.

$$\frac{\rho A H}{n}$$

$$\frac{n \sigma' A G}{H}$$

$$(T.R.)^2$$

Figures 5.1 to 5.4 show respectively plots of p , Z , V and MT versus α . In all the cases, it is observed that a C.S.B. could be an analogous theoretical model of M.S.F.S.

COMPARISON OF M.S.F.S. - C.S.B NATURAL FREQUENCY

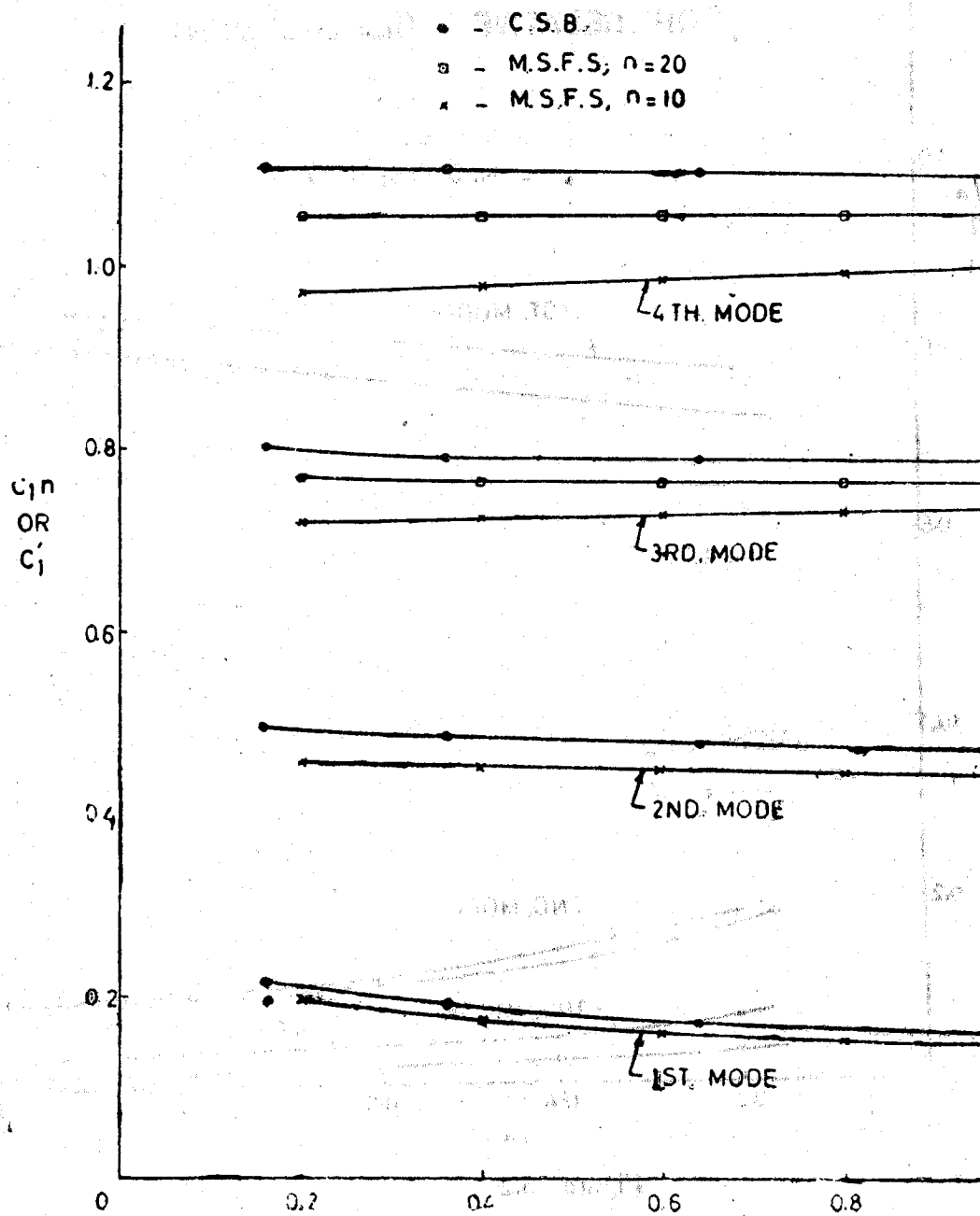


Figure 5.1

Figures 5.5 to 5.9 show plots of shear diagram. It is also observed that shear diagram for a C.S.B. is very close and similar to that of a corresponding shear diagram of M.S.F.S.

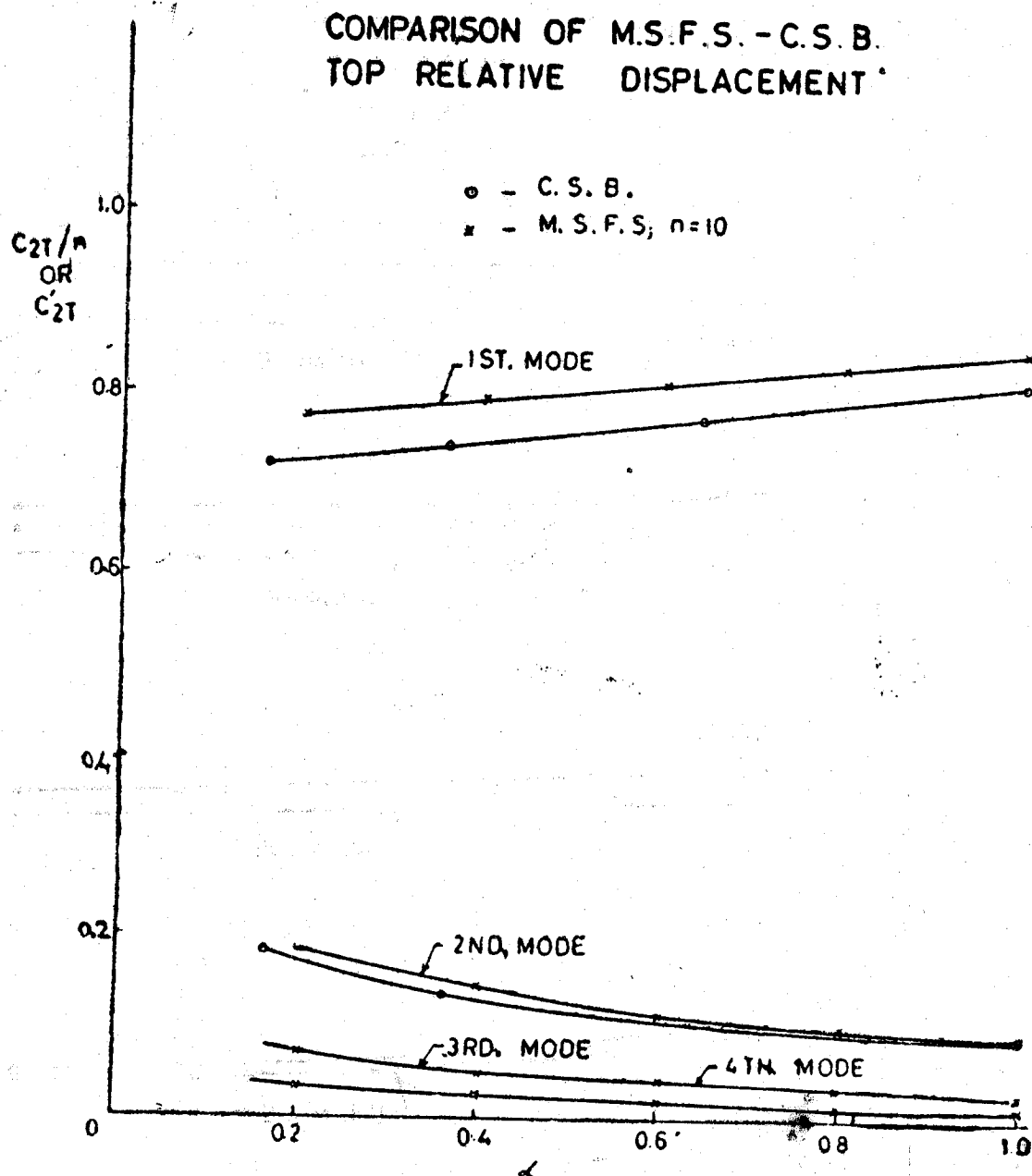


Figure 5.2

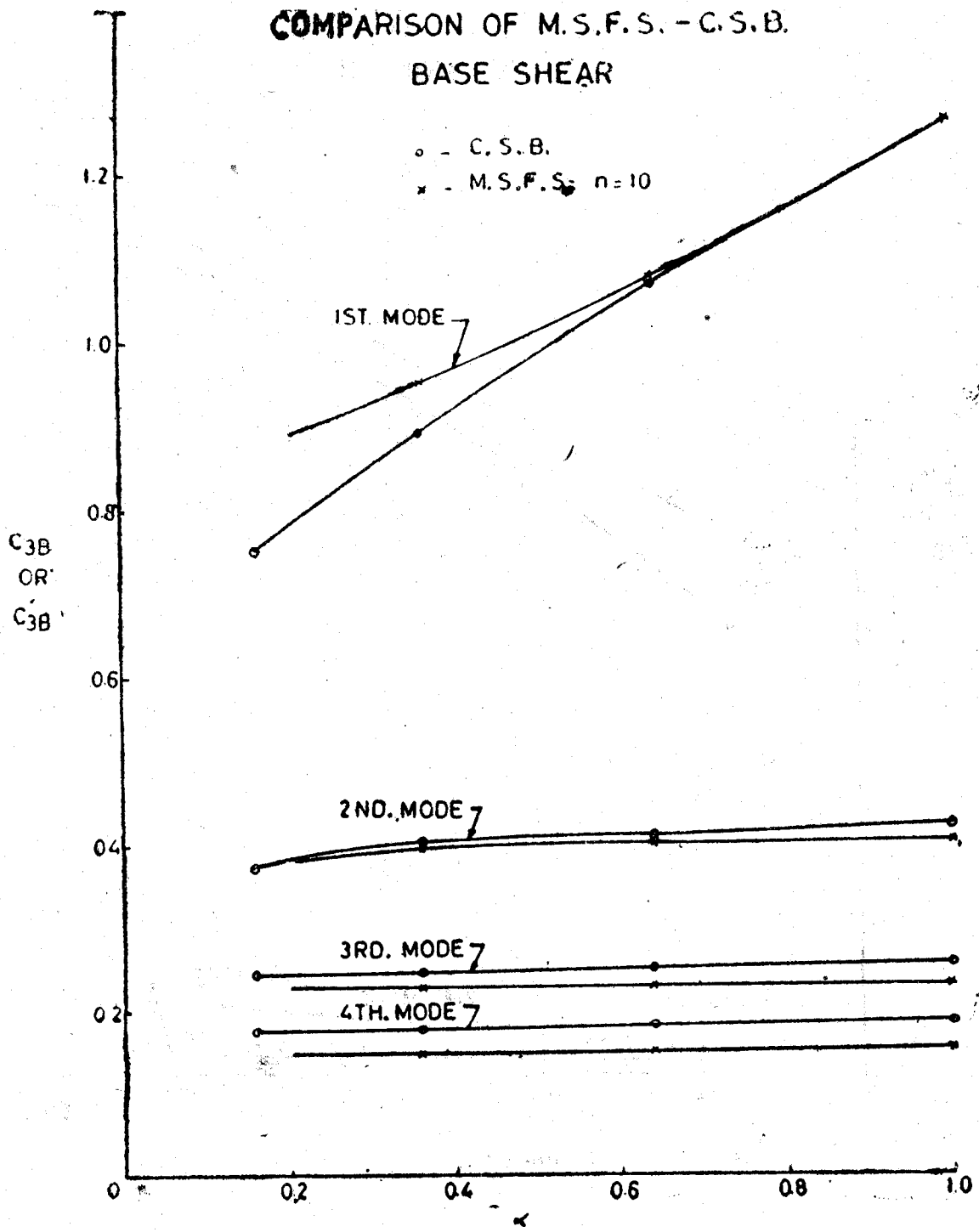


Figure 5.3

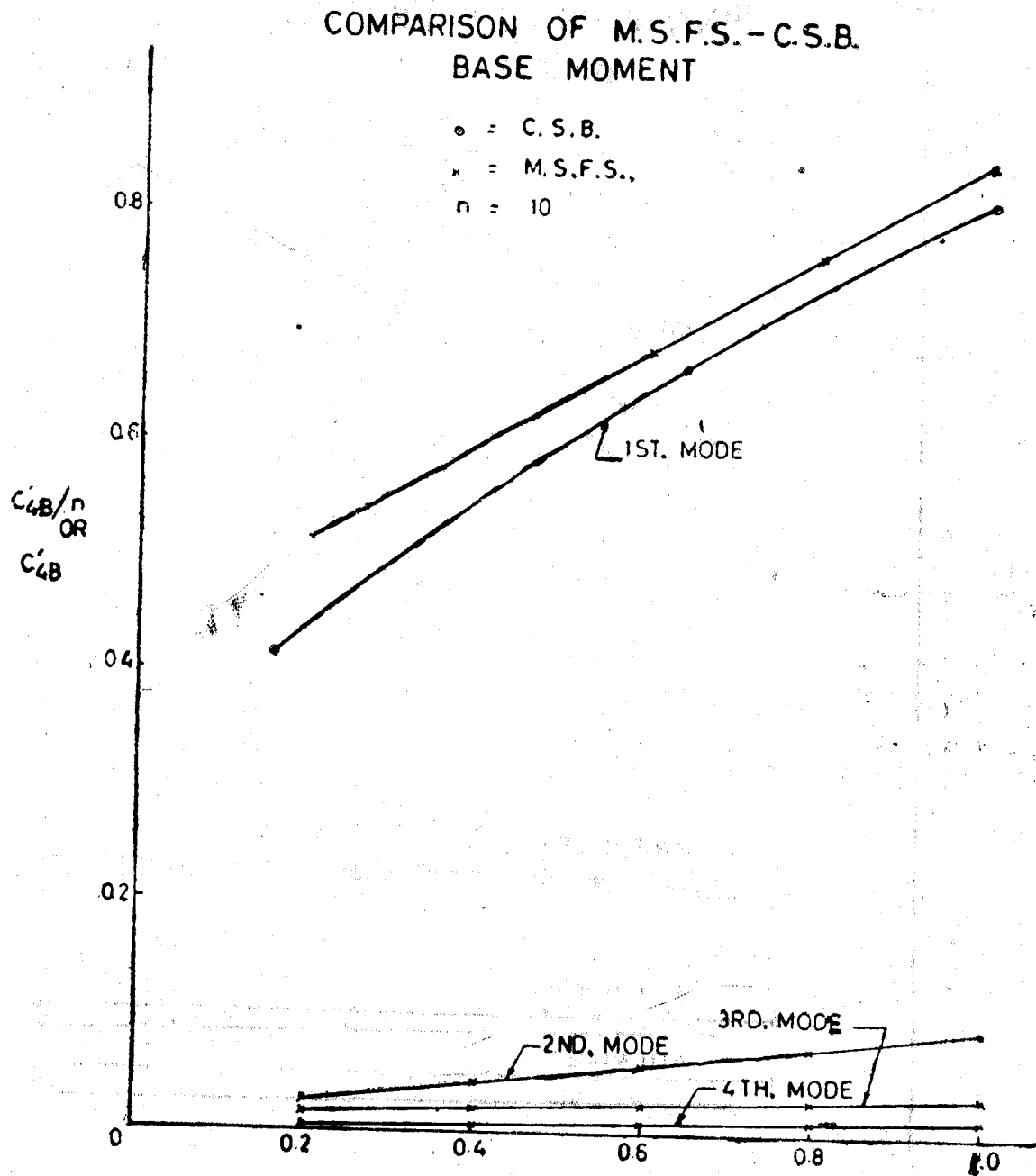


Figure 5.4

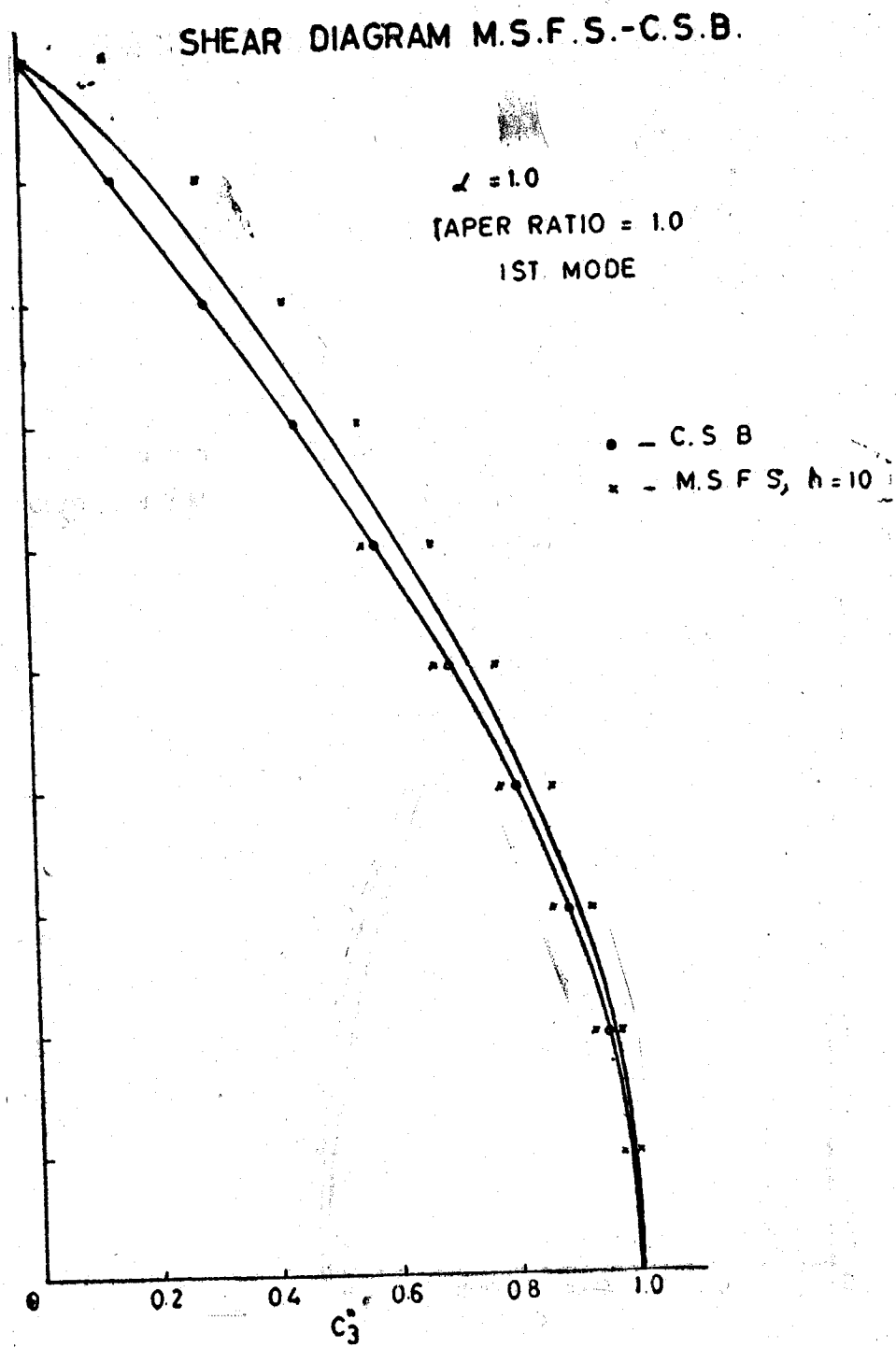


Figure 5.5

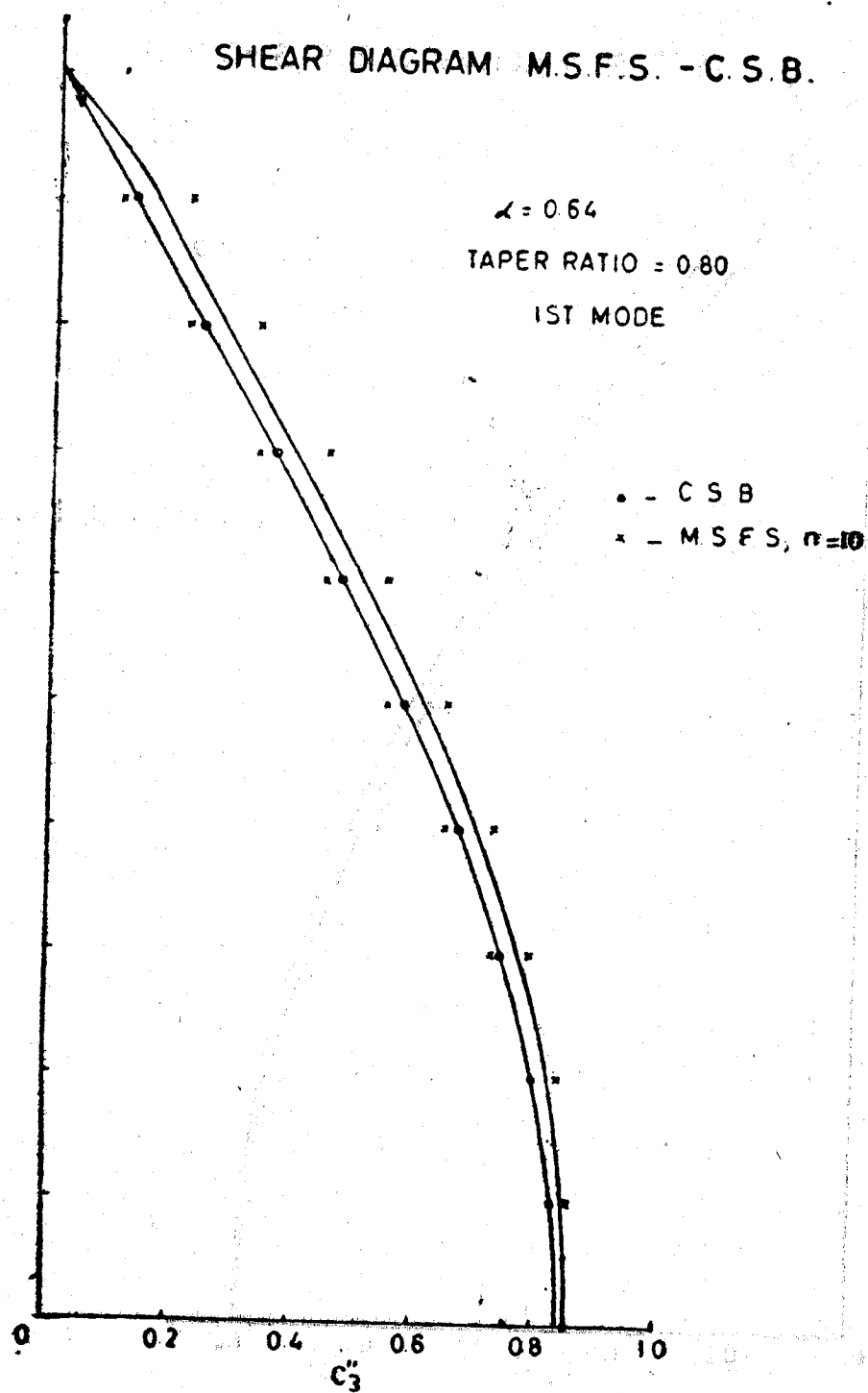


Figure 5.6

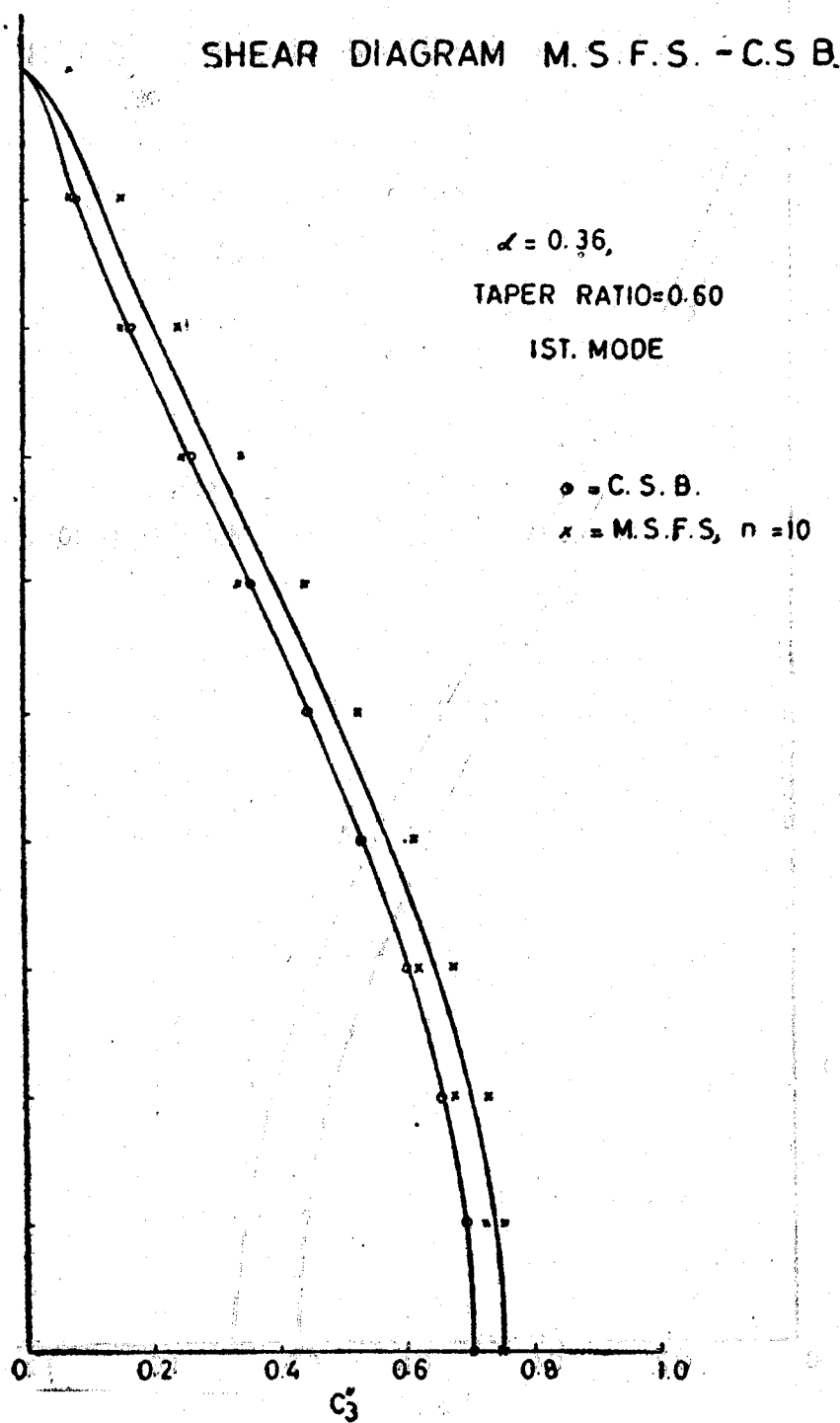


Figure 5.7

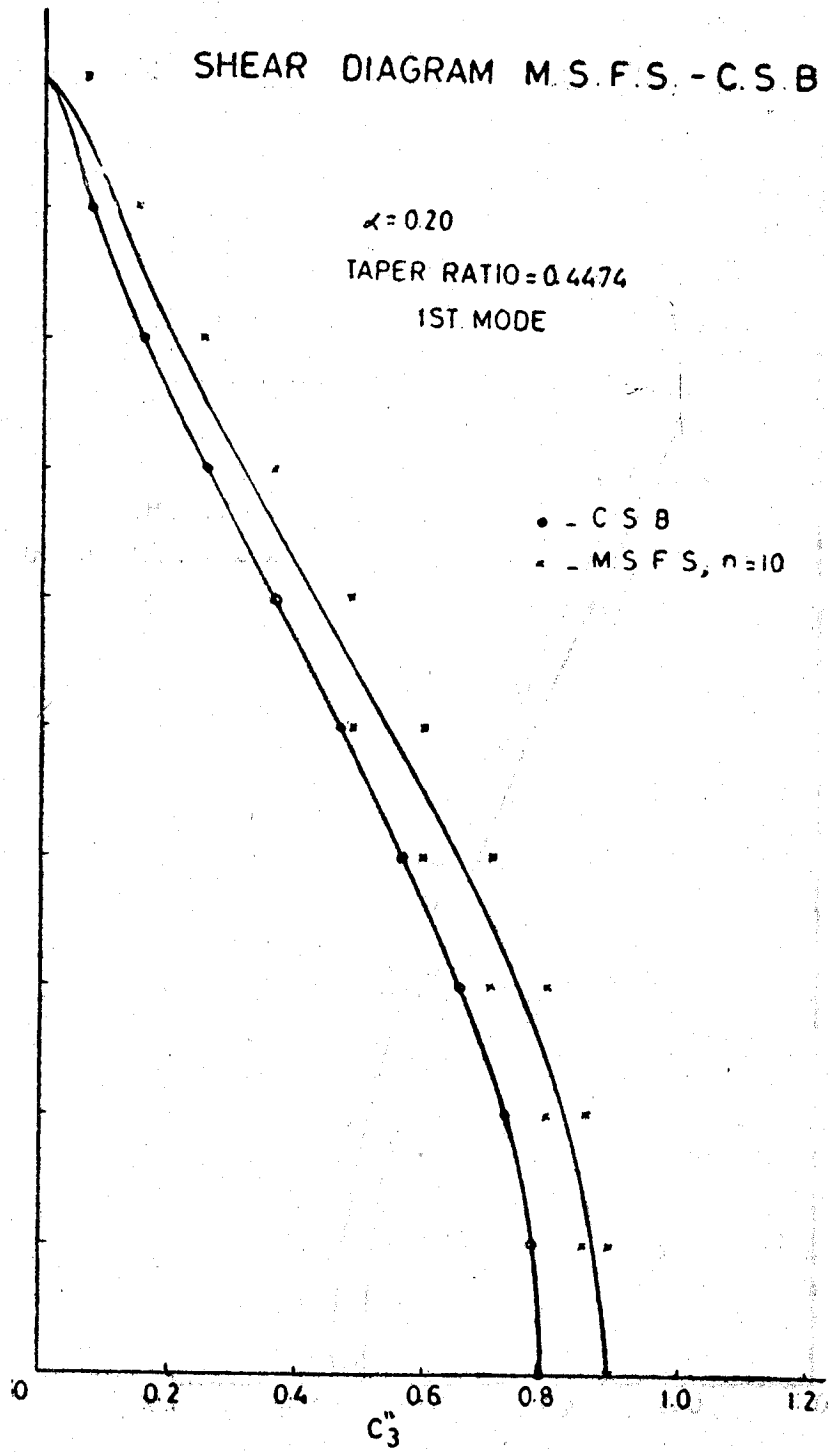


Figure 5.8

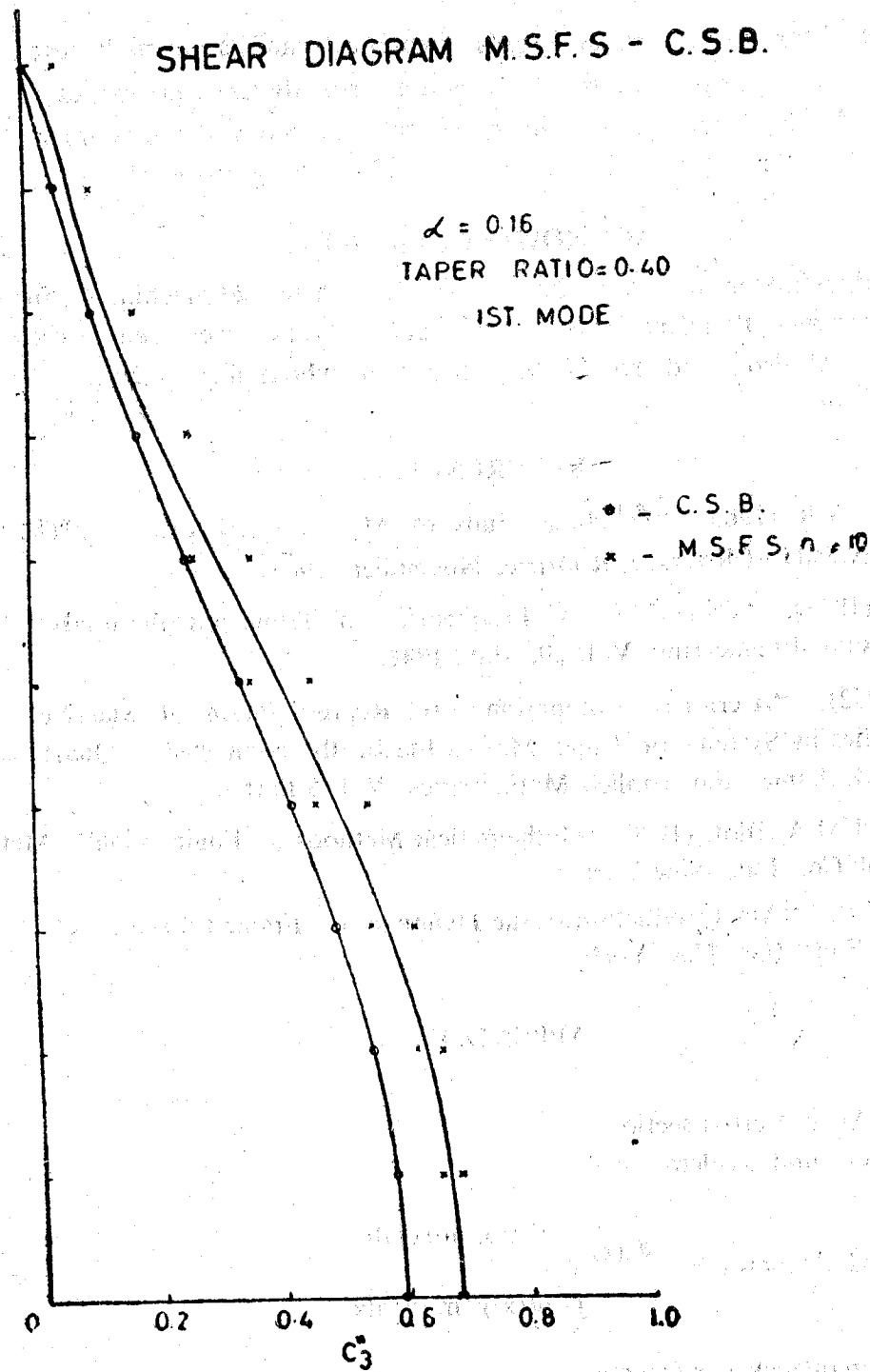


Figure 5.9

CONCLUSION

Cantilever shear beams are analogous theoretical models of multistoreyed framed structure. The concept of shear beam indicates that once dynamic properties are calculated for a multistoreyed framed structure (say for $n=5$), then the behaviour of similar multistoreyed structures (that is for all values of n above 5) could be easily predicted.

ACKNOWLEDGEMENTS

The digital computer work was done on a Burroughs 220 machine at the California Institute of Technology, Pasadena, U.S.A. The author is extremely thankful to Dr. G.W. Housner, Dr. D.E. Hudson and Dr. Jai Krishna under whose able guidance this research work was carried out.

REFERENCES

- Chandrasekaran, A.R. (1963), "Dynamic Study of Multistoreyed Frames", Ph. D. Thesis, University of Roorkee, Roorkee, November, 1963.
- Conway, H.D. (1948), "Calculation of Frequencies of Truncated Pyramids", Journal of Aircraft Engineering, Vol. 20, May, 1948.
- Duncan, W.J. (1952), "A critical Examination of the Representation of Massive and Elastic Bodies by Systems of Rigid Masses Elastically connected", Quarterly Journal of Mechanics and Applied Mathematics, Vol. 5 Part I.
- Karman, T.V. and M.A. Biot, (1940) "Mathematical Methods in Engineering", McGraw Hill Book Co., Inc., New York.
- Rogers, G.L. (1959), "An Introduction to the Dynamics of Framed Structures", John Wiley and Sons, Inc., New York.

APPENDIX

Notations

- A — Area of cross section
 a(t) — Ground acceleration

$$B_x \text{ — Mode factor} = \frac{\phi(x) \int_0^H \phi(x) \cdot m(x) dx}{\int_0^H (\phi(x))^2 m(x) dx}$$

- C_1, C_1' — Frequency coefficients
 C_2, C_2' — Displacement coefficients; subscript 'T' used along with this represents values at top
 C_3, C_3' — Shear coefficients; subscript 'B' used along with this represents values at base
 C_3'' — $C_3' / 1.2732$

- C_4, C_4' — Moment coefficients; subscript 'B' used along this represents values at base
 D — arbitrary constant to be determined from initial or boundary conditions
 E — modulus of elasticity
 G — modulus of rigidity
 H — Total length of beam
 k — spring constant
 m — mass
 MT — moment at any section
 n — number of masses
 p — natural frequency of system
 p_d — damped natural frequency of system; $\approx p$ if ζ is small, say, ≤ 0.20
 r — index representing mode of vibration
 S_v — Response velocity spectrum

$$= \left| \int_0^t a(t) \cdot e^{-\zeta p(t-\tau)} \sin p_d(t-\tau) d\tau \right|_{\text{maximum}}$$

- t — time interval
 $T.R.$ — Taper Ratio, defined as per fig. 3.6
 V — shear force at any section
 w — intensity of load at any section
 x — distance measured along the length of the beam
 y — displacements measured transverse to the longitudinal axis of the beam
 Z — relative displacement of any section with respect to the base
 α — mass and spring constant variation parameter defined as per figure 3.7
 ζ — coefficient of damping expressed as a fraction of critical damping value
 θ — phase angle between input and output
 ξ — normal coordinate
 ρ — mass density of beam
 σ' — ratio of average shear stress on a section to the product of shear modulus and angle of shear at the neutral axis.
 ϕ — mode shape coefficient

1940

1940

1940

1940

1940

1940

1940

1940

1940

1940

1940

1940

1940

1940

1940

1940

1940

1940

1940

A NOTE ON THE EARTHQUAKE OBSERVATIONS

P.N. Agrawal*

The importance of earthquake observations has been discussed, and a questionnaire has been prepared with a view to rendering the reported observations more objective.

In the absence of an adequate net work of seismological observatories it is hardly necessary to emphasize the importance of earthquake observations, as obviously these alone can provide the data necessary for earthquake studies. We broadly know the seismic belts of the world, and also the particular regions where earthquakes have occurred most frequently in the past and where they are most likely to occur again. We also understand something about the various geological and geophysical activities connected with their origin. In order to determine more precisely as to where they are most likely to originate, as well as the conditions which may minimise the damage caused by them, earthquake observations are of immense importance. In the seismic regions of this country, we have only a few seismological observatories and as the cost involved in building, equipping and maintaining them is enormous, one cannot hope that their number will increase in the near future. Moreover, the instruments normally installed in these observatories give hardly any ready data to earthquake engineers regarding the displacement, acceleration and strain of the ground in the wake of an earthquake. Also the instrumental records do not directly yield any information of public interest. The benefits of instrumental records are thus slow in materialising. Whereas, at times, quicker and more practical information may be obtained from the earthquake observations. It can therefore be stated that the importance of the earthquake observations does not diminish even when the instrumental records are adequately available.

An earthquake may occur anywhere and at any time and one cannot expect an observer to be ready at the spot for making observations. This difficulty can be overcome by employing a fairly large number of observers or, even better, by getting the information through those who have observed the earthquake. The short duration of the earthquake vibrations imposes some limitations on the observations made, but if one starts looking into the effects of earthquakes on people, objects and structures built by man, as well as on

* Senior Scientific Officer, Regional Research Laboratory, Jorhat, Assam. Attached to School of Research and Training in Earthquake Engineering, University of Roorkee, Roorkee (India).

animals and plants, he may be able to get a good deal of useful information, even though much still remains to be observed. The greatest handicap in earthquake observation arises from the fact that we are not able to see with an open mind what is happening but try to see some thing which we expect to occur, based on some preconceived notions imparted to us in childhood by dear old grandmother. An attempt on the part of an observer to forget all earlier impressions about the earthquakes and then observe what has actually happened will make the observations more useful and reliable. With this in view the following questionnaire has been prepared and would, it is hoped, prove very useful to the engineering studies in connection with earthquake effects.

EARTHQUAKE QUESTIONNAIRE.

1. General.

- (i) Location of the observer :
- (ii) Nature of the ground : Alluvial / Sandy / Rocky / Swampy / Loose / Compact
- (iii) Type and condition of the construction in the area of observation. : Masonry / Timber / Reinforced-concrete / Steel. Single/Double storied. Poor/Satisfactory/Good condition.
- (iv) Density of inhabitation : Thick/Normal (as in that region)/thin.

2. Earthquake Effect on People.

- (i) Date and time of feeling the earthquake :
- (ii) Estimate of duration of shock (s) their number, interval between successive shocks :
- (iii) Sound heard : No/Booming/Roaring
- (iv) Nature of vibration : Slow-rolling/Sudden/Rapid and continuous/Violent/Destructive.
- (v) Direction of approach of wave (s) : Observed/Not observed, Direction.....
- (vi) People felt earthquake : At rest/In car/Unable to walk/Stand.
 People frightened : None/Few/Many/All.
 People died : None/Few/Many.

3. Earthquake Effects on Objects and Structures Built by Man.

- (i) Hanging objects like, pictures : Did/Didnot swing. In.....direction.
 doors

- (ii) Wall clocks : Stopped/Not stopped/Not available for observation.
- (iii) Rattling of windows, doors and dishes : Observed/Not observed.
- (iv) Loose objects like furniture : Not shifted/Shifted/Overturned. In....direction
- (v) Crack (s) in Plaster/Wall (s) : Observed/Not observed in wall (s) facing..... direction.
- (vi) Fall/Swing of building(s)/Post(s)/Chimney(s)/Tower(s) : Observed/Not observed. In.....direction.
- (vii) Rail Road / Road / Telegraph line : Yes/No. Give direction of bend..... out of line
- (viii) Damage to bridge/Culverter/Under-ground pipe(s)/Cable(s) : Observed / Not observed / No such objects Present.

4. Earthquake Effects on Animals and Plants.

- (i) Animals disturbed : Yes/No/Not observed.
- (ii) Animals died : None/Few/Many.
- (iii) Trees broken/up rooted : Observed/Not observed. Size.....Height of break.....Direction of fall.....

5. Earthquake Effects on Topography etc.

- (i) Settling of Loose earth land slide/ Fracture : Observed/Not observed
- (ii) Depression(s) Uplift(s)/Pond(s) / Crack(s) along crests of waves in ground formed : Yes/No.
- (iii) Change in well/Ground/River/Pond water level : Observed/Observation not possible/Not observed.
- (iv) Change in ground level : Observed/Not observed.

6. Remarks.

7. Observer.

Name, address and Signature of observer with the date of entries.

(Note: Directions should be approximated as N, NE, E, SE, S. SW, W and NW).

The above questionnaire is not intended to give an exhaustive list of what could be observed, but only to render the reports, as far as possible, free from personal error and prejudice. It is hoped that it will greatly enhance the value of the data provided by a volunteer who wishes to participate in the great venture of understanding the nature and consequences of earthquakes.

THE HISTORY OF THE UNITED STATES

The history of the United States is a story of growth and change. From the first settlers to the present day, the nation has evolved through various stages of development. The early years were marked by exploration and the establishment of colonies. The American Revolution led to the birth of a new nation, and the subsequent years saw the expansion of territory and the growth of industry.

The American Civil War was a pivotal moment in the nation's history, leading to the abolition of slavery and the strengthening of the Union. The Reconstruction era followed, a period of significant social and political change. The late 19th and early 20th centuries saw the rise of industrialization and the emergence of the United States as a world power.

The 20th century has been a time of great challenges and achievements. The two world wars tested the nation's resolve and led to the establishment of the United Nations. The civil rights movement fought for equality and justice for all. The space age opened new frontiers for exploration and discovery.

The future of the United States is uncertain, but the values of freedom, democracy, and justice remain the foundation of the nation. As the world changes, the United States must continue to adapt and evolve, ensuring that it remains a beacon of hope and progress for all people.

The history of the United States is a testament to the resilience and spirit of its people. It is a story of a nation that has overcome many challenges and emerged as a global leader. The future is bright, and the United States remains committed to the principles of liberty and justice for all.

STUDY OF EARTHQUAKE SEQUENCES IN ASSAM AND NEIGHBOURHOOD FOR THE PERIOD 1918-62.

T. K. Dutta*

SYNOPSIS

Frequency distribution of earthquakes in Assam region has been studied for the period 1918—1962. Earthquake sequence in general, and after shock sequences of major shocks in particular, indicate the influence of regional structural features on the nature of release of earthquake strain energy.

INTRODUCTION

Placing of Assam region in one of the known seismic belts of the world presents difficulties. That Assam Himalaya is a part of tran-Asiatic Alpide belt of tectonic feature is evident enough. The seismicity of Assam, however, is so closely linked with Burma that it is difficult to view these two features separately. It was mainly to avoid this difficulty that Gutenberg (1954), overriding seismic and structural data to the contrary, considered the Himalayan and Burmese areas as coming under the Himalayan system. The author (1964) in his examination of seismic regionalisation of Assam pointed out the basic differences in the two arcuate activities of the region. It was also pointed out that these two arcuate features are separated by a 'block' tectonic environment running along the length of Assam in a general north-easterly direction. This view, based mainly on seismic data, is supported by the frontal pattern of mountain arcs of the region. Alpide belts in Asia (of which Himalayas form a part) all show convexity towards south while the Burmese arcs, in close resemblance to the Sunda arc continuation, show west-ward convexity. Gutenberg (1954) has however, pointed out that seismic evidences are insufficient to establish a direct connection between the activities of Burmese and Sunda arc sectors. From all these indications, it appears that the Burmese activity should be considered as a feature different from that of Himalayan activity.

The regional complexity of Assam thus arises out of the positioning of the fold resistant Archean wedge sandwiched between two compressive stress fields. The process results in the development of complex force field within and around the basically 'stable'

* Senior Scientific Officer, Regional Research Laboratory, Jorhat (Assam).

platform. The four zones of tectonic activities of this region, earlier discussed by the author (1964), are based upon both structural complexities and stress field distribution of this area.

In the present study, an analysis of the frequency distribution of significant tectonic movements of the region has been made and the influence of the environment of such frequency distribution examined.

DATA AND METHOD OF ANALYSIS

The period covered in the present study is from 1918-1962 (45 years). All significant tectonic disturbances with lower magnitude limit 4 on the Gutenberg-Richter scale of seismic magnitude were used for the present study. Scarcity of reliable instrumental data however severely restricted the scope of the study. Epicentres of earthquakes used in the study were all checked afresh on the basis of available data. Travel time values used for all determinations were those given in "Seismological tables by Jeffreys and Bullen" (1948). The table at the end gives year and region wise distribution of earthquake epicentres in and around Assam. Figures 2 through 5 present graphically the frequency distribution of earthquakes of the four zones separately while figure 1 gives the frequency distribution of earthquakes of the region as a whole. Though all available data were freely used, yet following sources were found outstandingly valuable :

1. International Seismological Summary.
2. Bulletin of the Bureau Central International de Seismologie.
3. Seismological bulletins of India Meteorological Department.
4. Bulletins and other publication of the United States coast and Geodetic Surveys.
5. Unpublished records and data of India Meteorological Department.

Prior to 1951 no seismological station was operating within the region and the efficiency of the recording seismographs, both within and outside India, was rather low. With the commissioning of a powerful seismograph station at Shillong and a subsidiary station at Tocklai (Jorhat) from 1951, considerable improvement in the recording efficiency of the earthquakes of the region was noticed. Data used in the table for the period 1952 onwards are quite complete for the purpose of present study, but for earlier periods such high order of completeness cannot be claimed.

FREQUENCY DISTRIBUTION OF EARTHQUAKES

For the purpose of present study, annual occurrences of major shocks and the total number of shocks of all categories, for all four regions, have been treated separately. Shocks of magnitude ≥ 7 and above have been treated as major shocks. This criterion has been used mainly for the understanding of the frequency of occurrence of earthquakes which are capable of causing damages to engineering structures over wide areas. Major shocks have been

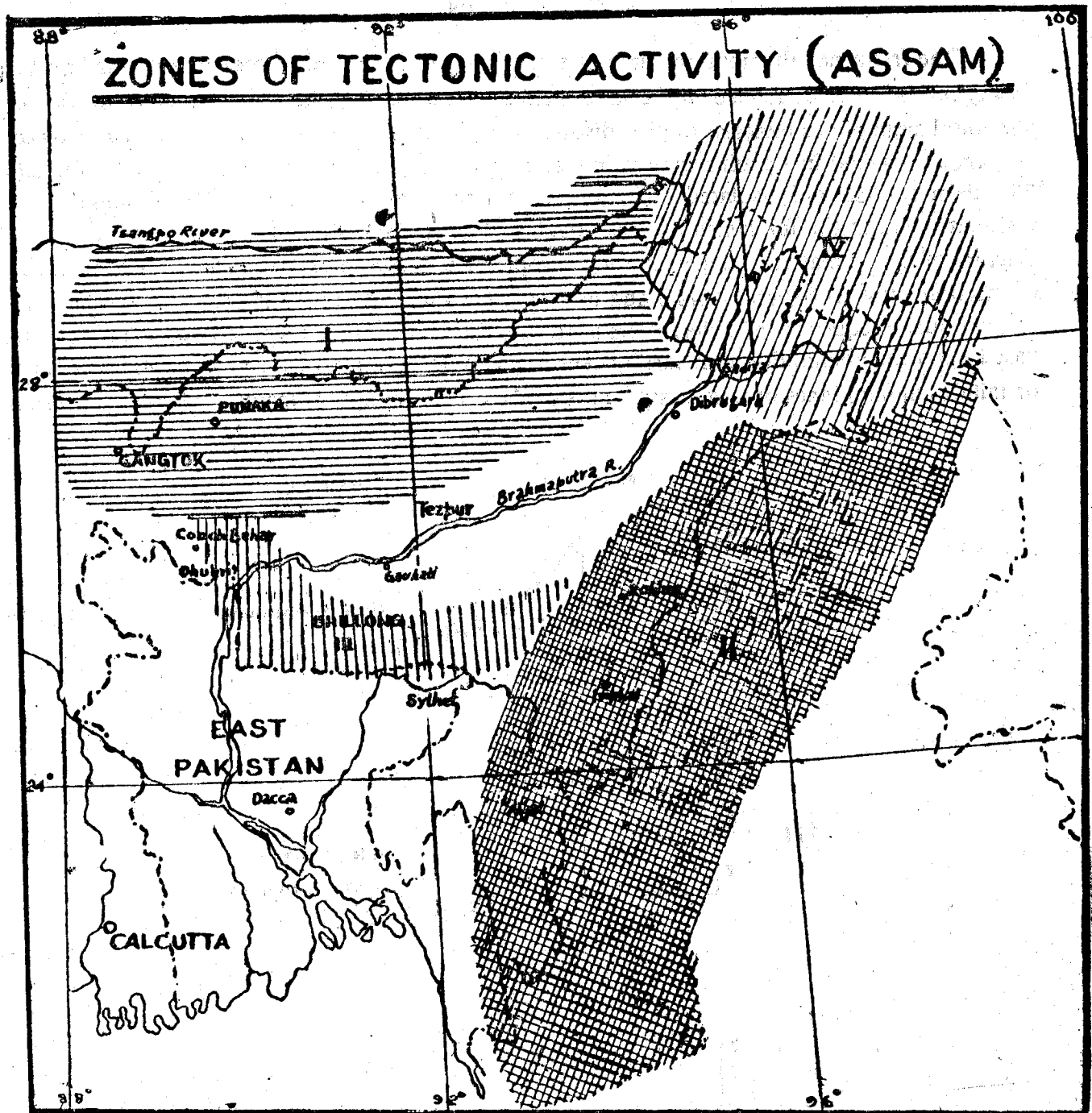


Figure 6

represented in Figs. 1 through 5, by vertical columns with lengths proportional to the number of such shocks. The continuous curves in all figures give the frequency distributions of total number of earthquake shocks. Total number of earthquakes used for the present study is 473. Fig. 6 indicates the four zones of seismic activity of the region as discussed earlier by the author (1964).

DISCUSSION

The frequency distribution curve of a zone indicates the general sequence of earthquake energy release and are related to the stress field responsible for the process as well as the structural state of the material of the disturbed region. The author (1964) earlier showed that the stress field in Assam region is fundamentally compressive and uniformly distributed. The shear type stress in isolated areas originate only out of local reaction of stable and resistant strata to the fundamental stress field. Mogi (1963) studied the nature of brittle fracture of model materials under uniform compressive stress and pointed out an intimate connection between structural state and nature of fracture. The interpretation of the nature of earthquake sequences of different areas on the basis of Mogi's experimental results are based upon the assumption that earthquakes are caused by brittle or semi-plastic fractures or failures along planes of weaknesses in earth's crust or upper mantle. Recently Evison

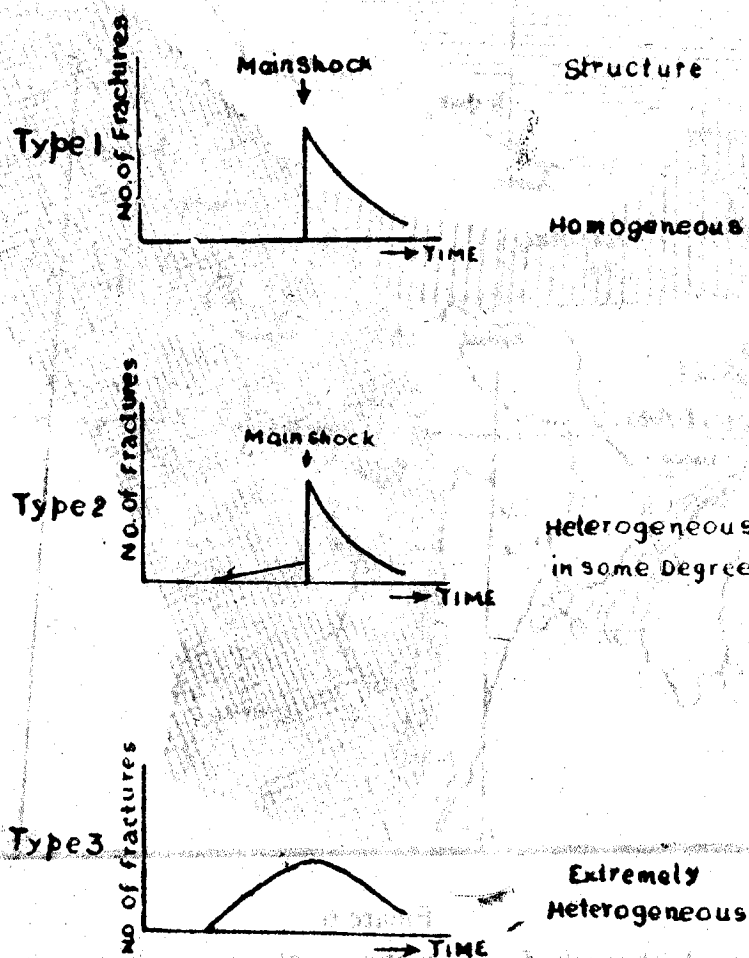


Fig. 7 Schematic Representation of Frequency Curves of Brittle Fracture in Different Model Materials under Compressive Stress (based on Mogi's experimental data)

(1963) reviewed the weakness of such assumption but nevertheless observations of both earthquake mechanism at source and surface effect near epicentral regions of major earthquakes still seem to overwhelmingly support this view. Mogi's experimental data can thus be used for examining the effects of structural inhomogeneity upon the earthquake sequence of zones of tectonic activities in Assam. Fig. 7 above schematically presents the frequency distribution curves of elastic shocks, under compressive stress (based on Mogi's experiments).

Frequency distribution of earthquake of different regions of earth shows striking resemblance to the above schematic presentation of brittle fractures. As the stress field in Assam region is basically compressive in nature, the frequency distribution curves of this region may be examined for an indication of the structural state of the different zones of the region. But because of inherent incompleteness of the basic data, it is possible to examine this aspect of seismicity on general terms only. If the earthquake sequences of the four zones of Assam region are examined in the above light, then it is observed that sequences of both zones I and II resemble the fracture pattern of type II while sequences of zone III and IV resemble that of type I in Fig. 7 above. However for this purpose it is necessary to treat the upheaval of 1950 on a different footing. The instability that resulted in the earthquake sequences of 1950 effected the neighbouring areas also through elastic rebound and analysis of aftershock sequences of the main shock of 15th August 1950 (Epc-28°7N 96°6E, origin time-14h 09m 30s GMT Magnitude-8.6) show that the main shock originating from Zone IV had in its sequence of aftershocks a series of shock (some of them major) originating from bordering areas of zone I and II.

From Figs. 2 and 3 it will also be seen that generally major shocks of zones I and II are preceded by a slight increase in the normal seismic activity of the region and that after shock sequences for major shocks are either absent or fall off rather rapidly. Again from Figs. 4 & 5 it will be observed that major shocks of zones III and IV are generally preceded by a period of quiescence during which the seismic activity is lower than the normal level. However all major shocks from zones III and IV are followed by large trains of after shocks which die off slowly. In some cases energy levels of a few aftershocks are quite high and the sequence of aftershock is complicated by the presence of such secondary sequences.

Both Dhubri earthquake of 1930 and Assam earthquake of 1950 (originating from Zone III and IV respectively) exhibited such complicated phenomena. Thus in both zones III and IV the mechanism of elastic strain release is in the form of intense energy bursts followed by periods of quiescence, while in zones I and II though the normal level of activity, in terms of frequency of disturbances, is relatively high yet the burst of high energy releases are not as high as in other two zones and viewed on frequency distribution curves

the energetic bursts are very much less conspicuous for Zones I and II as compared to Zones III and IV.

The nature of earthquake sequences of different zones of Assam, viewed in the light of Mogi's (1963) observation of fracture pattern of model materials, indicate a comparatively homogenous structure for zones III and IV as compared to zones I and II. It seems that the seismicity of both zones I and II are connected to the development of folded mountains of the arcuate Himalayan and Indo-Burmese system, through comparison of Geosynclines while activities of zones III and IV are caused by the block tectonic degeneration of the ancient platform represented by the Assam plateau. The nature of activity of the platform seems to be a similar to that of Central Asian platform as observed by Gorshkov (1959).

ACKNOWLEDGEMENT

This paper is published with the kind permission of Shri E. Ehsanullah, Assistant Director-in-Charge, Regional Research Laboratory, Jorhat. Dr. B. N. Mitra, formerly Director of Regional Research Laboratory, Jorhat suggested the problem and helped the author through his constant interest and valuable advice. The author also acknowledges with thanks the facilities offered to him at Central Seismological Observatory Shillong by the Director General of Observatories.

YEAR WISE AND REGION WISE DISTRIBUTION EARTHQUAKE EPICENTRES IN AND AROUND ASSAM (1918—1962)

Year	No. of shocks originating from Region					Major shocks Magnitude = 7 & above	Remarks
	I	II	III	IV	Total		
1918	—	—	1	—	1	1	Major shock originated from Zone III
1919	—	—	—	—	—	—	—
1920	—	1	—	—	1	—	—
1921	—	1	—	—	1	1	Major shock originated from Zone II
1922	—	—	—	—	—	—	—
1923	—	1	1	—	2	1	Major shock originated from Zone III
1924	1	3	1	—	—	5	—
1925	—	—	—	—	—	—	—
1926	—	4	1	1	6	—	—
1927	—	2	1	1	4	—	—
1928	1	1	1	2	5	1	Major shock originated from II
1929	1	8	—	1	10	—	—

(Continued)

Year	No. of shocks originating from Region					Major shock Magnitude = 7 & above	Remarks
	I	II	III	IV	Total		
1930	—	16	9	—	25	1	Major shock originated from III
1931	—	9	1	4	14	1	Major shock originated from II
1932	1	5	4	—	10	1	Major shock originated from II
1933	—	7	1	2	10	—	—
1934	—	3	—	—	3	—	—
1935	1	3	1	—	5	—	—
1936	1	3	2	—	6	—	—
1937	2	4	—	—	6	1	Major shock originated from II
1938	2	3	1	1	7	2	Both major shocks originated from II
1939	—	2	—	—	2	1	Major shock originated from II
1940	2	1	—	—	3	1	Major shock originated from I
1941	6	4	1	1	12	3	One major shock originated from I and two from II
1942	1	—	1	—	2	—	—
1943	1	—	—	—	2	1	The major shock originating from near Jorhat and outside the marked region.
1944	1	1	1	—	3	—	—
1945	—	—	1	—	1	—	—
1946	1	8	—	1	11	2	Both the major shocks originated from II, one shock originated from near Nowgong and outside the marked region.
1947	2	6	—	—	8	1	Major shock originated from I
1948	1	2	2	—	7	—	Two shocks originated from near Jorhat and outside the marked region.
1949	—	4	1	1	6	1	Major shock originated from III
1950	33	11	2	42	88	13	Major shocks :- 4 from I, 2 from II and 7 from IV
1951	9	5	2	9	25	2	Major shock :- 1 from I and 1 from III
1952	3	6	—	2	11	—	—
1953	—	1	1	2	4	—	—

(Continued)

Year	No. of shocks originating from Region					Major shock Magnitude = 7 & above	Remarks
	I	II	III	IV	Total		
1954	1	1	—	2	4	1	The major shock originated from II
1955	2	7	3	1	13	—	—
1956	2	12	3	3	20	1	The major shock originated from II
1957	—	10	1	2	13	1	The major shock originated from II
1958	5	10	1	—	16	—	—
1959	9	12	1	9	31	—	—
1960	4	11	3	4	22	—	—
1961	9	14	2	3	28	—	—
1962	2	10	3	5	20	—	—
45 Years	104	212	54	99	473	38	Four shocks with origin outside marked region.

REFERENCE

- Banerjee, S. K.; (1957) "Earthquakes in the Himalayan Region" Indian Association for the Cultivation of Science.
- Dutta, T. K.; (1964) "Seismicity of Assam—Zones of Tectonic Activity" (will be published in next issue of Bulletin of N. G. R. I.)
- Evison, F. E., (1963) "Earthquakes and Faults" Bulletin, Seismological Society of America Vol. 53, No. 5.
- Gorshkov, G. P., (1959) "On Seismic Regioning of Assam Countries" I. U. G. G. Travaux Scientifiques Fascicule 20.
- Gutenberg, B and Richter, C. F., (1954) "Seismicity of Earth" Princeton University Press, 2nd edition.
- Mogi, K., (1963) "Some Discussions of Aftershocks, Foreshocks and Earthquake Swarms—the Fracture of Semi-infinite body Caused by an Inner stress origin and its Relation to the Earthquake Phenomena" Bulletin of the Earthquake Research Institute, Vol. 41, Part 3.
- Division of Earthquake Engineering and Seismology,
Regional Research Laboratory, Jorhat, Assam.

Dutta an Earthquake Sequence in Assam

ANNUAL DISTRIBUTION OF EARTHQUAKES ORIGINATING FROM ASSAM & NEIGHBOURHOOD (1918-1962)

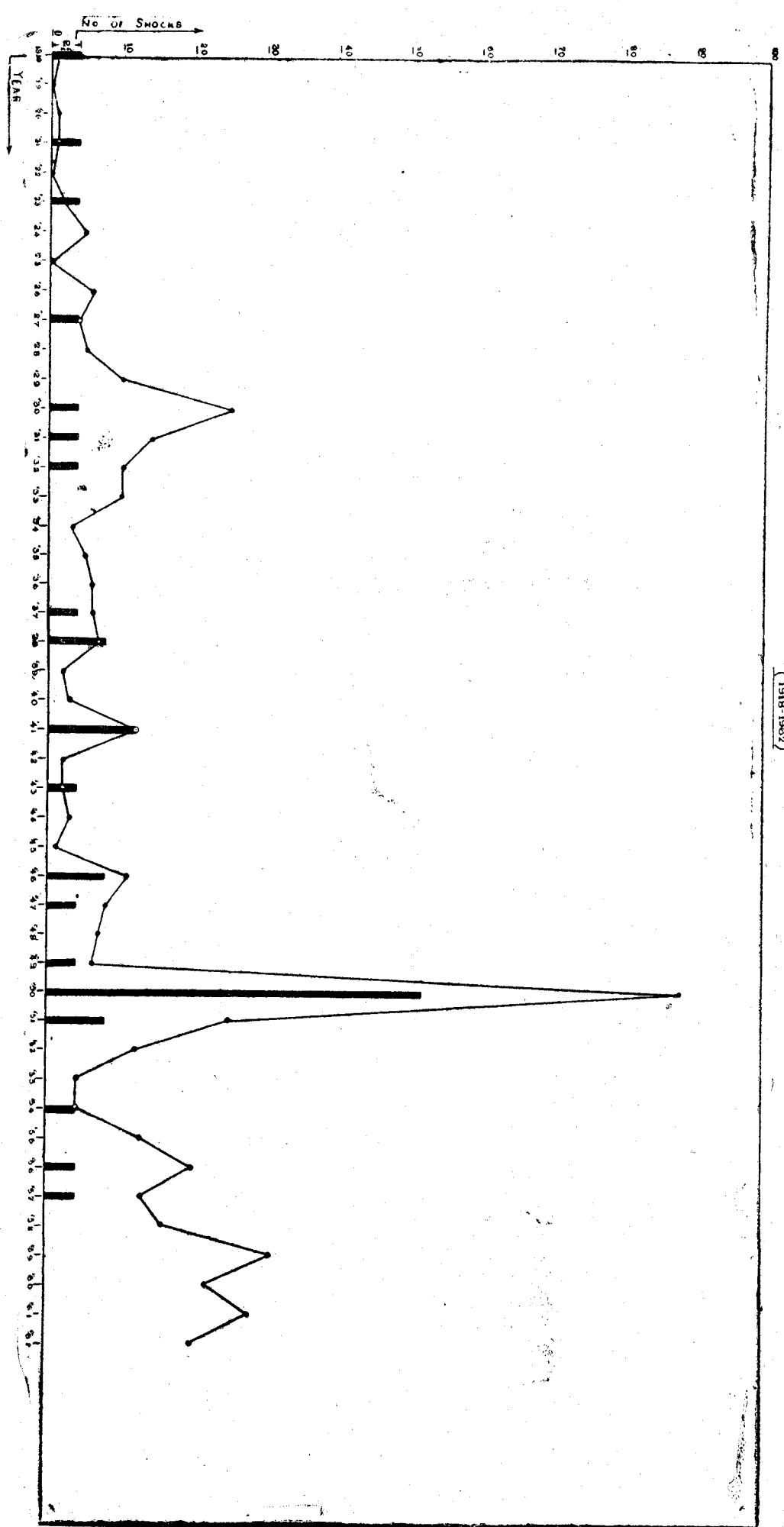


Figure 1

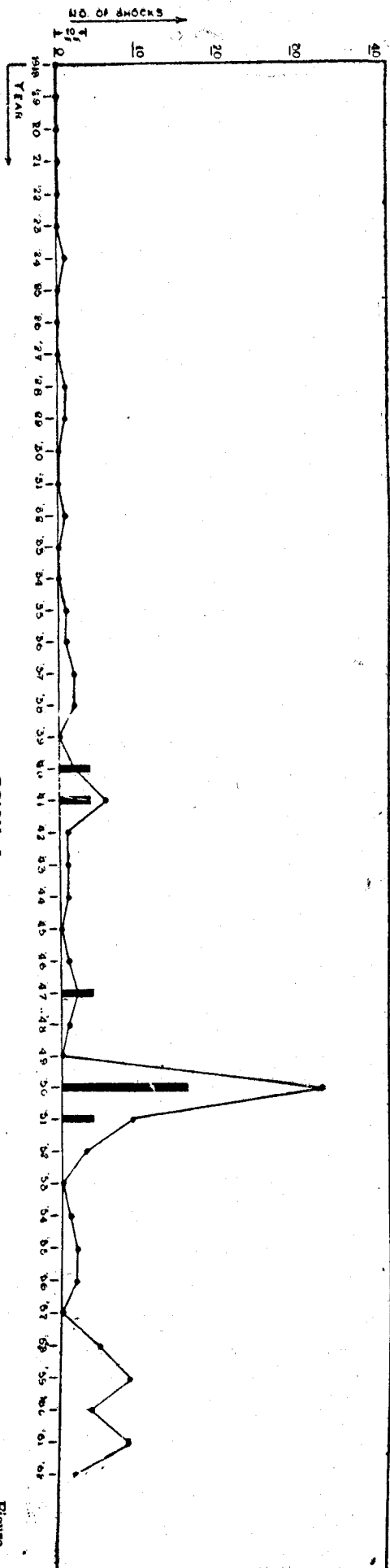


Figure 2

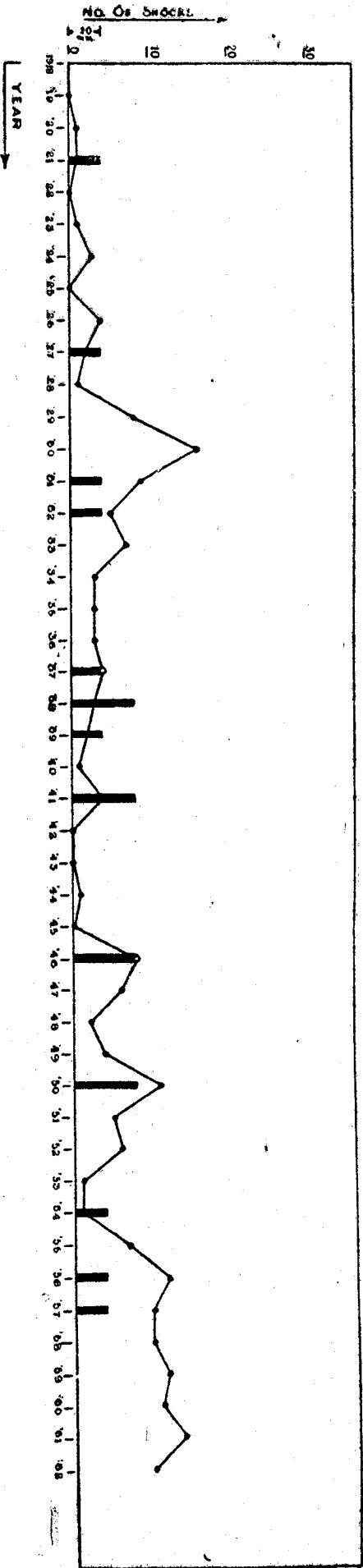


Figure 3

ANNUAL DISTRIBUTION OF EARTHQUAKES ORIGINATING FROM REGION - III
(1918-1962)

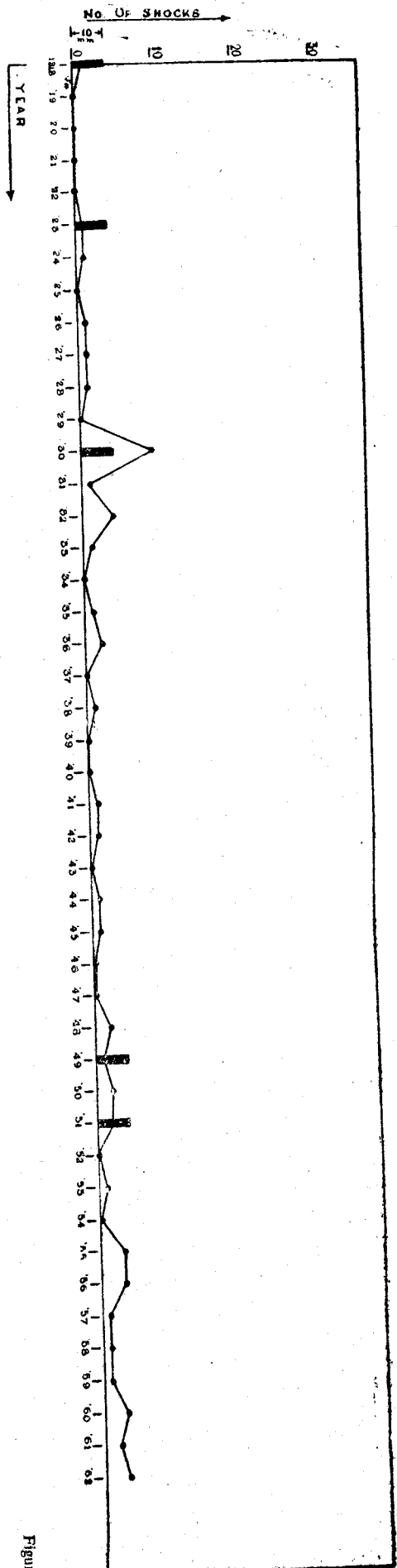


Figure 4

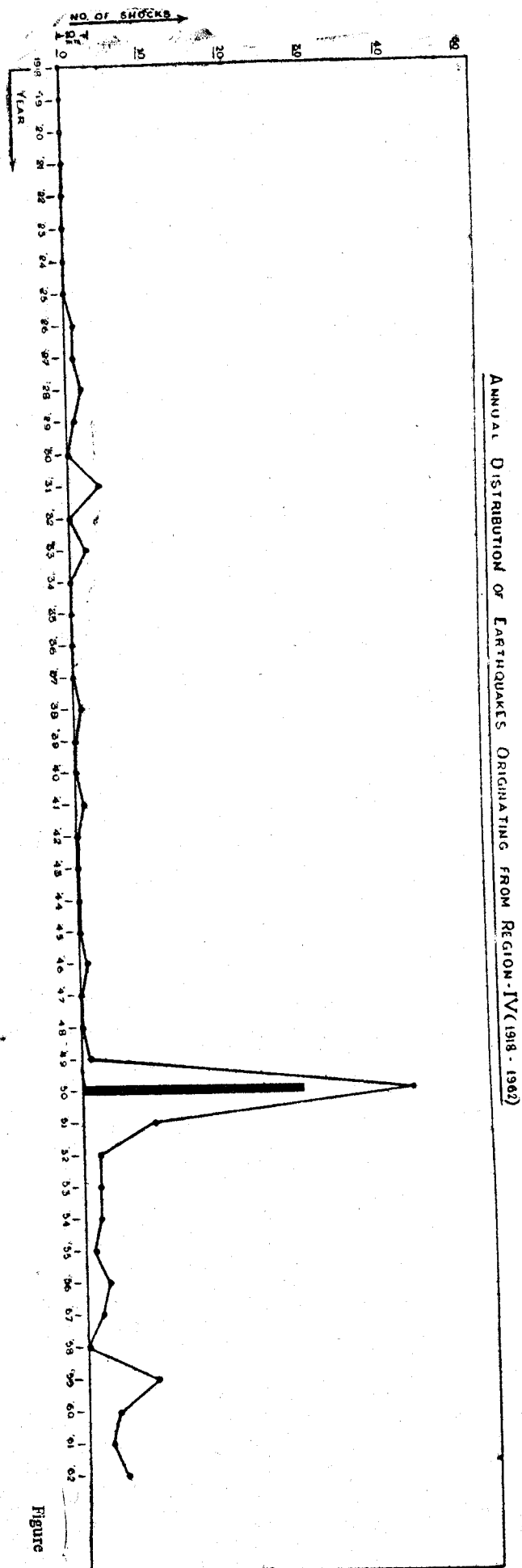


Figure 5

GROUND DISPLACEMENT AND ACCELERATION CAUSED BY EARTHQUAKES

Vinod Kumar Gaur* and Umesh Chandra*

SYNOPSIS

This paper is an outcome of an enquiry into the processes which lead to the attenuation of seismic waves in the earth. A knowledge of the variation of their amplitude with distance, and with depth, in the case of surface waves, would be of considerable interest to Seismology in general, and to Earthquake Engineering in particular.

The factors governing the amplitude of the ground displacement at a given epicentral distance have been examined in detail. However, as a progressive wave suffers from the cumulative effects of all these causes, the individual effects can be inferred only indirectly. Typical values representing the dissipation of seismic energy are also discussed.

INTRODUCTION

Most of the studies on the amplitude of seismic waves have been made with a view to understanding the structure of the earth and the nature of earthquakes. To an Earthquake Engineer the problem is an inverse one i.e., to estimate the amplitude of the seismic waves or the displacements caused by them when they emerge at the surface. Energy travels outwards from a focus, usually regarded as being small enough to approximate to a point, in the form of waves. These include body waves which may penetrate to all parts of the Earth's interior, as well as surface waves which only travel along surfaces of discontinuity, especially over the free surface of the earth. An advancing wave is normally attenuated as its energy spreads out over the enlarging wavefront, and also by the partitioning of energy at the elastic discontinuities. Other factors contributing to this include diffraction, scattering, dispersion and deviation from perfect elasticity.

1. Geometrical Spreading of the Wavefront

In the simplest case of spherical symmetry about a focus, the solution of the wave equation, for waves advancing outward from the focus, has the form $A = \frac{1}{r} F(r-vt)$, where F is a function representing initial conditions. The solution implies that A decreases inversely as the distance. This accounts for most of the decrease in amplitude at distances not too close to the focus, where more complicated phenomena predominate.

*Department of Geology and Geophysics, University of Roorkee, Roorkee, U.P., India.

The expression for the displacement of the outer surface arising from a wave travelling towards it from a focus without change of type can be written as (see Appendix),

$$y = K T. Z. \sqrt{E. \frac{\cos i}{\sin e. \sin \Delta} \left(\frac{di}{dt} \right)} \quad (1)$$

where K = a constant depending upon the fraction of the energy E passing into the wave

$$Z = \frac{\text{ground displacement (y)}}{\text{amplitude of the incident wave}}$$

Δ = epicentral distance

i = angle which the ray leaving F makes with the level surface through it

e = angle between the emergent ray and the surface.

Part of the energy released by an Earthquake travels along the free surface of the Earth and along other surfaces of discontinuity in the Earth (Jeffreys, 1963 pp. 56-57). The amplitudes of surface waves arising from a shock of a given size decrease with focal depth according to factor e^{-Gh} where h is the depth of focus and G a function of wave velocities (Jeffreys 1959 page 58). Thus when the focus is not too deep, surface waves will spread outward over the other surface falling in amplitude according to the inverse square root of the distance. However, surface waves exhibit considerable dispersion.

2. Partitioning of Energy at the Elastic Discontinuities

At each discontinuity encountered, where either the velocity changes discontinuously or its gradient is abnormally high, a wave is partly reflected and partly refracted into the new medium causing a division of its energy. In general an incident wave results in four transformed waves, the reflected and the refracted P and S waves except in certain special cases when the nature of the incident vibration may preclude some of these components (Jeffreys, 1963, pp.29-30). In order to calculate amplitude of any of these derived waves, it is only necessary to apply the boundary conditions corresponding to the continuity of stress and displacement across the entire boundary at all instants of time (Jeffreys, 1963 pp.31-32). For the limiting case when the differences in the physical properties of the region vary but slightly, the analysis shows that loss of energy by transmission amounts to a second order quantity only, and if the medium can be considered homogeneous enough within a wavelength, the energy is transmitted virtually undamped along rays.

The ratio of the refracted wave amplitude to the incident wave amplitude can be represented by an appropriate transmission factor

$$F = \left[1 - \left(\frac{A}{A_0} \right)^2 \right]$$

In general an emergent wave may have changed type at the various discontinuities. The foregoing argument, however, still holds but the appropriate transmission factor has to be

calculated for every encounter and introduced in equation (1) to allow for the losses discussed here. The resulting expression for the displacement would now be given by,

$$y = KTZ \sqrt{(F_1 F_2 \dots F_n)} E \cdot \frac{\cos i}{\sin e \cdot \sin \Delta} \left(\frac{di}{d\Delta} \right) \quad (2)$$

3. (a) Diffraction

However, if the discontinuity encountered involves a curvature large compared with that of the incident wavefront, the reflected and the refracted wavefronts will be sharply curved. This is the case of diffraction. It assumes great significance in the vicinity of the source of disturbances where the conditions of the ray theory do not obtain. The mathematical theory required to explain diffraction effects tends to be complicated owing to a wide variety of problems involved. No experimental work seems to have been done to elucidate these effects.

3. (b) Scattering

Scattering arises when the irregularities, very much smaller than the predominating wavelengths, are encountered. In such a case the incident wave will be irregularly scattered and partially degenerate into heat. Jeffreys (1963 p. 41) has developed a quantitative treatment of this effect with analogy to kinetic theory of gases and presents a quantity,

$$\tau \approx (1/3) a \epsilon' \quad (3)$$

corresponding to the kinematic viscosity in gases, to be incorporated in a firmoviscous law; where l is the average grain diameter, a the longitudinal wave velocity, and it is assumed that the wave velocities vary from grain to grain by a factor of ϵ' . The firmoviscous law in its simplest form may be written as

$$P_{ij} = 2\mu E_{ij} + 2\nu \frac{dE_{ij}}{dt} \quad (4)$$

and corresponds to the Kelvin model,

where, P_{ij} = deviatoric stress

E_{ij} = deviatoric strain

μ = rigidity

ν = viscosity

The perfect elasticity stress-strain relations and the elastic afterworking equations are respectively,

$$P_{ij} = 2\mu E_{ij} \quad (5)$$

and,
$$P_{ij} + \tau \frac{dP_{ij}}{dt} = 2\mu E_{ij} + 2\nu \frac{dE_{ij}}{dt} \quad (6)$$

It can be shown that the replacement of (5) by (4) introduces a damping factor of the order of $\exp(-\nu \gamma^2 x / 2\mu v)$ in the amplitudes of waves of period $2\pi/\gamma$ and speed v over a

distance x . For waves in the crust of the earth, a comparison with observations gives an effective value of $\nu/\mu = 0.003$ secs. For deeper portions of the earth the value seems to be still less. For surface waves with speeds of the order of 3 km/sec., the damping factor would be $(1/e)$ over distances of 50 and 5000 km. in waves of periods 1 and 10 secs., respectively. For body waves penetrating deeply into the earth, damping is still less.

Equation (6) similarly involves a damping factor, but in this case contrary to observation, short waves would not be more severely affected than longer ones, as in the case of firmoviscous relation (4). From this result Jeffreys concludes that scattering rather than the type of imperfections observed in laboratory experiments is the main source of departure from perfect elasticity theory in elastic wave propagation. He estimated the linear diameter of crustal irregularities responsible for scattering to be of the order of 5 meters.

Jeffreys further indicates that the wavefronts leaving the focus would be slightly blunted by scattering because of the associated small spread introduced into the values of the wave velocity. Using the firmoviscous law equation (4), he has shown that at a given point, the most rapid change of displacement in the onset would take place at the instant given by the perfect elasticity theory based on equation (5) but the blunting would be spread about this instant over a time-interval of the order of $\sqrt{2\nu t/\mu}$, where $\left(\frac{\nu}{\mu}\right)$ may be taken to be a measure of the average scattering during a time of transit t . For the longitudinal waves travelling through the earth's centre to the anticentre, $t \approx 20$ min., and if ν/μ has everywhere the suggested surface value of 0.003 secs., the blunting would be spread over about 2 secs., which does not fit in with the observations of seismograms. It is, therefore, concluded that scattering is largely confined to the outermost 40 km. of the earth.

Rayleigh scattering will predominate if the grain size is smaller than the wavelength λ of the seismic wave concerned. Scattering in such a case will be proportional to $(1/\lambda^4)$ being greater for shorter wavelengths and smaller for longer ones.

4. Internal Friction

Besides these effects both laboratory experiments on rock samples as well as field measurements on rocks in situ, point to the elastic absorption in rocks i.e., in a steady state vibration, the amplitude is found to decrease with time. The corresponding loss of energy appears as heat and the processes causing this are collectively known as internal friction.

Internal friction may be expressed in terms of a function Q analogous to that of an electrical system and can be similarly obtained from the shape of the resonance curve. Alternatively, the relation between Q and one of the following quantities may be used:

1. The logarithmic decrement ϵ
2. The fractional loss of energy per unit cycle $\left(\frac{\Delta E}{E}\right)$

3. The phase difference between the applied stress and the resulting displacement δ . Accordingly,

$$\text{Internal friction} \cong \frac{\Delta E}{E} = 2\epsilon = \frac{2\pi}{Q} = 2\pi \tan \delta \quad (7)$$

One may also define internal friction in terms of the attenuation of a plane wave. The amplitude A_x of a damped wave at a distance x from a reference position x_0 , including the effect of divergence of the wave front, is normally expressed by the following relation.

$$A_x = \left(\frac{A_{x_0}}{x^m} \right) e^{-kx} \quad (8)$$

where k is the absorption coefficient and m the appropriate geometrical factor for the wave. If k varies in the body, it has to be replaced by the corresponding integral $\int k(x) dx$.

A relation between $\frac{\Delta E}{E}$ obtained from a rock bar sample and k obtained from the damping of a wave in the field follows from a suggestion by Born (1941) which states that

$$\frac{\Delta E}{E} (\text{bar}) = (2.1) \frac{\Delta E}{E} (\text{bulk}), \quad (9)$$

so that

$$\frac{\Delta E}{E} (\text{bar}) = \frac{2kv}{f} \quad (10)$$

$$\therefore k = \frac{f}{2v} \frac{\Delta E}{E} (\text{bar}) = \frac{\pi}{T v Q} (\text{bar}) \quad (11)$$

No general theory is available to describe the actual physical mechanisms responsible for causing dissipation in a medium, for obvious mathematical difficulties. However, the simplest way to introduce dissipative effects in the equation of motion is to represent them either as a function of velocity or of the absolute value of all acting forces, i.e. COULOMB FRICTION (Förtsch, O., 1956).

Following this simple models have been proposed by various authors which suggest the elastic behaviour of solids for the particular mechanisms, some of these important models are briefly summarized in Table 1. The mathematical form wherever possible, has been translated in mechanical terms as a combination of springs (elastic elements), and dashpots (viscous elements).

Models 1 to 5 produce a frequency dependent variation in the internal friction. Model 4 proposed by Boltzmann implies that the behaviour of a solid under stress is a function of its entire previous history. The solid may be visualized as a combination of springs and dashpots, but the resulting equations, in general are not soluble. This difficulty has been partially overcome by Sokoloff and Scriabin who assumed, on experimental evidence, that the

function ψ (see Table 1) may be expressed as a negative exponential involving constants of the rocks, $\psi(T-t) = B e^{-b(T-t)}$ (12)

Models 5 and 6 were specifically designed to render Q independent of the frequency in order to satisfy the results obtained from some of the laboratory experiments such as those by Kimball and Lowell (1927), Ide (1937, 8,000 cps.), Birch and Bancroft (1938, 120-4, 500 cps.).

Knopoff and Mac Donald (1958) have shown that the dissipative characteristics of many solids cannot be accounted for by any linear mechanism of attenuation. A particular model explored by them involves a nonlinear hysteresis loop resulting from nonrecoverable deformation at small stresses. The model, as they conclude, is by no means unique and other models involving some frictional dissipation could also account for the observation. Försch (1956) attributes the Coulomb Friction to be a mechanism for attenuation.

Lomnitz (1962) observed, "there is no evidence that the deformation of solids is governed by linear mechanism at the intercrystalline or molecular level, therefore a linear empirical relation for the creep function in such as Boltzmann's equation,

$$\phi(t) = q \log_e(1+at) \quad (13)$$

can be expected to fit only a restricted region of the strain-time continuum". He further emphasized the need for more detailed data and that it would seem premature to reach any conclusions or to introduce further refinements into the mathematical treatment.

However, in most measurements of this type the errors are relatively large i.e.. of the order of 20 percent. Bruckshaw and Mahanta in 1954, working in the frequency range of 40-120 cps., noted a small increase in Q with decreasing frequency, the gradient being greater at the lower frequencies. Usher in 1962 (2-40 cps.) noted a similar frequency dependence of Q by an improved apparatus reducing the error to within 10 percent. The variation of Q amounted to as much as 100 percent but most of it occurred between 2 and 10 cps., thus explaining the failure of other workers, using higher frequencies, to observe it. A brief review of laboratory measurements of internal friction in different rock types over different frequency ranges by various investigators is given in Table 2. Usher (1962) studied the effect of oil and water also on internal friction (Table 3).

The variation of Q in rocks in situ can be studied by two different means,

- (i) by measuring the amplitude as a function of the distance, and
- (ii) by examining the frequency spectrum of the wave at various distances.

The first type of experiments were performed by Evison (1951), Collins and Lee (1956) and Mac Donald (1959), and point to the frequency independence of Q . But these results are largely inconclusive.

Gutenberg (1935), Kendal (1941), and Ricker (1953), have followed the second line of

approach using frequencies below 50 cps. and have found a linear relationship between Q and the time period. Born (1941), using frequencies in the range (200-4000 cps.) also concluded that Q was independent of frequency but varied when a certain amount of moisture was present. Internal friction would thus appear to have two components, one suggesting a solid friction type of mechanism and the other a viscous type. Usher's (1962) results are more relevant to the seismic wave propagation as they pertain to low frequencies encountered in seismic work. They suggest a solid viscous type of mechanism operating at low frequencies which are probably associated with the grain boundaries. However, more experimental work in the low frequency region under varying pressure would permit more realistic correlation between laboratory rock samples and the rocks in situ.

Table 4, contains a valuable set of field results giving absorption coefficient, k , and the corresponding internal friction ($1/Q$) for different waves with different periods. The data show that the absorption in the case of surface waves, varies considerably with period, being smaller for longer periods and vice versa. Karnik (1956) combined data for Rayleigh waves with periods of between 0.001 sec. ($k=200$ per kilometer) and 200 secs. ($k=0.00002$ per kilometer) and found that all data can be represented fairly well by the following expression,

$$k = 0.017 (T)^{-1.42} \quad (14)$$

Furthermore, the value of the absorption coefficient depends on the path which the corresponding wave has travelled. Gutenberg (1945a) obtained the following value of k corresponding to 20 secs. period for different paths.

Continental path,	$k = 0.00016$
Around the earth or across the Pacific,	$k = 0.00030$
Along the boundary of the Pacific,	$k = 0.00050$

He attributes the loss of energy along different paths, just mentioned, to reflection and diffraction of waves along the part of the path which crosses and recrosses repeatedly the discontinuity between the Pacific and the continental structure. The G waves with wave lengths of several hundred kilometers, much in excess of the probable maximum depth at which there is a distinct difference in elastic constants and density between the material below the Pacific Basin and the surrounding continents, do not seem to show any similar loss of energy.

However, the available data seem to be very scanty and more data for the value of absorption coefficients corresponding to different periods and paths, would be required to extend the methods of magnitude determinations of Gutenberg and Richter for maximum amplitudes of surface waves corresponding to 20 secs., to that corresponding to other periods.

On the other hand the data for body waves show that $k = 0.00006$ is fairly constant over waves of different periods.

Equation (2) could now be further modified as follows in order to include the dissipative effects discussed above. Thus,

$$y = KTZ \sqrt{(F_1 \dots F_n) E \cdot \frac{\cos i}{\sin e \cdot \sin \Delta} \left(\frac{di}{d\Delta} \right) \cdot e^{-2k\Delta}} \quad (15)$$

The distance along the wave path has been replaced by the epicentral distance Δ , as this involves only a small error within tolerable limits, for most seismic waves which do not encounter the core mantle boundary.

The various quantities involved in equation (15) can be computed for various conditions. Thus the term $\left(\frac{di}{d\Delta} \right)$ is a function of velocity along the path, Z is a function of the angle of emergence and the Poisson's ratio just below the surface, and the F_n depends upon the angle of incidence at the discontinuity, the wave type, and the value of density and wave velocity on either side of the discontinuity. It is, therefore, possible to prepare tables of Z and F_n for given types of waves and discontinuities.

5. Dispersion

The change of wave velocity with period is known as dispersion. This phenomenon in fact does not lead to any dissipation of energy, but to a lengthening of the pulse. The life-time of a pulse undergoing dispersion is thus increased at the expense of its amplitude. We may consider the dispersion of surface waves and body waves separately.

SURFACE WAVE DISPERSION

Whenever the velocity of seismic waves changes with depth h in the earth, the surface waves undergo dispersion, as the velocity of surface waves depends on λ/h where λ is the wave length.

The equation for the velocity of Rayleigh waves, propagating along the free surface, of the earth regarded as plane, is given by,

$$\frac{C^6}{\beta^6} - 8 \frac{C^4}{\beta^4} + C^2 \left(\frac{24}{\beta^2} - \frac{16}{\alpha^2} \right) - 16 \left(1 - \frac{\beta^2}{\alpha^2} \right) = 0 \quad (16)$$

where α , β , and C are respectively the longitudinal, transverse and the Rayleigh wave velocities in the medium.

The expression for C does not show any dispersion effect, but the earth is not homogeneous as is assumed here. The theory of Rayleigh waves in the presence of two and three layers have been worked out by Stoneley and Tillotson, and the equations for velocity show that the waves are dispersed.

The equation for the velocity C' of Love waves in the presence of a surface layer with transverse wave velocity β' overlying a homogeneous medium with transverse wave velocity β , so that $\beta' < C' < \beta$, is given as:

$$\mu \left(1 - \frac{C'^2}{\beta^2} \right)^{\frac{1}{2}} - \mu' \left(\frac{C'^2}{\beta'^2} - 1 \right)^{\frac{1}{2}} \cdot \tan \left[KH' \left(\frac{C'^2}{\beta'^2} \right)^{\frac{1}{2}} \right] = 0 \quad (17)$$

where $K = \frac{2\pi}{\lambda}$, λ being the wave length.

Equation (17) shows that the velocity depends on K i.e., the wave length and hence on the period, causing dispersion of Love waves.

The disturbance, in surface waves, propagates in groups of waves which tend to become sinusoidal as the travel time T and the epicentral distance Δ increase, the periods being approximately the same at different stations for groups whose group velocity $C = \frac{\Delta}{T}$ is the same. The group velocity C in terms of phase velocity C' is given as

$$C = C' - \lambda \left(\frac{dC'}{d\lambda} \right) \quad (18)$$

The surface wave equations as cited above and the more generalized ones may be used to fit the broad features of the observed dispersion of earlier arriving surface waves. The equation (17) for the velocity of Love waves entails a sinusoidal dispersion of an initially confined disturbance.

Jeffreys (1959, page 39), has given an approximate expression for the displacement caused by a surface wave undergoing dispersion. The main features of the expression include a factor common to all wave groups which will cause the ratios of the amplitudes of waves of given periods to be constant on the Earth's outer surface. However, the amplitude would vary according to the wave group, the nature of the initial disturbance and that of dispersion.

BODY WAVE DISPERSION

The cause of irregular dispersion, of body waves or more correctly of their oscillatory motion, is not yet clearly understood. Jeffreys has considered the effects of scattering, the complex initial conditions at the focus, fluctuations in the local gravity value during the passage of a disturbance, imperfections in elasticity and the departures from homogeneity within the earth. If the original disturbance at the focus is assumed to be oscillatory, it would explain oscillations in P and S , but in such a case the duration of the oscillations should be the same for all distances whereas it is actually observed to increase with distance. The cause of bodily wave dispersion must therefore be sought in terms of heterogeneities inside the earth, most probably in the outermost 40 km., but the precise way in which it occurs must await more detailed knowledge of the crustal structure than is yet available. The following suggestions seem to hold promise:

- (i) diffuse refraction at irregular interfaces in the crustal layers,
- (ii) subsidiary waves arising from the fact that the travel times of reflected waves, though stationary are not true minima,
- (iii) The longitudinal and transverse wave velocities have been derived on the assumption that the density ρ , compressibility k' and rigidity μ are constant.

But these conditions do not hold rigorously as they are functions of initial strain, temperature and chemical composition. To a first approximation we may take ρ , k' and μ as slowly varying functions of depth between a limited number of surfaces of discontinuity within the earth. Since in the derivation of the equation of motion, viz.,

$$\rho f_i = \left(k' + \frac{\mu}{3} \right) \frac{\partial \theta}{\partial x_i} + \mu \nabla^2 u_i \quad (19)$$

terms involving $\frac{\partial k'}{\partial x_i}$ and $\frac{\partial \mu}{\partial x_i}$ are assumed to be zero, which no longer holds if k' and μ are taken as variables, additional terms would appear in the wave equations,

$$\frac{\partial^2 \theta}{\partial t^2} = \left(\frac{k + \frac{4}{3}\mu}{\rho} \right) \nabla^2 \theta \quad (20)$$

$$\frac{\partial^2 \xi}{\partial t^2} = \left(\frac{\mu}{\rho} \right) \nabla^2 \xi \quad (21)$$

The result would be a dispersion of body waves analogous to the dispersion of surface waves. Such an effect would be pronounced if longitudinal and transverse wave velocities vary significantly over distances comparable with the predominating wavelengths of the disturbance, and such changes in both horizontal and vertical components are most likely to occur in the crust of the earth (outermost 40 km) and probably contribute to the observed dispersion of body waves. The details are not yet clearly understood. In the mantle, except perhaps in the neighbourhood of a limited number of discontinuities ρ , k' and μ change sufficiently slowly and the dispersion effects may be neglected.

CONCLUSION

Damage to structures is mainly caused by the horizontal component of the ground acceleration. The longitudinal waves are, therefore, relatively harmless to structures as the resulting acceleration is mainly in the vertical direction and hardly ever exceeds that due to gravity, which the structures are normally able to withstand. We are thus, chiefly interested in the various attenuating effects on shear waves. These will include the bodily transverse waves and the surface waves. The ground acceleration depends both upon the frequency of vibration and its amplitude. At greater distances from the epicentre the surface waves in spite of their longer periods have greater effect as they lose their energy less rapidly by divergence. It is also commonly assumed that both the effects of scattering and of internal friction are more significant for shear waves than for the compressional waves as the stresses involved are deviatoric rather than symmetrical. However, it is extremely difficult to give a quantitative definition of these effects particularly of scattering in the crust which widely varies in character.

Furthermore, the amplitudes of ground motion arising from nearby shocks are of great interest to Earthquake Engineers. But no general theory can be produced for these owing to extremely complicated conditions obtaining near the source. The amplitudes of near earthquake phases, however, seem to fall something like the inverse of distance, with an irregular variation superposed on it. An estimation of this latter effect seems to be fraught with difficulties at this stage owing to our lack of clear understanding of the actual mechanisms of the Earthquakes involved.

So far the general processes which contribute to the loss of energy in a progressive wave have been outlined. However, for particular cases additional terms would force consideration. Thus, while discussing the divergence effect, it was assumed that the energy is transmitted equally in all directions. Besides the anisotropy of the region surrounding the focus, the nature of the source and the manner of energy release may prevent the equipartition of energy by all azimuths.

Furthermore, it has been observed that the amplitudes of waves (Kazim Ergin, 1953) reflected at the mantle core boundary show anomalous behaviour i.e., they have larger amplitudes than could be predicted theoretically. This may be caused by a particular type of anisotropy which, however, lacks a general theory.

Similarly, while computing the amplitudes of surface waves it would be essential to consider additional factors which may arise from circumstances such as the linear extension of the focus, and from the occurrence of disturbances under varying depths of the oceans.

APPENDIX

An expression for the ground displacement at an epicentral distance Δ due to energy propagated in body waves can be obtained under simplified conditions. These are,

- (i) that the Earth is spherically symmetrical about its centre,
- (ii) that the conditions of ray theory obtain, and
- (iii) that the surfaces of discontinuity are distant enough from the source to permit the application of plane wave theory of reflection and refraction.

Let us consider a group of waves which travel outwards from F in all directions between the angles i and $(i+di)$ forming a conical shell (see figure 1) which will subtend a solid angle equal to $\frac{2\pi r^2 \cos i \, di}{r^2}$

If E be the energy passing through unit solid angle, the total energy in the shell will be equal to $2\pi E \cos i \, di$.

If the earth is treated as being spherically symmetrical and FO, a polar axis (figure 2) these group of waves will emerge on the surface of the earth bounded by the colatitudes Δ and $(\Delta+d\Delta)$. Using spherical coordinates, the area of this region can be readily seen to be

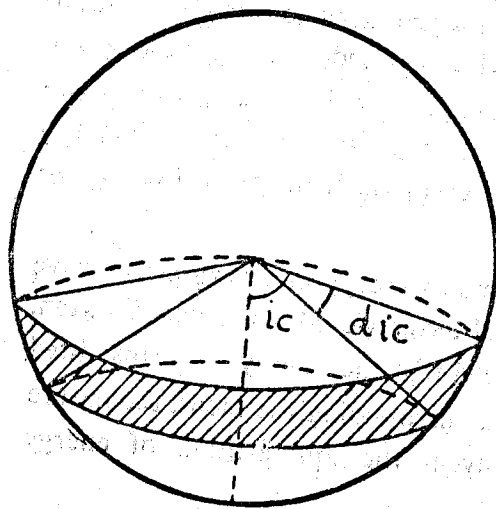


Figure 1

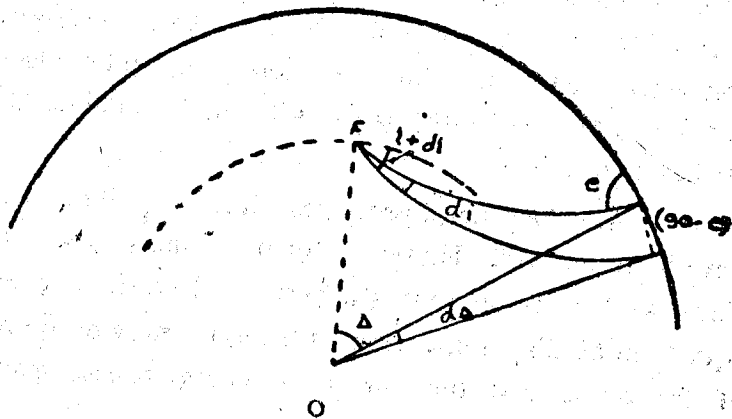


Figure 2

equal to $2\pi R^2 \sin \Delta d\Delta$ and that of the emergent wavefront to $2\pi R^2 \sin \Delta d\Delta \cdot \sin e$. Therefore the energy per unit area of the wavefront emergent at E can be written as

$$\frac{E \cos i \, di}{R^2 \sin e \sin \Delta \, d\Delta} \quad (A-1)$$

It can be further shown that the mean energy per unit wavelength of a train of waves is directly proportional to the square of its amplitude and inversely proportional to the amplitude of its period and therefore,

$$A = \frac{T}{C} \sqrt{\frac{E \cos i}{R^2 \sin \Delta \sin e} \left(\frac{di}{d\Delta} \right)} \quad (A-3)$$

where, C is a constant.

If K denotes another constant determining the fraction of the energy, E, actually passing into the wave under consideration (P, SV, or SH) and Z the ratio of ground displacement to the wave amplitude, we can write the resultant ground displacement y as,

$$y = K T Z \sqrt{\frac{E \cos i}{R^2 \sin \Delta \sin e} \left(\frac{di}{d\Delta} \right)} \quad (A-3)$$

REFERENCES



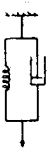
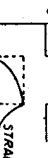
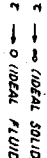
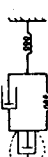
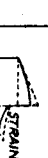
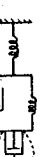
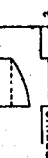
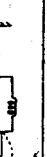


- Bath, M., (1958), "Ultra Long Period Motions from the Alaska Earthquake of July 10, 1958" *Geofis. Pura. e. Appl.*, 41, pp. 91-100;
 Bath, M., and A. L. Arroyo, (1962) "Attenuation and Dispersion of G Waves," *J. G. Res.*, 67, pp. 1933-1942.
 Birch, F., (1942) "Internal Friction in Vibrating Solids," *Handbook of Physical Constants*,

Geolog. Soc. Am., Spec. Paper, 36, pp. 89-92.

- Birch, F., and D. Bancroft (1938), "Elasticity and Internal Friction in a long Column of Granite," *Bull. Seism. Soc. Am.*, 28, pp. 243-254.
- Born, W. T., (1941) "The Attenuation Constant of Earth Materials," *Geophysics*, 6, pp. 132-148.
- Bruckshaw, J. M. and P. C. Mahanta, (1954) "The Variation of the Elastic Constants of Rocks with Frequency," *Petroleum*, 17, p. 14,
- Bullen, K. E., (1953) "An Introduction to the Theory of Seismology," C. U. P.
- Bullen, K. E., (1954) "Seismology," Methuen's Monographs on Physical subjects.
- Ewing, M., and F. Press, (1954a) "An Investigation of Mantle Rayleigh Waves," *Bull. Seism. Soc. Am.*, 44, pp. 127-147.
- Ewing, M. and F. Press, (1954b) "Mantle Rayleigh Waves from the Kamchatka Earthquake of November 4, 1952" *Bull. Seism. Soc. Am.* 44, pp. 471-479.
- Förtsch, O., (1956) "Die Ursachen der Absorption Elastischer Wellen," *Annali di Geofis.*, 9, pp. 469-524.
- Gutenberg, B., (1945a) "Amplitude of Surface Waves and Magnitudes of Shallow Earthquakes," *Bull. Seism. Soc. Am.*, 35, pp. 3-12.
- Gutenberg, B., (1945b) "Amplitudes of P, PP and S and Magnitudes of Shallow Earthquakes," *Bull. Seism. Soc. Am.*, 35, pp. 57-69.
- Gutenberg, B., (1958) "Attenuation of Seismic Waves in the Earth's Mantle," *Bull. Seism. Soc. Am.* 48, pp. 269-282.
- Gutenberg, B., (1959) "Physics of the Earth's Interior," Academic Press, New York.
- Jeffreys, H., (1926) "On the Amplitudes of Bodily Seismic Waves," *Mon. Not. Roy. Astr. Soc., Geophys. Suppl.*, 1, pp. 334-348.
- Jeffreys, H., (1931a) "Damping in Bodily Seismic Waves," *Mon. Not. Roy. Astr. Soc. Geophys. Suppl.* 2. pp. 318-323.
- Jeffreys, H., (1931b) "On the Cause of Oscillatory Movement in Seismograms," *Mon. Not. Roy. Astr. Soc., Geophys. Suppl.* 2, pp. 407-416.
- Jeffreys, H., (1958) "A Modification of Lomnitz's Law of Creep in Rocks," *Geophys. J.*, 1, pp. 92-95.
- Jeffreys, H., (1963) "The Earth," 4th ed., Cambridge University Press.
- Karnik, V., (1956) "Magnitudenbestimmung Europäischer Nahbeben," *Travaux. Inst. Geophys. Acad. Tchecoslov. Sci.* 47, p. 124.
- Knopoff, L., and G. J. F. Mac Donald, (1958) "Attenuation of Small Amplitude Stress Waves in Solids," *Reviews of Modern Physics.*, 30, pp. 1178-1192.

- Lomnitz, C., (1956) "Creep Measurements in Igneous Rocks," J. Geol., 64, pp. 473-479.
- Lomnitz, C., (1957) "Linear Dissipation in Solids," J. Appl. Phys., 28, pp. 201-205.
- Lomnitz, C., (1962) "Application of Logarithmic Creep Law to Stress Wave Attenuation in the Solid Earth" J. Geophys. Res., 67, pp. 365-367.
- Mac Donald, G. J. F., et al, (1958) "Attenuation of Shear and Compressional Waves in Pierre Shale." Geophysics, 23, p. 421.
- Mac Donald, G. J. F., (1959) "Rayleigh Wave Dissipation Functions in Low Media," Geophysics J., 2, pp. 89-100.
- Sato, Y., (1958) "Attenuation, Dispersion and the Wave Guide of the G Wave," Bull. Seism. Soc. Am, 48, pp. 231-251.
- Usher, M. J., (1962) "Elastic Behaviour of Rocks at Low Frequencies," Geophysical Prospecting, 2, pp. 119-127.

TABLE 1

Model	Strain-Stress relation	Mechanism	Effect upon $\frac{\Delta \epsilon}{\Delta t} \propto \dot{\epsilon}$	Strain Time Graph
1. Maxwell : (elasticoviscosity)	$2\mu \dot{\epsilon} = \dot{p} + p/\tau$		$\epsilon = \text{CONSTANT AT L.F.}$ $\epsilon \propto \frac{1}{f}$ AT H.F.	
2. Voigt : (firmoviscosity)	$\epsilon + \tau \dot{\epsilon} = p/\mu$		$\epsilon \propto f$ AT L.F. $\epsilon = \text{CONSTANT AT H.F.}$	
3. Solido-fluid :	—	VISCOS COMBINATION OF SPRING AND DASHPOTS OF VARIABLE RELATIVE SIZE	$\epsilon \propto f$ AT L.F. $\epsilon \rightarrow 0$ (LARGE τ)	
4. Boltzmann : (creep function, ϕ and memory function, ψ)	$\epsilon(\tau) = \frac{1}{\mu} \left[p(\tau) + \int_{-\infty}^{\tau} p(t) \dot{\phi}(\tau-t) dt \right], p(\tau) = \mu \left[\epsilon(\tau) - \int_{-\infty}^{\tau} \epsilon(t) \dot{\psi}(\tau-t) dt \right]$	A COMBINATION OF SPRINGS AND DASHPOTS	NOT GENERALLY SOLUBLE TO PRODUCE A MAXIMUM AT SOME FREQUENCY	
5. Sokoloff and Scriabin : Simplification of Boltzmann's memory function.	$\psi = B e^{-b(\tau-t)}$ in Boltzmann's relations, where B, b are constants.		$\epsilon \rightarrow 0$ AT V.L.F. $\epsilon \rightarrow 0$ AT V.H.F.	
6. Lomnitz : Simplification of Boltzmann's creep function.	$\dot{\phi} = q \log(1 + a t)$ in Boltzmann's relations, q, a are constants.		$\epsilon = \text{CONSTANT}$	
7. Jeffreys : Modification of Lomnitz's law of creep in Rocks.	$\dot{\phi}(t) = \frac{q}{a} \left\{ 1 + a t \right\}^a - 1$		$\epsilon = \text{CONSTANT}$	
8. Knopoff : Solid Friction.	Dissipative forces proportional to applied forces.		$\epsilon = \text{CONSTANT}$	
9. Thermal Mechanisms :	—	THERMAL ISOTHERMAL AND ADIABATIC	MAX ϵ AT V.L.F.	

Not:—The functions ϕ and ψ in models 4, 5, 6 and 7 are related as follows:

$$L(\psi) = L(\phi) / [1 + L(\phi)],$$

where $L(\psi)$ is the Laplace Transform of ψ .

TABLE 2

Internal Friction for Different Kinds of Rocks in Different Frequency Ranges.

Rock	Investigator	Frequency Range (Cycles per sec.)	Internal Friction $\frac{1}{Q} \times 10^{-3}$	$\frac{\Delta E}{E}$
Sylvan Shale	Born	3000-12,000	14.3	0.09
Hunton Limestone	"	2000-10,000	14.3	0.09
Amherst Sandstone	"	900-4000	17.5	0.11
Cockfield Yequa	"	3000-11,000	14.3	0.09
Solenhofen Limestone	Birch and Bancroft	about 10,000	6.7	0.042
Slate (Pa)	"	" "	3.8	0.024
Quincy Granite	"	" "	10.0	0.063
Rockport Granite	"	" "	7.7	0.048
Diabase	"	" "	1.7	0.011
Quincy Granite	"	140 - 1600	5.0-10.0	0.03-0.06
(Very soft) Sandstone	Bruckshaw and Mahanta	40 - 120	47.8	0.3
Oolite	"	" "	23.9	0.15
Shelly Limestone	"	" "	15.9	0.10
Granite	"	" "	15.9	0.10
Dolerite	"	" "	9.6	0.06
Diorite	"	" "	7.2	0.045
Chalk	Evison (seismic)	600	12.7	0.08
Various Sedimentary Rocks	Born "	Seismic	12.7-19.1	0.08-0.12
" "	Howell "	"		
Pierre Shale	MacDonal,,	500	7.7	0.048

(Contd.)

			Average $1/Q$ (2 c/S)	Average $1/Q$ (40 c/S)	Average $\Delta E/E$ (2 c/S)	Average $\Delta E/E$ (40 c/S)
Dolerite	Usher	2 - 40	2.2	5.4	0.014	0.034
Diorite	"	" "	2.4	5.1	0.015	0.032
Old Red Sandstone	"	" "	8.0	13.5	0.050	0.085
Micaceous Sandstone	"	" "	5.6	11.8	0.035	0.074
Oolite Limestone	"	" "	3.2	6.7	0.020	0.042
Slate	"	" "	1.9	4.1	0.012	0.026
Chalk	"	" "	5.6	9.1	0.035	0.057
Shelly Limestone	"	" "	1.6	3.8	0.010	0.024
Millstone grit	"	" "	5.91	23.9	0.10	0.15
Tufnol	"	" "	7.9	9.5	0.05	0.06
Wood	"	" "	6.4	7.0	0.040	0.044
Asbestos	"	" "	3.8	8.9	0.024	0.056

TABLE 3
Effect of Water and Oil on Internal Friction.

Rock	Saturation Moisture (by weight)	40 C/S, dry		40 C/S, Saturated	
		$\frac{\Delta E}{E}$	$\frac{1}{Q} \times 10^{-3}$	$\frac{\Delta E}{E}$	$\frac{1}{Q} \times 10^{-3}$
Dolerite	0.25%	not measurable			
Oolitic Limestone	5%	0.032	5.4	0.06	9.6
Millstone grit	9%	0.14	22.3	0.30	47.8
Micaceous Sandstone	1.0%	0.08	12.7	0.32	50.9
Old Red Sandstone	4.0%	0.07	11.1	0.24	38.2
Old Red Sandstone(OIL)	3.0%	0.07	11.1	0.41	65.3

TABLE 4

Absorption Coefficient (k) for Amplitudes, and the corresponding internal friction ($\frac{1}{Q}$) for different waves with different periods, obtained from the earthquake Records.

Reference	Wave Type	Period (Sec)	Absorption Coefficient K (km ⁻¹) x10 ⁻⁶		Internal Friction $\frac{1}{Q}$ x10 ⁻³	
(a) Surface Waves						
Gutenberg (1924)	Love	100 ±	100		14.29	
Sato (1958)	G	360	New Guinea	Kamchatka	New Guinea	Kamchatka
" "	G	216	23	28	13.5	19.0
" "	G	108	25	31	8.5	12.0
" "	G	72	58	35	9.0	11.0
" "	G	54	77	71	8.0	8.0
" "	G	43	79	—	6.0	—
" "	G	43	75	—	4.0	—
Press, Ben-Menaham and Toksoz (1961)	G	400	—		10.95	
" "	G	200	—		10.52	
" "	G	100	—		8.19	
Bath and A.L. Arroyo (1962)	G	300	28.2		13.76	
" "	G	200	25.6		7.92	
" "	G	150	34.9		7.90	
" "	G	120	53.0		9.47	
" "	G	100	69.4		10.25	
" "	G	86	82.3		10.35	
" "	G	75	88.7		9.72	
Gutenberg (1945 a)	Rayleigh	20	200		5.0	
Ewing and Press (1954 a)	Rayleigh	215	22		6.65	
" "	Rayleigh	140	36		6.73	
Ewing and Press (1964 b)	Rayleigh	250-350	8		4.10	
Bath (1958)	Rayleigh	120-260	—		4.80	
Press, Ben-Menahem, and Toksoz (1961)	Rayleigh	400	—		6.96	
" "	Rayleigh	200	—		5.72	
" "	Rayleigh	100	—		8.92	
(b) Body Waves						
Gutenberg (1945 b)	P,PKP	4 ±	60		.8	
Gutenberg (1958)	P,PP	2	60		.4	
" "	P,PP	12	60		2.5	
" "	S	12	60		1.4	
" "	S	24	60		2.5	
Press (1956)	S	11	(90)		2.0	
Benioff Press and Smith(1961)	Free Oscillations	375-500	—		5.7	
" "	"	666	—		7.5	
Jeffreys (1959)	Nutation	37 × 10 ⁶	—		25.0	

A STUDY OF LONGITUDINAL WAVE VELOCITY VARIATION IN THE CRUST

M. R. Thapar*

SYNOPSIS

In different parts of the earth seismic wave velocities in the crustal layers have been determined from mainly two sources (1) Seismic refraction technique as applied in explosion seismology (2) The observational or Earthquake Seismology. For the Indian Region, travel time curves have been drawn for different parts which show different velocities of transmission of longitudinal waves in the crustal layers under these parts.

INTRODUCTION

Various Geophysical and Geological investigations have shown that the crust of the earth can be divided into layers of varying thicknesses. It has been shown on the basis of the velocities of seismic waves obtained either from a natural earthquake or explosion seismology, that the crust can be divided into various layers. The main layers above the Mohorovicic discontinuity are called (1) Granitic Layer (2) Intermediate layer and below these layers is the Mantle and termed as Basaltic layer. The thicknesses of these layers vary accordingly as the thickness of the crust varies from 33 Km. to 50 Km. under the continents (exceptional thickness under the mountain ranges upto 70 Km.) to 16 Km. under the sea.

The longitudinal waves travelling through these three layers are termed as P_g , P^* and P_n . It is known that the crust possesses large amount of lateral inhomogeneities i.e. the elastic constants vary according to the distribution of material and thus accounting for the different velocities of P_g , P^* , P_n with which these waves have been found to travel in different parts of the earth's crust. Subsequently, from the calculated velocities of these waves, from observed travel times, give us an idea about the elastic inhomogeneities in the crustal structure.

DETERMINATION OF SEISMIC VELOCITIES IN THE CRUSTAL STRUCTURE

Seismologists have resorted to various measuring techniques in order to determine the crustal structures and the seismic wave velocities under the continents and oceans. Refraction techniques in explosion seismology and travel times in earthquake seismology have been used in the determination of these wave velocities.

I. Seismic Refraction Technique in Explosion Seismology as Applied in the Oceans

Seismic-Refraction Measurements in the Atlantic ocean, in the Mediterranean Sea, on

*Senior Scientific Officer, Regional Research Laboratory, Jorhat, Assam—Attached to School of Research and Training in Earthquake Engineering, University of Roorkee, Roorkee (India)

the Mid-Atlantic Ridge, and in the Norwegian Sea, have shown the following values for seismic wave velocities and the crustal structure under the oceans.

(i) Western Basins of the North Atlantic Ocean

(a) Crustal section of 1/2 to 1 Km. thick of low velocity sediments.

(b) Crustal rock 4 to 6 Km. thick and of seismic velocity is about 6.5 Km/Sec.

(c) Sub bottom reflections have shown that there is a layer of 1-2 Km. thick and of 4.5 - 5.5 Km/Sec. between layers (a) and (b).

(d) Below these layers is the mantle with a velocity of 8 Km/sec. at the Mohorovicic discontinuity.

(ii) Measurements in the eastern basin show similar values except a velocity of 7.7 - 7.8 Km/sec. at the Moho's discontinuity.

(iii) Measurements in the Mediterranean Sea show only low velocity sediments underlain by a refracting layer in which the average velocity is about 4.5 Km/sec.

(iv) On the Mid Atlantic Ridge the sediments are underlain by two refracting layers with velocities averaging 5.6 and 7.4 Km/sec. respectively. The results indicate that the ridge has been built by the upwelling of the great amounts of basalt magma come from convection currents deep in the mantle. Low velocity layer 1.70 - 1.80 Km/sec. is assumed.

(v) Between North America and Mid Atlantic Ridge.

5.15 Km. of water

1.49 Km. of sediments velocity 1.7 to 4.5 Km/sec.

4.02 Km. of "Oceanic-Layer" rocks,

Mean velocity 6.36 - 6.88 Km/sec.

Subcrustal mantle has a velocity 7.81 to 8.08 Km/sec.

(vi) Seismic refraction measurements in the Gulf of Mexico show that the layers with velocities between 2.25 and 6.0 Km/sec. are the only additions to a standard Atlantic Oceanic column. The third layer has been found to be of 5.0 Km/sec. velocity and predicted to be a thin limestone underlain by huge thicknesses of sediments, because the wave with the velocity of 5.0 Km/sec. disappears from the travel time curves after greater distances.

II. Seismic Refraction Technique in Explosion Seismology as Applied in the Continents

(i) *Measurements over Emerged and Submerged Atlantic Coastal Plain*

Seismic refraction profiles shot on the continental rise and slope south of the Grand banks show great sediments thickness which reaches a maximum of 10 Km. and thins down under the banks. These sedimentary layers are present, with average velocities of 1.83, 2.47, and 3.97 Km. per second. The basement is

thickest under the south edge of the continental shelf and thins down to 2 or 3 Km. to the north and to the south. Its average velocity is 5.77 Km/sec. and on the southernmost profile where it is 6.70 Km/sec. Sub-basement is reached at a depth of about 13 Km. and has velocity of about 7.76 Km/sec. to 7.24 Km/sec.

Unconsolidated sediments have got a thickness of 0.5 Km. and an average velocity of 1.83 Km/sec. Semiconsolidated sediments are of 2.7 Km. thickness and average velocity 2.47 Km/sec. Consolidated sediments have an average velocity of 3.97 Km/sec. and the thickness is 6.8–3 Km. The average basement and sub-basement velocities are 5.73 Km/sec. and 7.53 Km/sec. respectively.

(ii) *Measurements on the floor of Yosenite Valley California*

The uppermost layer in the valley fill has a velocity of 1.7 Km/sec. and is only 150 m. in thickness. The intermediate layer in the valley fill has a velocity of 2.5 Km/sec. and 220 m. in thickness and at the Bridalveil Meadow where it becomes the surface layer having a velocity of 2.1 Km/sec. The basal layer is 300 m. in thickness and of 3 Km/sec. velocity.

(iii) *Seismic Explosion and refraction measurements in the Vancouver Island-strait of Georgia area of western Canada.*

The average structure derived for the area consists of a layer of volcanic and granite strata less than 5 Km. in thickness and an intermediate layer with a constant velocity for compressional waves of 6.66 Km/sec, 46 Km. thick. A velocity of about 7.7 Km/sec. for the mantle has been observed.

(iv) *A seismic survey in the Canadian shield*

Average velocity for the intermediate layer has been found to be 6.234 ± 0.012 Km/sec.

(v) *Rock bursts at Kirkland Lake Ontario*

'P' velocities for the intermediate layer and at the Mohoronic discontinuity are 6.246 ± 0.015 Km/sec. and 7.913 ± 0.125 to 8.176 ± 0.013 Km/sec. respectively. The average crustal thickness of this crust, based on the 'P' waves is 35.4 ± 5.5 Km.

III. Nuclear Detonations and their Recording at Seismological Observatories

Seismological Records of Nuclear detonations have been analysed for crustal investigations. Some measurements have also been done by this technique in Japan. The Seismic Refraction technique has been more successfully and commonly employed than the Earthquake Seismology in determining the seismic waves velocities and thicknesses of different crustal

layers. Many more examples of the successful application of this particular technique in this field can be cited.

VI. Earthquake Seismology

Determination of seismic wave velocities and crustal structure from the earthquake records can be carried out with the help of different phases of the record. P_g , P^* , P_n waves velocities can be calculated from the records of earthquakes and then used for determination of crustal thickness. Shear wave velocities have also been used along with longitudinal wave velocities to determine the thicknesses of the crustal layers. Dispersion curves of surface waves have also been used to find out the thicknesses of the crustal layers.

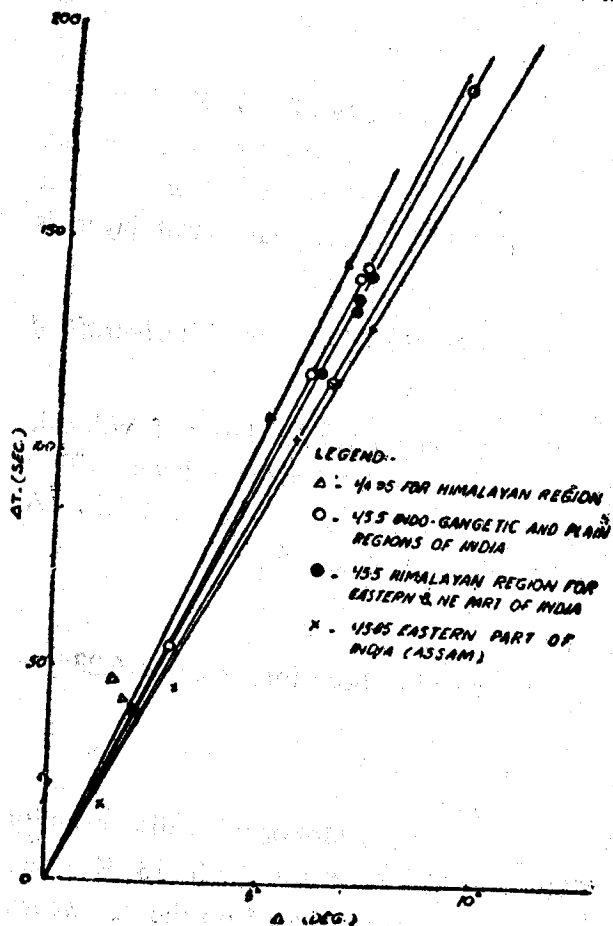


Figure 1 T Vs. Δ° For P_g .

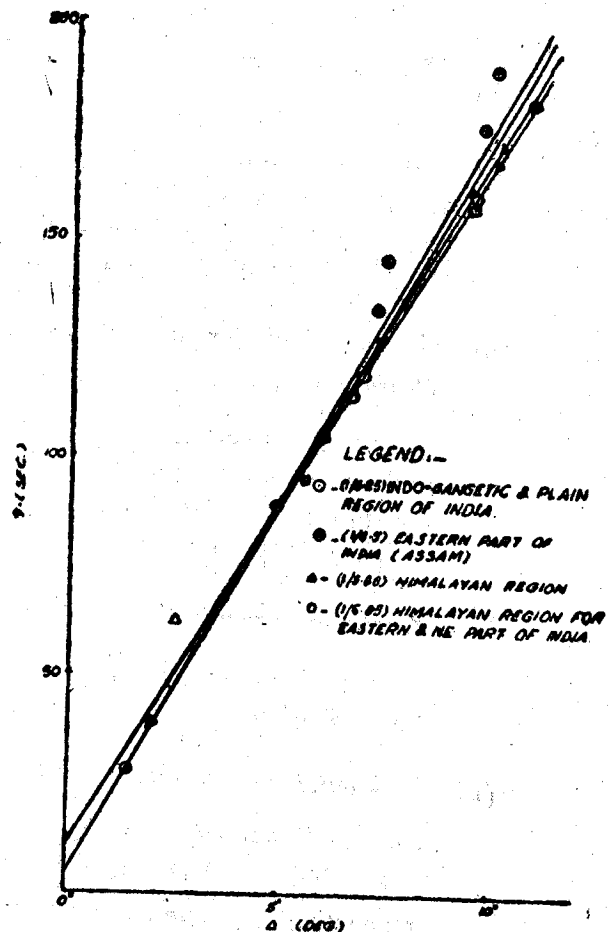


Figure 2 T Vs. Δ° For P^*

Velocities for the longitudinal waves propagated through different crustal layers can be known by plotting travel time curves for a region. If the distances involved are small then the travel-time curves are straight lines which is quite a good approximation. It is evident that these different phases known as P, P^* , P_g were discovered from the observation of earthquake records. A. Mohorovicic (1909) found out from earthquake records of Kulpa Valley, Grotia, on 1909 October 8, that two distinct P and two S pulses were present. The faster

pair were identified with the P and S traceable to large distances. The new pair were denoted by \bar{P} and \bar{S} , a notation still extensively used and this has been termed as P_g and S_g for convenience, P and S, however were refracted down into the deeper layers and propagated at a greater velocity and later on refracted upto the surface.

After this work of A and S. Mohorovicic and Gutenberg the next great advance was made by V. Conrad (1925) in a study of the Tavern (Austria) earthquake of 1923 Nov. 28. He discovered a fifth phase P^* in addition to the above mentioned phases. This appeared to have travelled in a intermediate layer having a velocity of propagation between P and P_g . P.L. Willmore (1949) made a detailed study of the Heligoland explosion of 1947 April 18. His results for the velocities were in Km/sec. P, 8.18 ± 0.14 , P^* , 6.4 ± 0.16 , P_g variables.

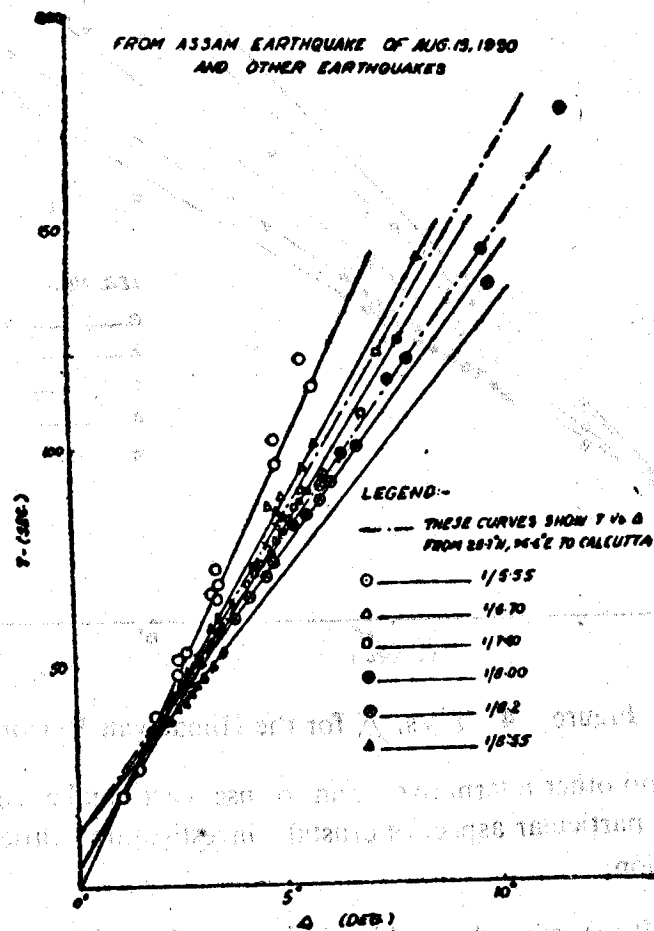


Figure 3 T Vs. Δ For Plains, Brahmaputra Valley & Assam Plateau

Extensive studies of near earthquakes have been made by Gutenberg, Byerly and their collaborators in California. Gutenberg's data (1932) for P_g correspond to 5.58 ± 0.023 Km/sec. for P, 7.92 ± 0.05 Km/sec. For intermediate layers Gutenberg associated two velocities of 6.83 and 6.05 Km/sec. Extensive studies of near earthquakes in Japan have been made by Matuzawa et al (1928). Velocities in Km/sec. are given as : P_g , 5.0 P^* , 6.2, P, 7.5.

Many more seismologists have made some studies regarding the velocities of these phases, in Japan, England and California.

INDIAN REGION

In this continental part of the earth no Seismic Refraction Technique in explosion seismology has been used to investigate the crustal layers. Seismologists engaged in such

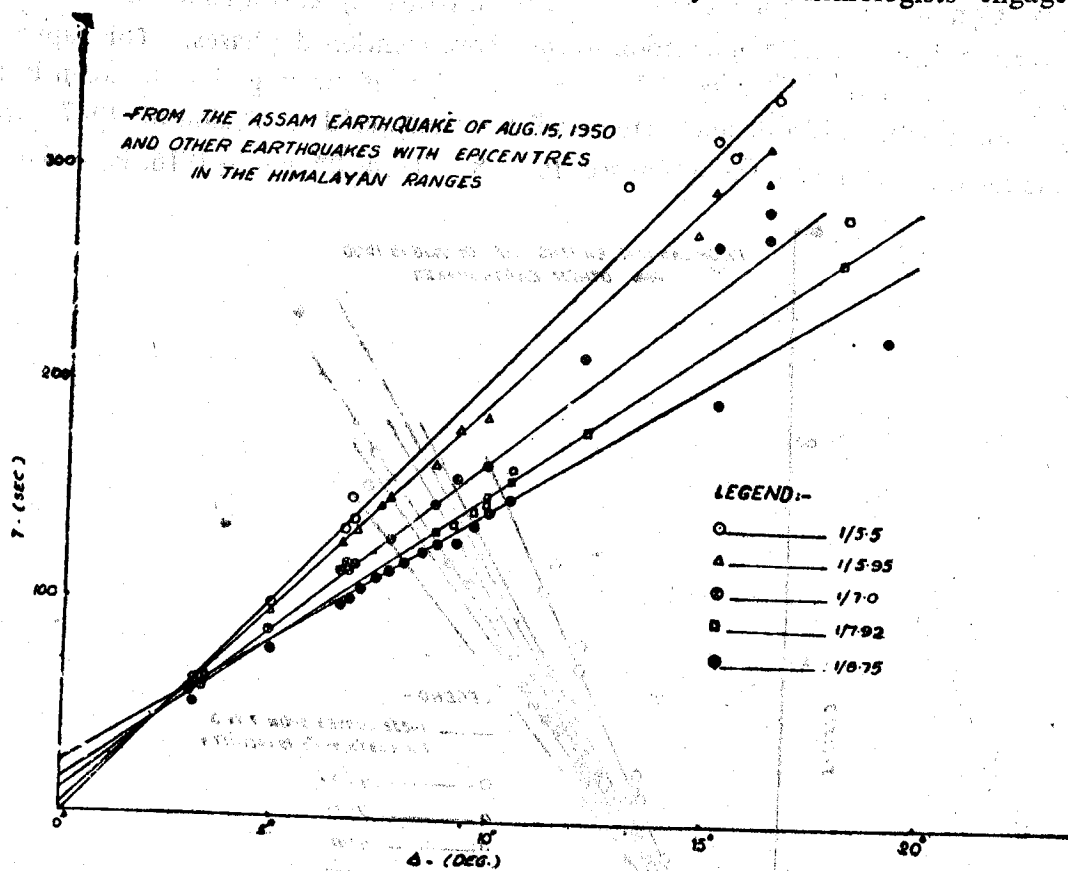


Figure 4 T Vs. Δ for the Himalayan Region

studies are left with no other alternative than to use earthquake seismology as their only tool. As regards this particular aspect of crustal investigation little amount of work has been done for this region.

A.N. Tandon (1955) carried out his studies on this subject of crustal investigations mainly from the Assam Earthquake of 1950, August 15 and its fiftyfour aftershocks. From the travel-time curves, he showed the values of velocities in Km/sec. as shown : P, 7.91, P*, 6.55, P_g 5.58. In the Asian continent, values of these velocities vary quite considerably. P_g 3.56 to 5.55 Km/sec., P 5.95 to 6.30 Km/sec. P 7.4 to 8.5 Km/sec. The author has made investigation for the velocities of longitudinal waves in the crustal layers in the Indian Region. This study has been done on the basis of data obtained from the Assam earthquake of 1950,

Aug. 15 and its fiftyfour aftershocks and thirty more near earthquakes as listed in the Table-1.

It has been attempted to divide the Indian sub-continent into different parts such as the Himalayan Region, Indo-Gangetic plains, Assam Region etc. This has been done for the purpose of drawing travel-time curves separately for these regions. The object of this study is to get an idea about the behaviour of the crustal layers in different regions, to the longitudinal wave velocities.

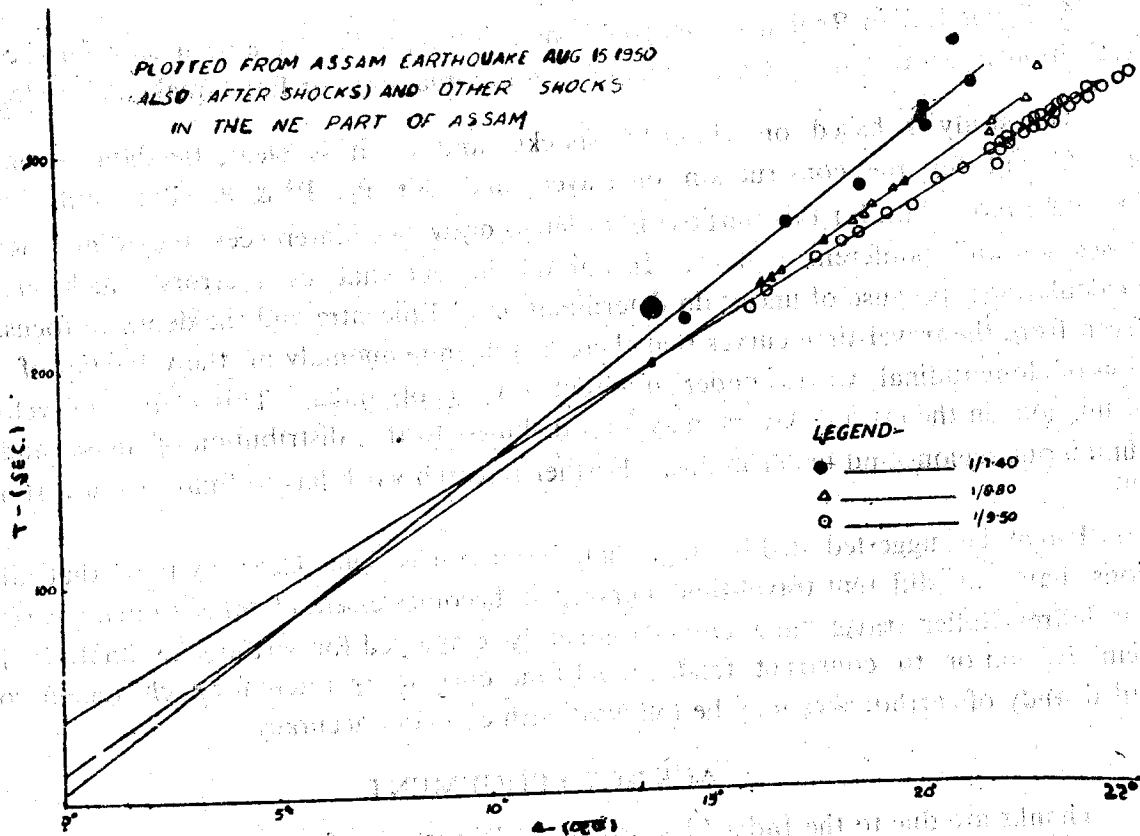


Figure 5 T Vs. Δ for the Directions of Propagation from NE Assam to Bombay, Poona and Hyderabad

Travel-time curves for P_g has been constructed as shown in figure 1. It is quite evident that different regions have got different velocities of P_g . Himalayan region has been found to have P_g to be 4.95 Km/sec. and the Indo-Gangetic plains region has a velocity of 5.5 Km/sec. as a value of P_g . It may be indicated that this indirectly supports the theory of isostasy which enunciates deficit of material under the mountains and excess of mass under the oceans. Atleast the first part of this theory can be supported by the anomaly obtained from the values of P_g and P^* (figs. 1&2) under the Himalayan Region and under the Indo-Gangetic plains. For the region of Assam, it is noted that the velocities of P_g and P^* (figures 1 & 2) are greater than these velocities in other regions. This indicates better transmission of elastic energy to the surface and thus to some extent accounts for greater damage. Also, this may be one of

the reasons why even small local shocks which otherwise may not be felt are frequently felt in Assam. Values for velocities in different crustal layers are found to a good approximation in Km/sec. as : P_g 4.95 – 5.80, P^* 6.5 – 6.85, P 7.4 – 8.35. (figs. 3, 4, & 5).

DISCUSSION AND CONCLUSION

In Earthquake Seismology, for almost any type of study to be made, we require accurate observational data in a large amount. This helps in making out some inferences from the study.

As for as Indian Region is concerned, no seismic profiles have been shot for the crustal investigations. So this study depends mainly on observational or Earthquake Seismology.

This study is based on about 85 shocks, and as it is clear, the data seem to be just sufficient for the construction of travel times for P_g , P^* & P . But, still it will be safer to use more data for this purpose in order to draw some inferences regarding velocity of propagation under different regions. In spite of the fact that usual errors which creep into the calculations, because of uncertain determination of Epicentre and the depth of focus, it can be seen from the travel-time curves that there is a definite anomaly in the velocities of propagation of longitudinal waves under different regions of India. This change in velocity of transmission in the crustal layers may be attributed to the distribution of mass under the mountainous regions and under plains. Further research work has to follow to ascertain this point.

It may be suggested at this stage that because it is quite clear by now that different regions have got different travel-time curves, it becomes essential either to make corrections to the Jeffrey-Bullen travel time curves frequently employed for earthquake analysis in the Indian Region or to construct fresh travel-time curves separately for each region so that detailed study of earthquakes may be followed with ease and accuracy.

ACKNOWLEDGEMENT

Thanks are due to the India Meteorological Department for supplying the records used in the above study. The author acknowledges with thanks the facilities given by Director, School of Research and Training in Earthquake Engineering, for preparing the manuscript.

REFERENCES

- Ewing, M., G.H. Sutton, C.B. Officer (1956) "Seismic Refraction Measurements I the Atlantic Ocean (Part VI) North America Basin"; Bull. Geol. Soc. of Am. Vol. 67, pp. 1647-1658.
- Gutenberg, B., (1959) "Wave Velocities Below the Mohorovicic Discontinuity," Bull. of Seism. Soc. of Am. Vol. 41 pp.143-163.
- Jeffreys, H., (1962) "The Earth" Cambridge University Press, London pp. 70-71.
- Katz, S. (1955) "Seismic Study of Crustal Structure In Pennsylvania and New York" Bull. of Seism. Soc. of Am., 1955, Vol. 45, pp. 303-325

Tandon, A.N. (1955) "A Study of Assam Earthquake of August 15, 1950" I.J.M. & G., Vol. 5, No. 2, p. 95. Records and Reports Referred.

Annual Report (1961-62), Institute of Earth Sciences, University of British, Columbia.

International Seismological Summary

Records of Seism. Bull. of Ind. Met. Deptt.

TABLE 1

Data from the following earthquakes have been used for drawing the travel time curves for different regions of India.

Sl.No.	Epicentre	Date	Remarks
1	2	3	4
1.	28.7° N, 96.6° E	Aug 15, 1950	Assam earthquake with 54 aftershocks. From Seismological Bulletin of India Meteorological Department.
2.	29.0° N, 95.0° E	Jan 3, 1951	
3.	29.0° N, 95.0° E	Jan 4, 1951	
4.	27.2° N, 95.0° E	Feb 8, 1951	
5.	30.8° N, 97.0° E	Feb 15, 1951	
6.	28.0° N, 93.5° E	Feb 21, 1951	
7.	29.3° N, 94.8° E	Mar 6, 1951	
8.	28.2° N, 94.0° E	Mar 12, 1951	
9.	31.4° N, 96.7° E	Mar 16, 1951	
10.	32.0° N, 96.5° E	Mar 17, 1951	
11.	26.0° N, 90.5° E	Apr 17, 1951	
12.	19.2° N, 70.8° E	Apr 8, 1951	
13.	33.3° N, 82.4° E	Jan 28, 1955	
14.	33.0° N, 83.0° E	Feb 9, 1955	Taken from International Seismological Summary.
15.	30.3° N, 67.1° E	Feb 19, 1955	
16.	28.0° N, 85.5° E	Feb 23, 1955	
17.	28.5° N, 85.3° E	Feb 24, 1955	
18.	36.8° N, 71.3° E	Mar 5, 1955	
19.	38.1° N, 72.9° E	Mar 6, 1955	
20.	34.0° N, 78.0° E	Mar 10, 1955	
21.	34.6° N, 74.2° E	Mar 12, 1955	
22.	23.8° N, 93.0° E	Mar 15, 1955	
23.	29.9° N, 90.2° E	Mar 27, 1955	
24.	32.4° N, 76.1° E	Apr 14, 1955	
25.	26.5° N, 90.0° E	Apr 17, 1955	
26.	32.5° N, 78.6° E	Jun 27, 1955	
27.	36.8° N, 71.0° E	Jun 3, 1955	
28.	30.8° N, 86.4° E	Aug 2, 1955	
29.	31.0° N, 71.5° E	Aug 23, 1955	
30.	25.2° N, 90.8° E	Aug 29, 1955	
31.	27.0° N, 91.0° E	Nov 23, 1955	

THE HISTORY OF THE UNITED STATES

The history of the United States is a story of growth and change. From the first settlers to the present day, the nation has evolved through various stages of development. The early years were marked by exploration and settlement, followed by a period of rapid expansion and industrialization. The American Revolution was a pivotal moment in the nation's history, leading to the establishment of a new government. The Civil War was another major event, which resulted in the abolition of slavery and the preservation of the Union. The 20th century has been a time of significant social and political change, with the United States playing a leading role in the world.

CHAPTER I: THE EARLY YEARS

Year	Event	Location
1492	Columbus discovers America	Santa Fe, New Mexico
1607	First permanent English settlement	Jamestown, Virginia
1620	Pilgrims arrive on the Mayflower	Plimouth, Massachusetts
1630	Massachusetts Bay Colony established	Boston, Massachusetts
1650	First printing press in America	New York City
1676	King Philip's War	New England
1703	First census in America	New York City
1733	Georgia founded	Savannah, Georgia
1763	Seven Years' War ends	Paris, France
1776	Declaration of Independence	Philadelphia, Pennsylvania
1781	British evacuated from Philadelphia	York, Pennsylvania
1787	Constitution signed	Philadelphia, Pennsylvania
1791	First Congress meets	Washington, D.C.
1800	Capital moved to Washington	Washington, D.C.
1803	Louisiana Purchase	St. Louis, Missouri
1812	War of 1812 begins	Washington, D.C.
1815	Treaty of Ghent signed	Ghent, Belgium
1820	Missouri Compromise	St. Louis, Missouri
1823	Monroe Doctrine	Washington, D.C.
1845	Texas Annexation	Washington, D.C.
1846	Mexican-American War begins	San Antonio, Texas
1848	Treaty of Guadalupe Hidalgo	Guadalupe, Mexico
1850	Compromise of 1850	Washington, D.C.
1854	Kansas-Nebraska Act	Washington, D.C.
1857	Dred Scott decision	St. Louis, Missouri
1860	Lincoln elected President	Springfield, Illinois
1861	Secession begins	South Carolina
1862	Emancipation Proclamation	Washington, D.C.
1863	Gettysburg Address	Gettysburg, Pennsylvania
1865	War ends	Appomattox, Virginia
1868	Reconstruction begins	Washington, D.C.
1870	First Reconstruction Act	Washington, D.C.
1876	Compromise of 1876	Washington, D.C.
1877	Reconstruction ends	Washington, D.C.
1889	Washburn Act	Washington, D.C.
1890	Wheeler Act	Washington, D.C.
1893	Overthrow of Hawaiian monarchy	Honolulu, Hawaii
1898	Spanish-American War	San Juan, Puerto Rico
1900	Tyler Act	Washington, D.C.
1901	McKinley Act	Washington, D.C.
1906	Antiquities Act	Washington, D.C.
1908	Wheeler Act	Washington, D.C.
1910	Wheeler Act	Washington, D.C.
1912	Wheeler Act	Washington, D.C.
1914	Wheeler Act	Washington, D.C.
1916	Wheeler Act	Washington, D.C.
1917	Wheeler Act	Washington, D.C.
1918	Wheeler Act	Washington, D.C.
1919	Wheeler Act	Washington, D.C.
1920	Wheeler Act	Washington, D.C.
1921	Wheeler Act	Washington, D.C.
1922	Wheeler Act	Washington, D.C.
1923	Wheeler Act	Washington, D.C.
1924	Wheeler Act	Washington, D.C.
1925	Wheeler Act	Washington, D.C.
1926	Wheeler Act	Washington, D.C.
1927	Wheeler Act	Washington, D.C.
1928	Wheeler Act	Washington, D.C.
1929	Wheeler Act	Washington, D.C.
1930	Wheeler Act	Washington, D.C.
1931	Wheeler Act	Washington, D.C.
1932	Wheeler Act	Washington, D.C.
1933	Wheeler Act	Washington, D.C.
1934	Wheeler Act	Washington, D.C.
1935	Wheeler Act	Washington, D.C.
1936	Wheeler Act	Washington, D.C.
1937	Wheeler Act	Washington, D.C.
1938	Wheeler Act	Washington, D.C.
1939	Wheeler Act	Washington, D.C.
1940	Wheeler Act	Washington, D.C.
1941	Wheeler Act	Washington, D.C.
1942	Wheeler Act	Washington, D.C.
1943	Wheeler Act	Washington, D.C.
1944	Wheeler Act	Washington, D.C.
1945	Wheeler Act	Washington, D.C.
1946	Wheeler Act	Washington, D.C.
1947	Wheeler Act	Washington, D.C.
1948	Wheeler Act	Washington, D.C.
1949	Wheeler Act	Washington, D.C.
1950	Wheeler Act	Washington, D.C.
1951	Wheeler Act	Washington, D.C.
1952	Wheeler Act	Washington, D.C.
1953	Wheeler Act	Washington, D.C.
1954	Wheeler Act	Washington, D.C.
1955	Wheeler Act	Washington, D.C.
1956	Wheeler Act	Washington, D.C.
1957	Wheeler Act	Washington, D.C.
1958	Wheeler Act	Washington, D.C.
1959	Wheeler Act	Washington, D.C.
1960	Wheeler Act	Washington, D.C.
1961	Wheeler Act	Washington, D.C.
1962	Wheeler Act	Washington, D.C.
1963	Wheeler Act	Washington, D.C.
1964	Wheeler Act	Washington, D.C.
1965	Wheeler Act	Washington, D.C.
1966	Wheeler Act	Washington, D.C.
1967	Wheeler Act	Washington, D.C.
1968	Wheeler Act	Washington, D.C.
1969	Wheeler Act	Washington, D.C.
1970	Wheeler Act	Washington, D.C.
1971	Wheeler Act	Washington, D.C.
1972	Wheeler Act	Washington, D.C.
1973	Wheeler Act	Washington, D.C.
1974	Wheeler Act	Washington, D.C.
1975	Wheeler Act	Washington, D.C.
1976	Wheeler Act	Washington, D.C.
1977	Wheeler Act	Washington, D.C.
1978	Wheeler Act	Washington, D.C.
1979	Wheeler Act	Washington, D.C.
1980	Wheeler Act	Washington, D.C.
1981	Wheeler Act	Washington, D.C.
1982	Wheeler Act	Washington, D.C.
1983	Wheeler Act	Washington, D.C.
1984	Wheeler Act	Washington, D.C.
1985	Wheeler Act	Washington, D.C.
1986	Wheeler Act	Washington, D.C.
1987	Wheeler Act	Washington, D.C.
1988	Wheeler Act	Washington, D.C.
1989	Wheeler Act	Washington, D.C.
1990	Wheeler Act	Washington, D.C.
1991	Wheeler Act	Washington, D.C.
1992	Wheeler Act	Washington, D.C.
1993	Wheeler Act	Washington, D.C.
1994	Wheeler Act	Washington, D.C.
1995	Wheeler Act	Washington, D.C.
1996	Wheeler Act	Washington, D.C.
1997	Wheeler Act	Washington, D.C.
1998	Wheeler Act	Washington, D.C.
1999	Wheeler Act	Washington, D.C.
2000	Wheeler Act	Washington, D.C.
2001	Wheeler Act	Washington, D.C.
2002	Wheeler Act	Washington, D.C.
2003	Wheeler Act	Washington, D.C.
2004	Wheeler Act	Washington, D.C.
2005	Wheeler Act	Washington, D.C.
2006	Wheeler Act	Washington, D.C.
2007	Wheeler Act	Washington, D.C.
2008	Wheeler Act	Washington, D.C.
2009	Wheeler Act	Washington, D.C.
2010	Wheeler Act	Washington, D.C.
2011	Wheeler Act	Washington, D.C.
2012	Wheeler Act	Washington, D.C.
2013	Wheeler Act	Washington, D.C.
2014	Wheeler Act	Washington, D.C.
2015	Wheeler Act	Washington, D.C.
2016	Wheeler Act	Washington, D.C.
2017	Wheeler Act	Washington, D.C.
2018	Wheeler Act	Washington, D.C.
2019	Wheeler Act	Washington, D.C.
2020	Wheeler Act	Washington, D.C.
2021	Wheeler Act	Washington, D.C.
2022	Wheeler Act	Washington, D.C.
2023	Wheeler Act	Washington, D.C.
2024	Wheeler Act	Washington, D.C.
2025	Wheeler Act	Washington, D.C.

A NOTE ON FLEXURAL VIBRATIONS OF AN INTERCONNECTED BEAM SYSTEM

R. Radhakrishnan*

SYNOPSIS

A method is developed to find the lowest natural frequency of vibration of an interconnected beam system (Fig. 1) with different edge conditions. The analysis is based on the elastic equivalence of a grid frame work to an orthotropic plate. The method used for the analysis is Galerkin's method which belongs to the same class as that of Rayleigh and Ritz. But this method makes the formulation of the physical problem simple and suitable for numerical calculation.

INTRODUCTION

The elastic equivalence of a rectangular gridwork to an orthotropic plate was first suggested by Timoshenko (1959). Yonezawa and Naruoka (1958) used this principle for studying the free vibrations of bridge decks made of interconnected beam systems by the frequency analysis of the equivalent orthotropic plate. Recently, Rajappa (1964) has used this method for finding out the flexural vibration of an interconnected beam system point supported at the corners. The principle applied in this paper is the same and the Galerkin's method which has been used by Stanisic and McKinley (1961) for isotropic plate, is used here to determine the frequency of the orthotropic plate. Frequencies are calculated for two different types of edge conditions.

ANALYSIS

The equivalence of a beam system to the orthotropic plate has been described in detail in a paper by Rajappa (1964). The expression for 'p' is given by:

$$p^2 = \frac{g \lambda^2}{\gamma h} - \left(\frac{gk}{2\gamma h} \right)^2 \quad (1)$$

where,

$$\lambda^2 = \frac{\iint \left(D_x \frac{\partial^4 w}{\partial x^4} + 2H \frac{\partial^4 w}{\partial x^2 \partial y^2} + D_y \frac{\partial^4 w}{\partial y^4} \right) f(x, y) dx dy}{\iint f^2(x, y) dx dy} \quad (2)$$

*Deptt. of Civil Engineering, Indian Institute of Technology, Madras-36.



The value of 'p' can always be found whenever the value of ' λ ' is calculated for any plate whose characteristic function $f(x, y)$ is given :

For a plate simply supported on all sides, $f(x,y)$ for the fundamental mode of vibration is given by :

$$f(x, y) = A \sin \frac{\pi x}{a} \sin \frac{\pi y}{b} \quad (3)$$

where, $x=0$, $x=a$, $y=0$ and $y=b$ are the edges of the plate. Substituting the value of $f(x,y)$ in equation (2), we get :

$$\lambda^2 = \pi^4 \left[\frac{D_x}{a^4} + \frac{2H}{a^2 b^2} + \frac{D_y}{b^4} \right] \quad (4)$$

and,

$$p^2 = \frac{g \pi^4}{\gamma h} \left[\frac{D_x}{a^4} + \frac{2H}{a^2 b^2} + \frac{D_y}{b^4} \right] - \left(\frac{gk}{2rh} \right)^2 \quad (5)$$

For the isotropic plate $D_x = D_y = H = D$ and hence:

$$p^2 = \frac{gD\pi^4}{\gamma h} \left[\frac{1}{a^4} + \frac{2}{a^2 b^2} + \frac{1}{b^4} \right] - \left(\frac{gk}{2rh} \right)^2 \quad (6)$$

and for a square isotropic plate where damping is neglected :

$$p^2 = \frac{4gD\pi^4}{\gamma h a^4} \quad (7)$$

which is a well-known result (Timoshenko, 1959).

CASE 2.

For a plate clamped along its sides :

$$f(x, y) = B \left(1 - \cos \frac{2\pi x}{a} \right) \left(1 - \cos \frac{2\pi y}{b} \right) \quad (8)$$

and substituting in equation (2) :

$$\lambda^2 = \frac{16\pi^4}{9} \left[\frac{3b D_x}{a^4} + \frac{2H}{a^2 b^2} + \frac{3b D_y}{b^4} \right] \quad (9)$$

On simplifying :

$$\lambda^2 = 523.5 \left(\frac{D_x}{a^4} \right) + 349 \left(\frac{H}{a^2 b^2} \right) + 523.5 \left(\frac{D_y}{b^4} \right) \quad (10)$$

By employing an algebraic function for $f(x, y)$ as :

$$f(x, y) = x^2 (x - a)^2 y^2 (y - b)^2 \quad (11)$$

the frequency will be obtained (Rajappa, 1963) as :

$$\lambda^2 = 504 \left(\frac{D_x}{a^4} \right) + 288 \left(\frac{H}{a^2 b^2} \right) + 504 \left(\frac{D_y}{b^4} \right) \quad (12)$$

which is smaller than the one obtained in equation (10). Hence, the value of $f(x,y)$ given by equation (11) is preferable for practical purposes.

REFERENCES

- Rajappa, N.R., (1963) "Free Vibration of Rectangular and Orthotropic Plates", Journal of the American Institute of Aeronautics and Astronautics, May, 1963, p.1194.
- Rajappa, N.R., (1964) "Flexural Vibration of an Inter-connected Beam system Point supported at the Corners", Institution of Engineers (India), March 1964.
- Stanisic, N.M. and R.M. McKinley, (1961) "On the Vibration of a Trapezoidal Plate clamped along each edge with Damping considered"—ZAMM, Vol. 41, pp. 414-419, 1961.
- Timoshenko, S. and W.S. Krieger, (1959) "Theory of Plates and Shells, McGraw Hill".
- Yonezawa, H., and M. Naruoka, (1958) "A study on the period of free Lateral Vibration of the Beam Bridge by the Theory of Orthotropic plate"—Ingenieur-Archiv, Vol. XXVI B., Springer-Verlag.

NOTATIONS

- | | | |
|---------------|---|-----------------------------------------------------------|
| a,b | — | Dimensions of grid along x and y axis |
| D | — | Flexural rigidity of an isotropic plate |
| D_x, D_y, H | — | Flexural and Torsional rigidities of an orthotropic plate |
| g | — | Acceleration due to gravity |
| k | — | Co-efficient of viscous damping |
| γ | — | Weight density of the plate |
| h | — | Thickness of the plate material |
| r,s | — | Spacing of the beam along x and y axis |

SEISMOLOGICAL NOTES

A.N. Tandon*

Earthquakes felt in and near about India during January-March, 1964.

Date	Origin time (GMT)			Epicentre Lat. Long.		Region	Approx.dep. (Km.)	Magnitude	Remarks
1	2	3	4	5	6	7	8	9	10
Jan. 17	03	25	02	35	69	Hindukush	—	5.5 (N.DLH)	Recorded at a few observa- tories in India.
	03	25	00.6	36.8	71.4	Hindukush	94	5.2 (CGS)	
Jan. 21	16	40	24	20 Kms to the NNW of Delhi.		—	—	2.1 (N.DLH)	—
Jan. 22	15	58	45	22	93	Arakan Hills	—	5.9 (N.DLH)	Recorded at all Indian ob- servatories.
	15	58	46.5	22.4	92.7	Burma	88	6.1 (CGS)	
Jan. 23	15	19	38	37	73	Hindukush	—	5.0 (N.DLH)	Recorded at a few observa- tories in India.
	15	19	31	36.9	71.2	Hindukush	28	4.4 (CGS)	
Jan. 25	07	13	35	27.7	85.8	Nepal	—	—	Recorded at many observa- tories in India.
	07	13	30.8	28.5	86.8	Tibet	44	4.5 (CGS)	
Jan. 28	14	09	15	36.5	70.6	Hindukush	220	—	Felt in west Pakistan and large parts of NW India.
	14	09	17.1	36.5	70.9	Hindukush	208	6.1 (CGS)	
Feb. 1	12	26	23	44 Kms away from Delhi		—	—	—	Felt in Delhi (MM. intensity II)
Feb. 2	05	38	05	27 Kms to the west of Delhi		—	—	—	—

(Continued)

* Director (Seismology), India Meteorological Deptt., New Delhi-3

1	2	3	4	5	6	7	8	9	10
	13 05 28 (N. Delhi)			23 Kms to the WSW of Delhi		—	—	2.1 (N.DLH)	—
	17 35 00 (N. Delhi)			27 Kms to the west of Delhi		—	—	—	—
Feb. 8	11 54 20 (Shillong)			29 82	West Nepal	—	—	4.9 (N.DLH)	Recorded by many obser- vatories in India.
	11 54 23.1 (USCGS)			29.0 82.2	Nepal	33	—	—	—
Feb. 10	17 11 27 (N. DLH)			100 Kms to the NE of Delhi	—	—	—	3.8 (N.DLH)	Felt in Delhi (M.M. intensity II)
Feb. 16	10 06 48.4 (N. DLH)			90 Kms to the WNW of Delhi	—	—	—	4.2 (N.DLH)	Felt in Delhi and neighbouring areas. (M.M. intensity III)
Feb. 18	03 48 35.6 (USCGS)			27.5 91.1	Bhutan	30	5.6 (CGS)	—	Recorded at a few Indian observatories.
Feb. 20	01 16 58 (N. DLH)			32 Kms away from Delhi	—	—	—	—	—
Feb. 26	06 24 38 (N. DLH)			32 Kms to the NE of Delhi	—	—	—	2.4 (N.DLH)	—
Feb. 27	15 10 45 (Shillong)			21 94	East of Arakan Hills	—	—	7.1 (N.DLH)	Recorded at all Indian observatories.
	15 10 48.4 (UCGS)			21.7 94.4	Burma Central Burma	102	6.4 (CGS)	—	—
Feb. 28	17 47 10 (Shillong)			18.5 94	Arakan coast	—	—	6.2 (N.DLH)	Recorded at many observatories, in India.
	17 47 05.9 (UCGS)			18.2 94.3	Burma Near west coast of Burma	43	5.3	—	—
Mar. 4	18 00 16 (N. DLH)			17 Kms away from Delhi	—	—	—	—	—
Mar. 15	17 41 47 (N. DLH)			30 Kms away from Delhi.	—	—	—	—	—
	22 50 10 (N. DLH)			20 Kms away from Delhi.	—	—	—	—	—
Mar. 20	19 01 00 (Shillong)			24 93	Lushai Hills	—	—	—	Recorded by many observatories, in India.
	19 00 52.7 (UDGS)			23.6 94.4	Assam North- western Burma.	186	5.7 (CGS)	—	—

(Continued)

1	2	3	4	5	6	7	8	9	10
Mar. 22	21	31	10	30 Kms away from Delhi.		—	—	—	—
	(N. DLH)								
Mar. 24	17	52	06	40 Kms away from Delhi.		—	—	—	—
	(N. DLH)								
Mar. 27	04	30	35	26	95	Naga Hills-Burma Border Northen Burma	—	6.3	Recorded at many observatories in India
	(Shillong)								
	04	30	33	25.9	95.8		93	5.4	
	(UCGS)							(CGS)	
Mar. 30	16	34	29	13 Kms away from Delhi.		—	—	—	—
	(N. DLH)								
	16	35	03.5	15 Kms away from Delhi.		—	—	—	—
	(N. DLH)								

THE UNIVERSITY OF CHICAGO

THE UNIVERSITY OF CHICAGO
LIBRARY
540 EAST 57TH STREET
CHICAGO, ILL. 60637

STATEMENT OF ACCOUNTS OF 'ISET' AS ON 31st MARCH 1964

RECEIPT	TOTAL	EXPENDITURE	TOTAL
1. Subscriptions from Institution Members 3 × 100	Rs. 300.00	1. Printing of Constitution	Rs. 37.25
2. Subscription from members 68 × 15	Rs. 1020.00	2. Printing letter heads etc.	Rs. 18.00
3. Charges of extra reprints supplied to one author	Rs. 10.00	3. Printining of Bills, forms etc.	Rs. 18.00
4. Charges of selling one Bulletin	Rs. 5.00	4. Rubber Stamp	Rs. 2.25
5. Charges of advertise- ment	Rs. 135.00	5. Typing, stationary, Postage, remuneration etc.	Rs. 90.00
Grand Total	Rs. 1470.00	6. Printing of First Bulletin	Rs. 1232.96
		7. Bank Commisson	Rs. 2.65
			Rs. 1401 11

BALANCE

Rs. 68.89

— Secretary

GOEL ELECTRIC CO.,
SARRAFA BAZAR, MEERUT CITY

Engineers, Suppliers and Government Approved 'A' Class Licenced Contractors.

Dealers in :—

ALL KINDS OF ELECTRICAL AND ELECTRONIC INSTRUMENTS

Manufacturers of :—

SPEED CONTROLLED MOTORS AND REDUCTION GEAR UNITS

Stockists of :—

**H.S. METERS, VOLT METERS, AMPERE METERS, AVO METERS,
SWITCHES AND SWITCHGEARS, WIRES AND CABLES.**

MAKNIG
ELECTRONIC & ELECTRICAL INSTRUMENTS
IS OUR BUSINESS

**THERE IS PRACTICALLY NO LIMIT TO THE
VARIETY OF THESE INSTRUMENTS THAT
CAN BE MADE, BUT WE DO NOT MAKE
ALL OF THEM.**

WE MAKE ONLY FEW OF THEM AND

WE MAKE THEM PERFECT

**THE QUALITY & RELIABILITY WE PUT
INTO THESE INSTRUMENTS IS FOR YOU
IF YOU NEED ANY**

ELECTRONIC APPLIANCES

Manufacturers of Electoronic & Electrical Instruments for Research & Industry

ROORKEE

INDIAN SOCIETY OF EARTHQUAKE TECHNOLOGY

Instructions for Authors

MANUSCRIPTS

1. Only papers, which have not been previously published or offered for publication elsewhere, will be considered. The authors must agree not to publish a paper elsewhere when it is under consideration and print in the Bulletin of the ISET. Two copies of the manuscript must be submitted.
2. Manuscripts must be type written in English or Hindi with two-line spacing on one side of the paper only.
3. The use of the first person should be avoided, the writer being referred to as "the Author".
4. All mathematical symbols should be defined, where they appear first in the text.
5. Drawings or sketches should not be included in, or pasted on to the pages of the manuscript, but should be entirely separate.
6. Each article should be accompanied by a "Synopsis" of its subject matter, with special reference to any conclusions, and it should not exceed 300 words.
7. A set of conclusions must be given at the end of the article.
8. Bibliographical references should be standardized as follows:—
 - (a) In the text the author's name and the year of publication should appear in parentheses as (Krishna 1960) or Krishna (1960).
 - (b) In a list of references (un-numbered) at the end of the article, the references should be listed in alphabetical order of authors' names, the general form of a complete reference being:—

Name, initials, year of publication.

Title of work, Source (in full), volume number, page number (beginning)—page number (end).

Examples:—

Prakash, S. and U.K. Bhatia (1964), "A Review of Machine Foundation Behaviour", Bulletin, Indian Society of Earthquake Technology, Vol. I No. 1, January, 1964, pp. 45-64.

Sekaran, A.R.C., (1962) "Effect of Joint Rotation on the Dynamics of Multistoreyed Frames", Proceedings, Second Symposium on Earthquake Engineering, University of Roorkee, Roorkee, Nov. 10-12, 1962, pp. 305-316.

ILLUSTRATIONS

1. Drawing should be made on tracing linen or paper in dense black drawing-ink, the thickness of lines being consistent with a reduction to one half or less in the process of reproduction, details shown should represent the minimum necessary for a clear understanding of what it is desired to illustrate.
2. The maximum final size of a single drawing or of a group of drawings which are intended to appear on the same page, is 7½ inches (19 centimeters) by 5 inches (13 centimeters). Drawings should be submitted larger than final size, the ideal being twice final size i.e. up to 15 inches (38 centimeters) by 10 inches (26 centimeters).
3. It should be ensured that printing of caption in the illustration is large enough so that it would be legible after reduction to one half linear size. 3/16" (0.5 cm.) size letters are recommended.
4. MSS. may also be accompanied by photographs (glossy prints) which should, however, represent the minimum number essential to a clear understanding of the subject. No lettering of any kind should be added to the face of a photograph: the Figure number and caption being printed lightly on the reverse side or upon the front of the mounting if mounted.
5. All illustrations should be numbered consecutively without distinction between photographs and drawings. Each illustration should have an appropriate reference in the text, and the figure number order should follow the order in which references appear in the text.

GENERAL

1. A total of 25 reprints are supplied free to authors. Additional reprints may be ordered well in advance @ Rs. 5/- per additional 25 reprints.
2. Reprints from the Bulletin may be made on the condition that full title, name of author, volume number and year of publication by the Society are given. The Society is not responsible for any statement made or opinions expressed in the Bulletin.
3. This Bulletin is published two times in a year by the Indian Society of Earthquake Technology with head quarters at Roorkee. Rs. 10.00 of a member's dues are applied as a subscription to this Bulletin.

EDITOR



GAUTAM PRINTING PRESS, ROORKEE (U.P.)